Effects of bulk viscosity in relativistic heavy ion collisions

Masters thesis, 19.12.2019

Author:

Henry Hirvonen

Supervisor:

Harri Niemi

UNIVERSITY OF JYVÄSKYLÄ
DEPARTMENT OF PHYSICS

Abstract

Hirvonen, Henry
Master's thesis
Department of Physics, University of Jyväskylä, 2019, 118 pages.

In relativistic heavy ion collisions substance called quark-gluon plasma (QGP) is created. The Quark gluon plasma is a matter which consists from a weakly coupled quarks and gluons and it can only be created on extreme temperatures or pressures. After QGP cools down it experiences phase transition to the hadron gas. The evolution of QGP and hadron gas can be modeled using the relativistic hydrodynamics, which is effective theory describing dynamics of the fluids. In this thesis we are particularly interested about effects of the bulk viscosity in Pb+Pb collisions with $\sqrt{s_{NN}} = 2.76$ TeV. Initial state for hydrodynamic evolution was calculated using the EKRT-model and freeze-out was done using Cooper-Frye procedure. We found out that the bulk viscosity caused expansion of the system to slow down which evidently decreased average transverse momentum of the final state particles.

Keywords: heavy ion collisions, QGP, hydrodynamics, kinetic theory, bulk viscosity

Tiivistelmä

Hirvonen, Henry
Pro gradu -tutkielma
Fysiikan laitos, Jyväskylän yliopisto, 2019, 118 sivua

Relativistisissa raskasionitörmäyksissä syntyy ainetta, jota kutsutaan kvarkki-gluoniplasmaksi (QGP). QGP on ainetta, joka koostuu heikosti kytketyistä kvarkeista ja gluoneista ja sitä syntyy ainoastaan erittäin korkeissa lämpötiloissa tai paineissa. Kun törmäyksessä syntynyt QGP alkaa jäähtymään, se kokee faasitransition hadronikaasuksi. QGP:n ja hadronikaasun kehitystä voidaan mallintaa käyttäen relativistista hydrodynamiikkaa, joka on fluidin dynamiikkaa kuvaava efektiivinen teoria. Tämä tutkielma käsittelee erityisesti tilavuusviskositeetin vaikutusta raskasionitörmäyksiin Pb+Pb törmäyksissä, joissa $\sqrt{s_{NN}} = 2.76$ TeV. Alkutila hydrodynaamiselle kehitykselle saatiin EKRT-mallin avulla ja irtikytkeytyminen toteutettiin Cooper-Frye menetelmällä. Saaduista tuloksista nähtiin, että tilavuusviskositeetti hidasti systeemin laajenemista ja sitä kautta pienesi lopputilan hiukkasten keskimääräisiä poikittaisliikemääriä.

Avainsanat: raskasionitörmäys, QGP, hydrodynamiikka, kineettinen teoria, tilavuusviskositeetti,

Contents

1 Introduction

One of the goals of the modern physics has always been to study matter at the extreme conditions in which temperature or density of the system is very high. One place where these kinds of conditions are met is in heavy ion collisions where two heavy nuclei collide to each other velocities near speed of light. As a consequence of the high collisions energies, even thousands of hadrons, such as protons, pions or kaons, can be created in a single collision.[1]

In heavy ion collisions most of the interactions happen via the strong interaction which described by theory called quantum chromodynamics (QCD). In QCD all the hadrons are considered as bound states of quarks and interactions between quarks are mediated by gluons. The quarks are spin-1/2 fermions which have three possible color charges, while gluons are spin-1 bosons which can have eight different color charges.[2]

One of the most interesting properties of QCD is so called color confinement which states that bound states of quarks must always exist in color neutral state. Another interesting property of QCD is the asymptotic freedom which expresses that interactions between quarks become asymptotically weaker as energy scale increases. These properties of QCD indicate that matter consisting from quarks and gluons should have two different states. At the low energies color confinement indicates that quarks and gluons form a gas of interacting hadrons while at the high energies this matter is expected to behave like weakly coupled gas of quarks and gluons due to asymptotic freedom.[1], [2]

The high energy state of QCD matter is usually referred as quark gluon plasma (QGP) and it is believed to exist in the early times of the universe, where temperatures were extremely high [1], [3]. The best way to experimentally replicate these conditions is by doing heavy ion collision experiments, where QGP is also expected to be created. First heavy ion collision experiments were done in the 1970s at BEVALAC where the center of mass energies of the collisions were around 2 GeV [4]. Since then particle accelerators have improved a lot and nowadays the highest energies are achieved in LHC where center of mass energies are as high as 5.02 TeV [5], [6].

In principle, modeling heavy ion collisions should be done by calculating all interactions between quarks and gluons with the help of QCD. However, there can be several thousands of particles created in one heavy ion collision which makes it difficult to use QCD directly. Instead, one usually uses hydrodynamics to model dynamics of the system. In this approach matter created in collision is described as a fluid which is close to thermal equilibrium. Because hydrodynamics describe collective behavior of the fluid, there is no need to calculate individual particle interactions. This makes modeling of the system much simpler.

The hydrodynamic fluid also has some thermal properties which are described by equation of state and some viscous properties which describe deviation from thermal equilibrium. Viscous properties of the fluid are usually divided into bulk viscosity and shear viscosity. The shear viscosity has been successfully used in context of heavy ion collision for many years and it has provided some excellent results [7]–[10]. The bulk viscosity has only recently added to simulations and amount of studies using it is still limited [11]–[14].

The goal of this thesis is to study effects of the bulk viscosity in relativistic heavy ion collisions and give theoretical overview about relativistic hydrodynamics and heavy ion collisions. To achieve this goal this thesis organized following way: In section 2 we discuss general structure of relativistic dissipative hydrodynamics and derive relativistic Navier-Stokes theory, which turns out to be acausal. We then proceed to derive causal Israel-Stewart theory by using the second law of thermodynamics. In section 3 we go through method to derive relativistic dissipative hydrodynamics directly from the kinetic theory. The modeling of the heavy ion collisions using hydrodynamics is then discussed in section 4. In section 5 we then introduce numerical methods used in the simulations and discuss a general structure of the numerical code. The results and final conclusions of this thesis are presented in sections 6 and 7 respectively.

2 Relativistic hydrodynamics

The relativistic hydrodynamics is an effective theory which describes macroscopic evolution of a relativistic fluid. In general describing behavior of fluid in microscopic scales is extremely complicated due to the fact that the fluid consists of many particles which interact with each other. This means that the system of interest has many degrees of freedom. Fortunately when studying the macroscopic behavior of the fluid most of the microscopic degrees of freedom are irrelevant and only overall effect of these complicated particle interactions are of interest. For example there is no need for information about velocity or position of every single particle in the fluid when considering macroscopic scales. Instead, the average quantities, like the velocity of the fluid, are much more prominent.

When applying hydrodynamics, there are some important assumptions that have to be made. First of all fluid has to considered continuous system where in close proximity of each point we have infinitesimal volume element where all properties of fluid remain constant. This means that this kind of fluid element has to be a very small compared to any macroscopic scales. Another assumption is that every fluid element is reasonably close to the thermodynamic equilibrium. This thermodynamic equilibrium is assured if fluid element is large enough relative to microscopic scales so that microscopic fluctuations can be ignored.

Both of these conditions are met if the difference between microscopic and macroscopic scales is large enough. All every day liquids and gasses fulfill this condition and that's why hydrodynamics is used to model their behavior in many applications. When studying QGP formed in heavy ion collisions this kind of separation is not trivial at all, because typical macroscopic distance scales in this kind of systems are ~ 1 fm. It has been pretty well established that the hydrodynamics are applicable when two heavy ions (e.g. Pb) collide, but the minimum size of a QGP droplet that can be formed is still under heavy debate [15]–[17].

In this section we go through formalism of relativistic hydrodynamics by first starting from ideal hydrodynamics and then proceeding to dissipative hydrodynamics. Most of this section, especially section 2.2, follows structure similar to one in Ref.[18]

2.1 Relativistic ideal hydrodynamics

The simplest case of the relativistic hydrodynamics is ideal hydrodynamics. In ideal hydrodynamics it is assumed that fluid element is exactly in thermodynamic equilibrium. In the most literature this kind of thermodynamic equilibrium is called the local thermal equilibrium. The local thermal equilibrium assures that in each space-time point x^μ there is well-defined temperature $T(x^\mu)$, chemical potential $\mu(x^\mu)$ and fluid velocity field $\vec{u}(x^\mu)$.

In hydrodynamics evolution of the fluid is controlled by different conservation laws: conservation of energy, momentum and particle number. For each of these conservation laws, there must be associated some conserved current. In case of relativistic hydrodynamics conserved currents connected to energy and momentum conservation are written in terms of one tensor $T^{\mu\nu}$ called energy-momentum tensor, which components are defined as [19]:

- T^{00} is the energy density,
- T^{j0} is the density of the j:th component of momentum (j=1,2,3),
- T^{0i} is the flux of energy along i-axis (i=1,2,3),
- T^{ij} is the flux of j:th momentum component along i-axis .

The momentum flux can also be thought as force per area so that components of T^{ij} are really the components of kinetic pressure. Conserved current used for particle number conservation is called particle 4-current N^μ, in which N^0 component is particle density and N^j components describe particle flux along i-axis. In addition, it is useful to define entropy 4 -current S^μ similar way than particle 4-current so that S^0 component is entropy density and S^j components describe entropy flux along i-axis. We also note that we use convention where metric tensor $g_{\mu\nu} = \mathrm{Diag}(-1,1,1,1)$.

When studying fluid in its rest frame, where fluid 4-velocity $u^\mu = (1,0,0,0)$, assumption of exact local thermal equilibrium demands that system is isotropic [19]. This isotropy implies that kinetic pressure components cannot be off diagonal and all diagonal components must equal to thermodynamic pressure meaning that $T^{ij}_{RF} = \delta^{ij}p$, where RF denotes rest frame. In rest frame there is also no flow of energy, entropy or particles and momentum density vanishes. Because of this energy-

momentum tensor in rest frame can be written as

$$T^{\mu\nu}_{RF} = \mathrm{Diag}(\varepsilon, p, p, p). \tag{2.1}$$

Similarly entropy and particle 4-currents take forms

$$N^{\mu}_{RF} = (n, 0, 0, 0), \tag{2.2}$$

$$S^{\mu}_{RF} = (s, 0, 0, 0), \tag{2.3}$$

where n is particle density and s is entropy density. Basically these equations tell that ideal fluid rest frame is frame where there is no energy or particle flow. More general form of these tensors in any boosted frame can now be obtained by doing general Lorenz -transformation to the rest frame tensors. General form of Lorenz transformation to a frame which moves with velocity $\vec{u}$ in respect of original frame is form of

$$\Lambda_{\mu\nu} = \begin{pmatrix} \gamma & -u^x & -u^y & -u^z \\ -u^x & 1+(1+\gamma)^{-1}u^x u^x & (1+\gamma)^{-1}u^x u^y & (1+\gamma)^{-1}u^x u^z \\ -u^y & (1+\gamma)^{-1}u^x u^y & 1+(1+\gamma)^{-1}u^y u^y & (1+\gamma)^{-1}u^x y^z \\ -u^z & (1+\gamma)^{-1}u^x u^z & (1+\gamma)^{-1}u^y u^z & 1+(1+\gamma)^{-1}u^z u^z \end{pmatrix}. \tag{2.4}$$

Now for the ideal fluid in boosted frame it is possible to write

$$T^{\mu\nu}_{(0)} = \Lambda^{\mu}_{\mu'}\Lambda^{\nu}_{\nu'}T^{\mu'\nu'}_{RF} = \varepsilon u^{\mu}u^{\nu} - \Delta^{\mu\nu}p, \tag{2.5}$$

$$N^{\mu}_{(0)} = \Lambda^{\mu}_{\mu'}N^{\mu'}_{RF} = nu^{\mu}, \tag{2.6}$$

$$S^{\mu}_{(0)} = \Lambda^{\mu}_{\mu'}S^{\mu'}_{RF} = su^{\mu}, \tag{2.7}$$

where lower index 0 denotes that we are talking about ideal fluid. In addition we introduced projection operator

$$\Delta^{\mu\nu} = g^{\mu\nu} - u^{\mu}u^{\nu}. \tag{2.8}$$

This kind of projection operator projectiles tensors into 3 dimensional space orthogonal to 4-velocity u^μ and it has following properties

$$\begin{aligned} u_\mu \Delta^{\mu\nu} &= u_\nu \Delta^{\mu\nu} = 0 \\ \Delta^{\mu\alpha}\Delta^{\nu}_{\alpha} &= \Delta^{\mu\nu} \\ \Delta^{\mu}_{\mu} &= g^{\mu}_{\mu} - u^\mu u_\mu = 3. \end{aligned} \tag{2.9}$$

As mentioned each conserved current is associated with some conservation law. These conservation laws cover conservation of energy, momentum and particle number. Using definitions of energy-momentum tensor and particle four current these conservation laws can be written as

$$\partial_\mu T^{\mu\nu}_{(0)} = 0, \tag{2.10}$$

$$\partial_\mu N^{\mu}_{(0)} = 0. \tag{2.11}$$

Conservation of energy-momentum tensor contains in total four equations. It is customary to divide these equation in to two parts, one which is parallel to 4-velocity and another which is orthogonal to 4-velocity. Parallel part reads

$$\begin{aligned} u_\nu \partial_\mu T^{\mu\nu}_{(0)} &= u_\nu (u^\mu u^\nu \partial_\mu \varepsilon + \varepsilon \partial_\mu (u^\mu u^\nu) + p\partial_\mu (u^\mu u^\nu) - \Delta^{\mu\nu}\partial_\mu p) \\ &= u^\mu \partial_\mu \varepsilon + (\varepsilon + p)\nabla_\mu u^\mu = \frac{d\varepsilon}{d\tau} + (\varepsilon + p)\theta = 0, \end{aligned} \tag{2.12}$$

where $d/d\tau = u^\mu \partial_\mu$ is the comoving derivative, $\nabla_\mu = \Delta^\nu_\mu \partial_\nu$ is the space-time like derivative and $\theta = \nabla_\mu u^\mu$ is the expansion rate. It is also convenient to notice useful relation between different kind of derivatives

$$\partial^\mu = \nabla^\mu + u^\mu \frac{d}{d\tau}. \tag{2.13}$$

Similarly we obtain energy-momentum conservation equations orthogonal to u^μ

$$\Delta^\mu_\alpha \partial_\beta T^{\alpha\beta}_{(0)} = (\varepsilon + p)\frac{du^\mu}{d\tau} - \nabla^\mu p = 0 \tag{2.14}$$

and particle number conservation equation

$$\partial_\mu N^{\mu}_{(0)} = \partial_\mu (n u^\mu) = \frac{dn}{d\tau} + n\theta = 0. \tag{2.15}$$

Equations (2.12), (2.14) and (2.15) together form the equations of motion for the ideal relativistic hydrodynamics and they read

$$\begin{aligned} &\frac{d\varepsilon}{d\tau} + (\varepsilon + p)\theta = 0, \\ &(\varepsilon + p)\frac{du^\mu}{d\tau} - \nabla^\mu p = 0, \\ &\frac{dn}{d\tau} + n\theta = 0. \end{aligned} \tag{2.16}$$

Because these equations contain 6 independent variables, ε, p and four components of u^μ, and there is only have 5 equations of motion, we need some additional constraint to solve this set of equations. This additional constrain is called equation of state which connects the pressure to energy and particle densities and it is discussed in more detail in section 2.

2.2 Covariant thermodynamics

Covariant thermodynamics is useful way to express usual thermodynamic relations in terms of covariant quantities, like entropy 4-current S^μ. In order to understand foundation of covariant thermodynamics better lets first take a quick look at the standard presentation of the thermodynamics.

Thermodynamics is theory which deals with the transfer of energy from one form to another. Its idea is to describe complicated microscopic processes in terms of macroscopic quantities like energy E, entropy S and particle number N. In this sense thermodynamics resembles a lot of hydrodynamics. This is not too surprising since hydrodynamics is based mostly on the thermodynamics. All of the thermodynamics can be derived from the four laws of thermodynamics. When considering hydrodynamics two of these four law are in particular interest: first and second laws of thermodynamics. The second law of thermodynamics turns out to be very useful, when considering dissipative fluid dynamics. It states that in an isolated system entropy can only increase or stay constant. First law on the other hand states that change of energy in system is caused by heat, mechanical work or change of particles. This law gives us basic thermodynamic relation and is extremely useful. The first law of thermodynamics can be written mathematically in terms of differentials [20]

$$dE = dQ - pdV + \mu dN, \tag{2.17}$$

where dQ is a transferred heat, V is a volume of the system, p is a pressure and μ is a chemical potential. When considering reversible processes heat can be written in terms of temperature and entropy, $dQ = TdS$. In this case first law of thermodynamics is

$$dE = TdS - pdV + \mu dN. \tag{2.18}$$

From this relation it is then easy to obtain other thermodynamic quantities

$$\begin{aligned} T &= \left(\frac{\partial E}{\partial S}\right)_{N,V} \\ p &= -\left(\frac{\partial E}{\partial V}\right)_{N,S} \\ \mu &= \left(\frac{\partial E}{\partial N}\right)_{S,V} = 0. \end{aligned} \tag{2.19}$$

Thermodynamic quantities are usually divided into intensive and extensive quantities. Intensive quantity doesn't depend on size of the system. Extensive quantity on the other hand depends linearly on the size of the system. In thermodynamics T, p, μ are intensive quantities and E, S, V, N are extensive ones. Because all E,S,V,N are extensive quantities it is possible to write

$$\lambda E = E(\lambda S, \lambda V, \lambda N), \tag{2.20}$$

where λ is some arbitrary constant. Now taking derivative from Eq.(2.20) with respect of λ and setting $\lambda = 1$, one obtains

$$E = \left(\frac{\partial E}{\partial S}\right)_{N,V} S + \left(\frac{\partial E}{\partial V}\right)_{N,V} V + \left(\frac{\partial E}{\partial N}\right)_{N,V} N. \tag{2.21}$$

When using definitions of thermodynamic quantities from Eq.(2.19) we get Euler's relation

$$E = TS - pV + \mu N. \tag{2.22}$$

Expressing this relation in terms of differentials and using Eq.(2.18), we find the Gibbs-Duhem equation

$$Vdp = SdT + Nd\mu. \tag{2.23}$$

In hydrodynamics we usually deal with densities so it is useful to divide Eqs. (2.18), (2.22) and (2.23) with volume V. This leads to

$$\begin{aligned} \varepsilon + p &= Ts + \mu n, \\ dp &= sdT + nd\mu, \\ ds &= \beta d\varepsilon + \alpha dn, \end{aligned} \tag{2.24}$$

where $\beta = 1/T$ and $\alpha = \mu/T$. These are the equations for which we would like to find covariant forms. In order to do so let's first define

$$\beta^\mu = u^\mu \beta. \tag{2.25}$$

Idea to convert Eqs.(2.24) into covariant form is to use normalization condition of 4 -velocity $u_\mu u^\mu = 1$ and following relations for energy and particle densities

$$\begin{aligned} \varepsilon &= u_\mu u_\nu T^{\mu\nu}_{(0)}, \\ n &= u_\mu N^\mu_{(0)}. \end{aligned} \tag{2.26}$$

Let's first take a look at Euler's relation, which can be written in form

$$\begin{aligned} &\varepsilon\beta + p\beta - s + \alpha n = u_\mu(u_\nu \beta T^{\mu\nu}_{(0)} + p u^\mu \beta - s u^\mu + \alpha n u^\mu) \\ &= u_\mu(\beta_\nu T^{\mu\nu}_{(0)} + p\beta^\mu - S^\mu_{(0)} + \alpha N^\mu_{(0)}) = 0. \end{aligned} \tag{2.27}$$

Similarly for Gibbs-Duhem equation

$$\begin{aligned} &\beta dp - \beta s dT + n d\mu = \beta dp + (\varepsilon + p - \mu n) d\beta - \beta n d\mu = d(\beta p) - n d\alpha + \varepsilon d\beta \\ &= u_\mu(d(\beta^\mu p) - N^\mu_{(0)} d\alpha + d\beta_\nu T^{\mu\nu}_{(0)}) = 0 \end{aligned} \tag{2.28}$$

and for first law of thermodynamics

$$ds - \beta d\varepsilon + \alpha dn = u_\mu(dS^\mu_{(0)} - \beta_\nu dT^{\mu\nu}_{(0)} + \alpha dN^\mu_{(0)}) = 0. \tag{2.29}$$

It would now seem to reasonable to suggest that covariant thermodynamics are described by equations

$$\begin{aligned} &dS^\mu_{(0)} - \beta_\nu dT^{\mu\nu}_{(0)} + \alpha dN^\mu_{(0)} = 0, \\ &d(\beta^\mu p) - N^\mu_{(0)} d\alpha + d\beta_\nu T^{\mu\nu}_{(0)} = 0, \\ &\beta_\nu T^{\mu\nu}_{(0)} + p\beta^\mu - S^\mu_{(0)} + \alpha N^\mu_{(0)} = 0, \end{aligned} \tag{2.30}$$

but one needs to be careful that these equations don't contain more information than original equations. Fortunately, taking projection orthogonal to u^μ from Eqs. (2.30) leads to trivial $0 = 0$ equations so that all information is covered in equations parallel to u^μ which are in fact just Eqs. (2.27-2.29). That is why we can use covariant equations (2.30) instead of Eqs. (2.24). Now taking differential ∂_μ from first law of thermodynamics in Eq. (2.30) we obtain

$$\partial_\mu S^\mu_{(0)} = \beta_\nu \partial_\mu T^{\mu\nu}_{(0)} - \alpha \partial_\mu N^\mu_{(0)}. \tag{2.31}$$

When considering the ideal fluid, conservation of energy-momentum tensor and particle 4-current just states that right hand side of Eq.(2.31) vanishes and we are left with

$$\partial_\mu S^\mu_{(0)} = \frac{ds}{d\tau} + s\theta = 0. \tag{2.32}$$

This equation tells that the entropy is conserved for the ideal fluids.

2.3 Relativistic dissipative hydrodynamics

Even though ideal hydrodynamics is a reasonable approximation in some cases, it relies purely on assumption about exact local thermal equilibrium. However, there is always some dissipative effects that has to be taken account. These dissipative effects are caused by irreversible thermodynamic processes, like friction or heat exchange between fluid elements. Because of these dissipative effects, our system is no longer isotropic and it is no longer possible to write energy-momentum tensor or particle 4-current in rest frame in such a convenient form. Instead, we assume that we are still close to thermal equilibrium and add some dissipative terms to ideal energy-momentum tensor and particle 4-current

$$T^{\mu\nu} = T^{\mu\nu}_{(0)} + \delta T^{\mu\nu} = \varepsilon u^\mu u^\nu - \Delta^{\mu\nu} p + \delta T^{\mu\nu}, \tag{2.33}$$

$$N^\mu = N^\mu_{(0)} + \delta N^\mu = n u^\mu + \delta N^\mu. \tag{2.34}$$

Even though the system is not anymore in equilibrium, angular momentum is still conserved and dissipative energy momentum must be symmetric. As seen before, the ideal part is a symmetric, so also dissipative part must be symmetric in order to keep a sum of ideal and dissipative parts symmetric.

2.3.1 Decomposition of dissipative parts

Equations (2.33) and (2.34) are still not in a very useful form because dissipative parts contain parts that are parallel to 4-velocity and parts that are orthogonal to 4-velocity. That is why it is very useful to decompose dissipative parts to their irreducible components. For the particle 4-current this is pretty straightforward:

$$\delta N^\mu = \delta n u^\mu + n^\mu, \tag{2.35}$$

where δn is the off-equilibrium contribution to the particle density which is parallel to the 4-velocity. n^μ is usually called the particle diffusion 4-current and it is orthogonal to the 4-velocity,

$$u_\mu n^\mu = 0. \tag{2.36}$$

Taking contractions from the particle 4-current N^μ, it is also easy to see that

$$n + \delta n = u_\mu N^\mu, \tag{2.37}$$

$$n^\mu = \Delta^\mu_\nu N^\nu. \tag{2.38}$$

In case of energy-momentum tensor situation is a little bit more complicated. Now there is two different scalar parts, vector part and tensor part:

$$\delta T^{\mu\nu} = \delta\varepsilon u^\mu u^\nu - \delta p \Delta^{\mu\nu} + 2h^{(\mu} u^{\nu)} + \pi^{\mu\nu}, \tag{2.39}$$

where the symmetrization notation $A^{(\mu\nu)} = (A^{\mu\nu} + A^{\nu\mu})/2$ for the parentheses is used. The two scalars $\delta\varepsilon$ and δp are just off-equilibrium contributions to energy density and pressure. The vector term, h^μ, is the energy diffusion 4-current, which is orthogonal to the 4-velocity and the tensor $\pi^{\mu\nu}$ is shear stress tensor, which is symmetric and traceless part that is orthogonal to the 4-velocity. The properties of h^μ and $\pi^{\mu\nu}$ state that

$$u_\mu h^\mu = 0, \tag{2.40}$$

$$u_\mu \pi^{\mu\nu} = u_\nu \pi^{\mu\nu} = \pi^\mu_\mu = 0. \tag{2.41}$$

Using these properties we can write dissipative quantities in terms of energy-momentum tensor and equilibrium quantities

$$\begin{aligned} \varepsilon + \delta\varepsilon &= u_\mu u_\nu T^{\mu\nu}, \\ p + \delta p &= \frac{1}{3}\Delta_{\mu\nu} T^{\mu\nu}, \\ h^\mu &= \Delta^\mu_\nu T^{\nu\alpha} u_\alpha. \end{aligned} \tag{2.42}$$

Writing shear stress tensor $\pi^{\mu\nu}$ in terms of energy-momentum tensor is a little bit harder. For that purpose we define the double symmetric, traceless projection operator orthogonal to 4-velocity

$$\Delta^{\mu\nu\alpha\beta} = \frac{1}{2}\Big(\Delta^{\mu\alpha}\Delta^{\nu\beta} + \Delta^{\mu\beta}\Delta^{\nu\alpha}\Big) - \frac{1}{3}\Delta^{\mu\nu}\Delta^{\alpha\beta}. \tag{2.43}$$

This kind of projection operator satisfies following properties, which can be derived easily using properties of projection operator $\Delta^{\mu\nu}$

$$\begin{aligned}
&\Delta^{\mu\nu\alpha\beta} = \Delta^{\alpha\beta\mu\nu} = \Delta^{\beta\alpha\mu\nu}, \\
&\Delta^{\mu\nu}_{\lambda\sigma}\Delta^{\lambda\sigma}_{\alpha\beta} = \Delta^{\mu\nu}_{\alpha\beta}, \\
&u_\mu\Delta^{\mu\nu\alpha\beta} = g_{\mu\nu}\Delta^{\mu\nu\alpha\beta} = \Delta_{\mu\nu} = 0, \\
&\Delta^{\mu\nu}_{\mu\nu} = 5.
\end{aligned} \tag{2.44}$$

Contracting energy-momentum tensor with projection operator $\Delta^{\mu\nu}_{\alpha\beta}$ we obtain

$$\begin{aligned}
\Delta^{\mu\nu}_{\alpha\beta}T^{\alpha\beta} &= -(p+\delta p)\Delta^{\mu\nu} + \frac{1}{3}(p+\delta p)\Delta^{\mu\nu}\Delta^{\alpha}_{\alpha} + \Delta^{\mu}_{\alpha}\Delta^{\nu}_{\beta}\pi^{\alpha\beta} - \frac{1}{3}\Delta^{\mu\nu}\Delta_{\alpha\beta}\pi^{\alpha\beta} \\
&= \pi^{\mu\nu}.
\end{aligned} \tag{2.45}$$

2.3.2 Landau matching conditions

At this point the particle 4-current and energy-momentum tensor are in form of

$$\begin{aligned}
N^\mu &= (n+\delta n)u^\mu + n^\mu, \\
T^{\mu\nu} &= (\varepsilon+\delta\varepsilon)u^\mu u^\nu - (p+\delta p)\Delta^{\mu\nu} + 2h^{(\mu}u^{\nu)} + \pi^{\mu\nu}.
\end{aligned} \tag{2.46}$$

Left hand side of Eqs.(2.46) contain in total six scalars (n,δn,ε,$\delta\varepsilon$, p, δp), three vectors (u^μ, n^μ, h^μ) and one second rank tensor. All vectors contain only three independent components, because of their orthogonality. In addition, shear stress tensor is symmetric and traceless second rank tensor which is orthogonal to 4-velocity, so it contains five independent components. Adding all components together we end up with total 20 independent components. On the other hand energy-momentum tensor is symmetric so therefore N^μ and $T^{\mu\nu}$ together only have 14 independent components.

This problem is partially due to fact that in dissipative hydrodynamics the system cannot be considered to be in a local thermal equilibrium. This is why we have to construct artificial equilibrium state that is defined by thermodynamic variables $n_0, \varepsilon_0, p_0, s_0$,$\beta_0$ and α_0, where subscript 0 denotes that we are talking about artificial equilibrium state. This artificial equilibrium state has to be constructed so that the usual equilibrium relations for the thermodynamic quantities are valid. Because all the other thermodynamic quantities can be derived from energy and particle densities using equation of state or other thermodynamic relations, we can arbitrary choose

energy and particle densities for this artificial equilibrium state. This is usually done by so-called Landau matching conditions:

$$\varepsilon_0 = \varepsilon = u_\mu u_\nu T^{\mu\nu}, \tag{2.47}$$

$$n_0 = n = u_\mu N^\mu. \tag{2.48}$$

Using definitions of energy-momentum tensor and particle 4-current from Eqs.(2.46) we immediately obtain that

$$\delta\varepsilon = \delta n = 0. \tag{2.49}$$

Now the entropy density can be obtained using equation of state $s_0 = s_0(\varepsilon,n)$. All other thermodynamic variables are now defined from thermodynamic relations in Eqs.(2.24):

$$\begin{aligned} \alpha_0 &= \left(\frac{\partial s_0}{\partial n}\right)_\varepsilon, \\ \beta_0 &= \left(\frac{\partial s_0}{\partial \varepsilon}\right)_n, \\ p_0 &= T_0 s_0 + \mu_0 n - \varepsilon. \end{aligned} \tag{2.50}$$

Alternatively p_0 can be obtained directly from equation of state $p_0 = p_0(\varepsilon,n)$. On the other hand pressure p in Eq.(2.46) is quantity, which is similarly obtained from ε and n using equation of state. This means that we can replace p in Eq.(2.46) with p_0. Unlike for particle and energy densities off-equilibrium contribution for pressure δp is not zero. Instead, it can be thought as correction to the isotropic equilibrium pressure p_0. Usually δp is called bulk viscous pressure and it is denoted by Π. Using this notation Eqs.(2.46) can be written as

$$\begin{aligned} N^\mu &= n u^\mu + n^\mu, \\ T^{\mu\nu} &= \varepsilon u^\mu u^\nu - (p_0(\varepsilon,n) + \Pi)\Delta^{\mu\nu} + 2h^{(\mu}u^{\nu)} + \pi^{\mu\nu}, \end{aligned} \tag{2.51}$$

where $p_0(\varepsilon,n)$ is from now on denoted as p_0. Right hand side of Eqs.(2.51) still contains 17 independent components, which is still three more than in the left hand side. This is because 4-velocity in a dissipative hydrodynamics is not uniquely defined.

2.3.3 Fluid rest frame and equations of motion

In ideal hydrodynamics fluids rest frame was defined as a frame where there was no particle or energy flow. This kind of definition is no longer possible in dissipative hydrodynamics due to dissipative currents. This means that definition of velocity would be arbitrary. However, there are two particular definitions for 4-velocity that have clear physical meaning. First of all, there is the Eckart picture where 4-velocity is defined such a way that it is parallel with particle 4-current

$$u^\mu = \frac{N^\mu}{\sqrt{N_\alpha N^\alpha}}. \tag{2.52}$$

From this definition it directly follows that dissipative particle current n^μ vanishes

$$n^\mu = \Delta^\mu_\nu N^\mu = \Delta^\mu_\nu u^\nu \sqrt{N_\alpha N^\alpha} = 0. \tag{2.53}$$

When dealing with the Eckart picture and there is multiple particle types, the 4-velocity must be defined by choosing only one particle type. Another way to define 4-velocity is so-called Landau picture. In Landau picture 4-velocity is defined such a way that it follows energy current

$$u^\mu = \frac{T^{\mu\nu}u_\nu}{\sqrt{u^\lambda T_{\lambda\alpha}T^{\alpha\beta}u_\beta}}. \tag{2.54}$$

When defining 4-velocity this way energy diffusion current h^μ vanishes:

$$h^\mu = \Delta^\mu_\nu T^{\nu\sigma}u_\sigma = \Delta^\mu_\nu u^\nu \sqrt{u^\lambda T_{\lambda\alpha}T^{\alpha\beta}u_\beta} = 0. \tag{2.55}$$

Now we see that defining 4-velocity using either Eckart or Landau definition causes one of the dissipative currents to vanish, which means that we got rid of 3 extra components in Eq.(2.51). Both of these definitions for 4-velocity are usable, but from now on we only use Landau's picture. In Landau picture Eqs.(2.51) take more simplified form

$$\begin{aligned} N^\mu &= nu^\mu + n^\mu, \\ T^{\mu\nu} &= \varepsilon u^\mu u^\nu - (p_0 + \Pi)\Delta^{\mu\nu} + \pi^{\mu\nu}. \end{aligned} \tag{2.56}$$

Lets now write equations of motion for dissipative hydrodynamics to similar form than for ideal fluid in section 2.1. Ideal parts of these equations are identical to Eqs.(2.16) and only dissipative parts have to be calculated:

$$\begin{aligned} u_\nu \partial_\mu(-\Delta^{\mu\nu}\Pi + \pi^{\mu\nu}) &= u_\nu \Pi \partial_\mu(u^\mu u^\nu) + \partial_\mu(u_\nu \pi^{\mu\nu}) - \pi^{\mu\nu}\partial_\mu u_\mu \\ &= \Pi\theta - \pi^{\alpha\beta}\Delta^{\mu\nu}_{\alpha\beta}\partial_\mu u_\mu = \Pi\theta - \pi^{\mu\nu}\sigma_{\mu\nu}, \end{aligned} \tag{2.57}$$

where we introduced shear tensor $\sigma^{\mu\nu}$

$$\sigma^{\mu\nu} = \Delta^{\mu\nu}_{\alpha\beta}\partial^{\alpha}u^{\beta} = \frac{1}{2}(\nabla^{\mu}u^{\nu} + \nabla^{\nu}u^{\mu}) - \frac{1}{3}\Delta^{\mu\nu}\theta. \tag{2.58}$$

In addition

$$\Delta^{\mu}_{\alpha}\partial_{\beta}(-\Delta^{\alpha\beta}\Pi + \pi^{\alpha\beta}) = \Pi\frac{du^{\mu}}{d\tau} - \nabla^{\mu}\Pi + \Delta^{\mu}_{\alpha}\partial_{\beta}\pi^{\alpha\beta}. \tag{2.59}$$

Now using Eqs.(2.16),(2.57) and (2.59) we can write the equations of motion for dissipative hydrodynamics:

$$\begin{aligned} u_{\nu}\partial_{\mu}T^{\mu\nu} &= \frac{d\varepsilon}{d\tau} + (\varepsilon + p + \Pi)\theta - \pi^{\mu\nu}\sigma_{\mu\nu} = 0, \\ \Delta^{\mu}_{\alpha}\partial_{\beta}T^{\alpha\beta} &= (\varepsilon + p + \Pi)\frac{du^{\mu}}{d\tau} - \nabla^{\mu}(p + \Pi) + \Delta^{\mu}_{\alpha}\partial_{\beta}\pi^{\alpha\beta} = 0, \\ \partial_{\nu}N^{\mu} &= \frac{dn}{d\tau} + n\theta + \partial_{\mu}n^{\mu} = 0. \end{aligned} \tag{2.60}$$

In ideal fluid case these equations of motion were enough to solve evolution of the fluid, because there were only 5 independent variables. However, in dissipative hydrodynamics there is in total 14 independent variables, so we need 9 more constraints in order to get complete equations of dissipative hydrodynamics. Turns out that these missing constraints are ones which define dissipative quantities Π, n^{μ} and $\pi^{\mu\nu}$ in terms of equilibrium quantities.

2.3.4 Navier-Stokes equations

One way to get relations for the dissipative quantities Π, n^{μ} and $\pi^{\mu\nu}$ is to make use of a second law of thermodynamics. In ideal case entropy was conserved. This is generally no longer true when there are dissipative currents. Entropy conservation law for ideal hydrodynamics was derived from Eq.(2.31)

$$\partial_{\mu}S^{\mu}_{(0)} = \beta_0 u_{\nu}\partial_{\mu}T^{\mu\nu}_{(0)} - \alpha_0\partial_{\mu}N^{\mu}_{(0)}. \tag{2.61}$$

Difference compared to ideal fluid case is that now there are no conservation laws for equilibrium parts of energy-momentum tensor and particle 4-current. Instead, only total energy-momentum and particle number are conserved so,

$$\begin{aligned} \partial_{\mu}N^{\mu} &= \partial_{\mu}N^{\mu}_{(0)} + \partial_{\mu}n^{\mu} = 0, \\ \partial_{\mu}T^{\mu\nu} &= \partial_{\mu}T^{\mu\nu}_{(0)} + \partial_{\mu}(\pi^{\mu\nu} - \Delta^{\mu\nu}\Pi) = 0. \end{aligned} \tag{2.62}$$

Using these equations together with Eq.(2.57) it is possible to write Eq.(2.61) in form

$$\begin{aligned}\partial_\mu S^\mu_{(0)} &= \beta_0 u_\nu \partial_\mu(\Delta^{\mu\nu}\Pi - \pi^{\mu\nu}) + \alpha_0 \partial_\mu n^\mu \\ &= \beta_0(\pi^{\mu\nu}\sigma_{\mu\nu} - \Pi\theta) + \alpha_0 \partial_\mu n^\mu.\end{aligned} \tag{2.63}$$

It is convenient to write Eq.(2.63) in a such a form that it doesn't contain any derivatives of dissipative quantities on the right hand side. This is done by writing

$$\alpha_0 \partial_\mu n^\mu = \partial_\mu(\alpha_0 n^\mu) - n^\mu \nabla_\mu \alpha_0$$

and rearranging terms in Eq.(2.63) to obtain

$$\partial_\mu(S^\mu_{(0)} - \alpha_0 n^\mu) = \beta_0 \pi^{\mu\nu}\sigma_{\mu\nu} - \beta_0 \Pi\theta - n^\mu \nabla_\mu \alpha_0. \tag{2.64}$$

The left hand side of this equation now contains divergences of the ideal entropy 4-current and some dissipative current, where the right hand side only contains terms with dissipative currents. This would suggest that the left hand side of Eq.(2.64) is the divergence of the total entropy 4-current S^μ, i.e.

$$S^\mu = S^\mu_{(0)} - \alpha_0 n^\mu, \tag{2.65}$$

and the right hand side could be identified as a source of entropy production. This kind of choice of entropy 4-current is not necessarily the correct one, but it is one which leads to the relativistic Navier-Stokes equations. Now that the entropy 4-current S^μ is known we can make use of the second law of thermodynamics which requires that entropy production is always positive. Applying this to Eq.(2.65) leads to

$$\partial_\mu S^\mu = \beta_0 \pi^{\mu\nu}\sigma_{\mu\nu} - \beta_0 \Pi\theta - n^\mu \nabla_\mu \alpha_0 \geq 0. \tag{2.66}$$

In order to satisfy this condition for all different configurations it is necessary to require that each individual term must be positive, which is achieved by setting a linear relation between dissipative currents and quantities $\sigma^{\mu\nu}, \theta$ and $\nabla^\mu \alpha_0$:

$$\Pi = -\zeta\theta, \tag{2.67}$$

$$n^\mu = \kappa \nabla^\mu \alpha_0, \tag{2.68}$$

$$\pi^{\mu\nu} = 2\eta\sigma^{\mu\nu}. \tag{2.69}$$

Here proportionally coefficients ζ, η and κ are called bulk viscosity, shear viscosity and heat conductivity, respectively. It is important to notice that $n^\mu n_\mu$ is negative. This can be shown by going to fluids rest frame where $u^\mu = (1,0,0,0)$ so that

$$u_\mu n^\mu = n^0 = 0, \tag{2.70}$$

$$n^\mu n_\mu = (n^0)^2 - \sum_{i=1}^{3}(n^i)^2 = -\sum_{i=1}^{3}(n^i)^2 \leq 0. \tag{2.71}$$

Because scalar quantities are Lorentz invariant $n^\mu n_\mu$ is also negative in general frame. In addition $\pi^{\mu\nu}\pi_{\mu\nu}$ is positive, which can be shown by going to frame where $\pi^{\mu\nu}$ is diagonal. This kind of frame must exist, because $\pi^{\mu\nu}$ is symmetric. In this kind of frame

$$\pi^{\mu\nu}\pi_{\mu\nu} = g_{\alpha\mu}g_{\beta\nu}\pi^{\mu\nu}\pi^{\alpha\beta} = \sum_{\mu=0}^{4}(\pi^{\mu\mu})^2 \geq 0. \tag{2.72}$$

Again this must also hold in general frame so $\pi^{\mu\nu}\pi_{\mu\nu}$ is allways positive. Now we can see that entropy production can be written in terms of dissipative quantities as

$$\partial_\mu S^\mu = \frac{\beta_0}{\zeta}\Pi^2 - \frac{1}{\kappa}n^\mu n_\mu + \frac{\beta_0}{2\eta}\pi^{\mu\nu}\pi_{\mu\nu}, \tag{2.73}$$

which is indeed positive when the proportionally coefficients ζ,κ and η are all positive.

From Eqs.(2.67)-(2.69), one can also deduce physical effects of each dissipative quantity. The bulk viscous pressure was correction to the equilibrium pressure and it is proportional for expansion rate θ. This would indicate that the bulk viscosity reduces pressure and slows down expansion. The particle diffusion current is proportional to the temperature gradients so it would seem reasonable to assume that it would act as a particle diffusion. The shear stress tensor is proportional to shear tensor $\sigma^{\mu\nu}$ which indicates that the shear viscosity drives system towards more isotropic state.

The relativistic Navier-Stokes equations are now recovered by substituting Eqs.(2.67),(2.68),(2.69) into the equations of motion (2.60):

$$\begin{aligned}
&\frac{d\varepsilon}{d\tau} + (\varepsilon + p - \zeta\theta)\theta - 2\eta\sigma^{\mu\nu}\sigma_{\mu\nu} = 0,\\
&(\varepsilon + p - \zeta\theta)\frac{du^\mu}{d\tau} - \nabla^\mu(p - \zeta\theta) + 2\Delta^\mu_\alpha\partial_\beta(\eta\sigma^{\alpha\beta}) = 0,\\
&\frac{dn}{d\tau} + n\theta + \partial_\mu(\kappa\nabla^\mu\alpha_0) = 0.
\end{aligned} \tag{2.74}$$

These equations were first derived by Landau and Lifshitz in 1959, and they were one of the first proposals for the relativistic dissipative fluid dynamics [21]. However, these equations have a major problem. The relativistic Navier-Stokes theory is unstable, which means that even small perturbations in hydrostatic equilibrium grow exponentially [22]–[24]. Reason why this kind of instability exist is that relativistic Navier-Stokes equations are parabolic. Because of this, changes in fluid properties will immediately effect on dissipative currents. This kind of infinite signal propagation speed is forbidden in relativistic case where the information cannot travel faster than the speed of light.

2.3.5 Second-order hydrodynamics

Because relativistic Navier-Stokes theory ended up being acausal it seems reasonable to assume that definition for S^μ in Eq.(2.65) is not correct. Instead, we need more general expression for the entropy 4-current. In this thesis we follow Israel and Stewart approach and expand entropy 4-current in terms of powers of the dissipative currents all the way up to second order [25],

$$\begin{aligned} S^\mu &= S^\mu_{(0)} - \alpha_0 n^\mu - \frac{1}{2}u^\mu(\delta_0\Pi^2 - \delta_1 n^\alpha n_\alpha + \delta_2\pi^{\alpha\beta}\pi_{\alpha\beta}) - \gamma_0\Pi n^\mu - \gamma_1\pi^\mu_\nu n^\nu \\ &= S^\mu_{(0)} - \alpha_0 n^\mu + Q^\mu, \end{aligned} \tag{2.75}$$

where we introduced expansion coefficients $\delta_0, \delta_1, \delta_2, \gamma_0$ and γ_1 and defined

$$Q^\mu = -\frac{1}{2}u^\mu(\delta_0\Pi^2 - \delta_1 n^\alpha n_\alpha + \delta_2\pi^{\alpha\beta}\pi_{\alpha\beta}) - \gamma_0\Pi n^\mu - \gamma_1\pi^\mu_\nu n^\nu. \tag{2.76}$$

The expansion coefficients cannot be directly calculated using thermodynamics. Instead, they must be calculated from microscopic principles which are described by kinetic theory. How this is practically done is discussed in more detail in section x. From Eq.(2.75) we can see that the relativistic Navier-Stokes theory is obtained by setting $Q^\mu = 0$. It is also interesting to notice that entropy density in fluids rest frame s is no longer equivalent to artificial equilibrium entropy density $s_0(n,\varepsilon)$, i.e.

$$s = u_\mu S^\mu = u_\mu S^\mu_0 + u_\mu Q^\mu = s_0 + u_\mu Q^\mu \neq s_0. \tag{2.77}$$

Now like in case of the relativistic Navier-Stokes equation we calculate divergence of entropy 4-current which is obtained by adding $\partial_\mu Q^\mu$ to the both sides of Eq.(2.64),

$$\partial_\mu S^\mu = \beta_0\pi^{\mu\nu}\sigma_{\mu\nu} - \beta_0\Pi\theta - n^\mu\nabla_\mu\alpha_0 + \partial_\mu Q^\mu. \tag{2.78}$$

Straight forward calculation shows that $\partial_\mu Q^\mu$ can be written in a form

$$\begin{aligned}\partial_\mu Q^\mu &= \Big(u_\mu \frac{d}{d\tau} + \nabla_\mu\Big)\Big(- \frac{1}{2}u^\mu(\delta_0\Pi^2 - \delta_1 n^\alpha n_\alpha + \delta_2\pi^{\alpha\beta}\pi_{\alpha\beta}) - \gamma_0\Pi n^\mu - \gamma_1\pi^\mu_\nu n^\nu\Big)\\ &= -\frac{1}{2}\Big(\dot\delta_0\Pi^2 + 2\delta_0\Pi\dot\Pi - \dot\delta_1 n^\alpha n_\alpha - 2\delta_1 n_\alpha\dot n^\alpha + \dot\delta_2\pi^{\alpha\beta}\pi_{\alpha\beta} + 2\delta_2\pi_{\mu\nu}\dot\pi^{\mu\nu}\Big)\\ &- \frac{1}{2}\Big(\delta_0\Pi^2 - \delta_1 n^\alpha n_\alpha + \delta_2\pi^{\alpha\beta}\pi_{\alpha\beta}\Big)\theta - (\Pi\nabla_\mu\gamma_0 + \gamma_0\nabla_\mu\Pi)n^\mu - \gamma_0\Pi\nabla_\mu n^\mu\\ &- n^\nu\pi_{\mu\nu}\nabla^\mu\gamma_1 - \gamma_1\pi_{\mu\nu}\nabla^\mu n^\nu - \gamma_1 n^\nu\nabla^\mu\pi_{\mu\nu}.\end{aligned} \tag{2.79}$$

Now substituting Eq.(2.79) back to Eq.(2.64) we obtain

$$\begin{aligned}\partial_\mu S^\mu &= \beta_0\Pi\Big(- \theta - \frac{1}{2\beta_0}\dot\delta_0\Pi - \frac{\delta_0}{\beta}\dot\Pi - \frac{\delta_0}{2\beta_0}\Pi\theta - \frac{\gamma_0}{2\beta_0}n_\mu\nabla^\mu\Pi - \frac{\gamma_0}{\beta_0}\nabla^\mu n_\mu\Big)\\ &+ n_\mu\Big(- \nabla^\mu\alpha + \frac{n^\mu}{2}\dot\delta_1 + \delta_1\dot n^\mu + \frac{\delta_1}{2}n^\mu\theta - \frac{\Pi}{2}\nabla^\mu\gamma_0 - \gamma_0\nabla^\mu\Pi - \frac{\pi^{\mu\nu}}{2}\nabla_\nu\gamma_1 - \gamma_1\nabla_\nu\pi^{\mu\nu}\Big)\\ &+ \beta_0\pi_{\mu\nu}\Big(\sigma^{\mu\nu} - \frac{\pi^{\mu\nu}}{2\beta_0}\dot\delta_2 - \frac{\delta_2}{\beta_0}\dot\pi^{\mu\nu} - \frac{\delta_2}{2\beta_0}\pi^{\mu\nu}\theta - \frac{n^\nu}{2\beta_0}\nabla^\mu\gamma_1 - \gamma_1\pi\nabla^\mu n^\nu\Big).\end{aligned} \tag{2.80}$$

As in the case of relativistic Navier-Stokes theory, the second law of thermodynamics requires that entropy production must be positive which is generally satisfied only if it can be written in a form

$$\partial_\mu S^\mu = \beta_0\varpi_\Pi\Pi^2 - \varpi_n n^\mu n_\mu + \beta_0\varpi_\pi\pi^{\mu\nu}\pi_{\mu\nu}, \tag{2.81}$$

where ϖ_Π, ϖ_n and ϖ_π are positive constants. This constraint together with Eq.(2.80) leads to following dynamical equations for dissipative currents

$$\frac{\delta_0}{\beta_0}\dot\Pi + \varpi_\Pi\Pi = -\theta - \frac{\delta_0}{2\beta_0}\Pi\theta - \frac{\gamma_0}{2\beta_0}n_\mu\nabla^\mu\Pi - \frac{\gamma_0}{\beta_0}\nabla^\mu n_\mu, \tag{2.82}$$

$$\delta_1\dot n^\mu + \varpi_n n^\mu = \nabla^\mu\alpha - \frac{\delta_1}{2}n^\mu\theta + \frac{\Pi}{2}\nabla^\mu\gamma_0 + \gamma_0\nabla^\mu\Pi + \frac{\pi^{\mu\nu}}{2}\nabla_\nu\gamma_1 + \gamma_1\nabla_\nu\pi^{\mu\nu}, \tag{2.83}$$

$$\frac{\delta_2}{\beta_0}\dot\pi^{\mu\nu} + \varpi_\pi\pi^{\mu\nu} = \sigma^{\mu\nu} - \frac{\delta_2}{2\beta_0}\pi^{\mu\nu}\theta - \frac{n^\nu}{2\beta_0}\nabla^\mu\gamma_1 - \gamma_1\pi\nabla^\mu n^\nu, \tag{2.84}$$

where we have neglected couple of higher order terms. These equations are relaxation-type equations and they are usually called Israel-Stewart equations. In general relaxation equations for quantity A are form of

$$\tau_A\dot A + A = f, \tag{2.85}$$

where τ_A is relaxation time and f contains all source terms. In absence of the source terms solution for Eq.(2.85) vanishes exponentially i.e.

$$A = A_0 e^{-t/\tau_A}, \tag{2.86}$$

where A_0 is initial value of A. In case of dissipative currents all source terms include some gradients. Now, unlike in relativistic Navier-Stokes theory, dissipative currents don't immediately react to the gradients. In fact dissipative currents relax to the value of corresponding source terms on relaxation time timescales. This is why relaxation type equations have finite signal propagation speed and Eqs.(2.82),(2.83) and (2.84) are causal and stable equations for relativistic dissipative hydrodynamics. Writing Eqs.(2.82),(2.83) and (2.84) to the relaxation equation form and comparing coefficient of terms to Eqs.(2.67),(2.68), (2.69) and (2.85) we can identify viscosity, diffusion and relaxation time coefficients

$$\zeta = \frac{2\beta_0}{2\beta_0 \varpi_\Pi}, \tag{2.87}$$

$$\kappa = \frac{2}{2\varpi_n}, \tag{2.88}$$

$$\eta = \frac{\beta_0}{2\beta_0 \varpi_\pi}, \tag{2.89}$$

$$\tau_\Pi = \frac{\delta_0}{\beta_0}\zeta, \tag{2.90}$$

$$\tau_n = \delta_1 \kappa, \tag{2.91}$$

$$\tau_\pi = \frac{2\delta_2}{\beta_0}\eta. \tag{2.92}$$

It is still important to remember that all these constant are complicated functions of thermodynamic quantities and we still haven't derived exact form of these coefficients, but they must be derived from kinetic theory. In addition, when deriving equation for dissipative currents from kinetic theory there will be some additional second order terms added to the right hand side of Eqs.(2.82), (2.83) and (2.84).

2.4 Applicability of hydrodynamics

Validity of hydrodynamics is important question that has to be addressed, because it is not always so clear if conditions for local thermal equilibrium and infinitesimal size of the fluid element are satisfied. Most direct way to find out how well theory of relativistic fluids works is to compare its solutions to the solutions of relativistic Boltzmann equation which describes evolution of particle distribution functions. However, this kind of method is often very tedious. Instead, applicability of hydrodynamics is often quantified by a couple of parameters:

- The Knudsen number $Kn \equiv l_{micr}/L_{macr}$ is the ratio between some microscopic and macroscopic scales. Typically in relativistic case relaxation time is used as a microscopic scale and inverse of expansion rate θ^{-1} as a macroscopic one.

- The inverse Reynolds number R^{-1} which describes ratio of dissipative quantity compared to similar equilibrium quantity. In relativistic case we had three different dissipative quantities so it is possible to define three different Reynolds numbers:

$$R_{\Pi}^{-1} \equiv \frac{|\Pi|}{p_0}, R_n^{-1} \equiv \frac{\sqrt{|n^\mu n_\mu|}}{n_0}, \; R_\pi^{-1} \equiv \frac{\sqrt{|\pi^{\mu\nu}\pi_{\mu\nu}|}}{p_0}.$$

As discussed earlier in this section applicability of hydrodynamics requires that difference between microscopic and macroscopic scales is large enough. This condition immediately tells that we should have $Kn \ll 1$. In addition, when we expanded entropy 4-current in terms of dissipative current in section 2.3.5 we assumed that dissipative currents are small enough that we don't have to take account terms higher than first order in dissipative currents. This condition corresponds to requirement that $R^{-1} \ll 1$.

In relativistic heavy-ion collisions using hydrodynamics is produced some excellent results. Nevertheless, when looking at the Knudsen and Reynolds numbers applicability of hydrodynamics seems to strongly depend on viscosity parameterization and size of the collision system [26], [27].

3 Relativistic kinetic theory

When considering fluid or any many particle system there are usually two different way to approach the subject. It is possible to consider the overall macroscopic phenomena, which was done is section 2. Another way to tackle this kind of problems is to consider the microscopic phenomena, where properties of single particle are of interest. Kinetic theory takes a look at the microscopic world and in a way allows to connect these microscopic and macroscopic worlds. Instead of trying to describe behavior of every single particle in the system, kinetic theory relies on statistics of the system. Statistical tool used to describe whole system is the single particle phase-space distribution function f_k, which describes how particles are distributed in position and momentum spaces.

3.1 Macroscopic variables in relativistic kinetic theory

Lets start with considering system of particles with each having rest mass m and 4-momentum $k^\mu = (k^0,\vec{k})$, where $\vec{k}$ is the momentum vector and $k^0 = \sqrt{p^2 + m^2}$ is the relativistic energy of the particle. Single particle phase-space distribution function f_k is defined such a way that the total number of particles in the system is given by

$$N \equiv \int \frac{d^3x\, d^3k}{(2\pi)^3}\, g f_k(k,x), \tag{3.1}$$

where g is number of internal degrees of freedom. From this equation it is obvious that particle density is defined as

$$n(x) = \frac{dN}{d^3x} = \int \frac{d^3k}{(2\pi)^3}\, g f_k(k,x). \tag{3.2}$$

and the particle flux along i-axis as

$$N^i = \int \frac{d^3k}{(2\pi)^3}\, g v^i\, f_k(k,x), \tag{3.3}$$

where $v^i = k^i/k^0$ is the particle velocity along i-axis. Now it is possible to use Eqs.(3.2) and (3.3) in order to write particle 4-current N^μ in covariant form

$$N^\mu = \int dK\, k^\mu\, f_k(k,x), \tag{3.4}$$

where $dK = gd^3k/[(2\pi)^3 k^0]$ is the Lorenz-invariant momentum-space volume. Similarly, using the definitions of energy momentum tensors components introduced in section 2.1 and the fact that k^0 is energy of the single particle it is possible to write energy-momentum tensor in terms of particle distribution function,

$$T^{\mu\nu} = \int dK\, k^\mu k^\nu\, f_k(k,x). \tag{3.5}$$

To make notations look cleaner we introduce following notation for the averages:

$$\langle \cdots \rangle = \int dK\, \cdots\, f_k. \tag{3.6}$$

Using this notation particle 4-current and energy-momentum tensor can be written in simple looking form

$$N^\mu = \langle k^\mu \rangle, \quad T^{\mu\nu} = \langle k^\mu k^\nu \rangle \tag{3.7}$$

It is also important to note that throughout this section we are working in Landau picture, where 4-velocity, particle 4-current and energy-momentum tensor are defined as in Eqs.(2.54) and (2.56). In order to write equilibrium and dissipative quantities n,ε, p_0,Π, n^μ and $\pi^{\mu\nu}$ in terms of distribution function f_k we first must divide 4-momentum into parts parallel and orthogonal to u^μ:

$$k^\mu = E_k u^\mu + k^{\langle\mu\rangle}, \tag{3.8}$$

where $E_k = u_\mu k^\mu$ is the projection of 4-momentum along the 4-velocity. We also used notation $A^{\langle\mu\rangle} = \Delta^\mu_\nu A^\nu$ for the orthogonal part. Now with use of Eq.(3.8) we can modify Eqs.(3.7) into form

$$N^\mu = \langle E_k \rangle u^\mu + \langle k^{\langle\mu\rangle} \rangle, \tag{3.9}$$

$$\begin{aligned} T^{\mu\nu} &= \langle E_k^2 \rangle + 2\langle E_k k^{(\langle\mu\rangle} \rangle u^{\nu)} + \langle k^{\langle\mu\rangle} k^{\langle\nu\rangle} \rangle \\ &= \langle E_k^2 \rangle + 2\langle E_k k^{(\langle\mu\rangle} \rangle u^{\nu)} + \langle k^{\langle\mu} k^{\nu\rangle} \rangle + \frac{1}{3}\Delta^{\mu\nu} \langle \Delta_{\alpha\beta} k^\alpha k^\beta \rangle, \end{aligned} \tag{3.10}$$

where $A^{\langle\mu\nu\rangle} = \Delta^{\mu\nu}_{\alpha\beta} A^{\alpha\beta}$. We also used the fact that

$$\begin{aligned} k^{\langle\mu} k^{\nu\rangle} &= \Big(\frac{1}{2}\Big(\Delta^\mu_\alpha \Delta^\nu_\beta + \Delta^\mu_\beta \Delta^\nu_\alpha\Big) - \frac{1}{3}\Delta^{\mu\nu}\Delta_{\alpha\beta}\Big) k^\alpha k^\beta \\ &= k^{\langle\mu\rangle} k^{\langle\nu\rangle} - \frac{1}{3}\Delta^{\mu\nu}(\Delta_{\alpha\beta} k^\alpha k^\beta). \end{aligned} \tag{3.11}$$

This relation will be used extensively throughout this section. Comparing Eqs.(3.9) and (3.10) to definition of particle 4-current and energy-momentum tensor from Eqs.(2.56) we can now identify macroscopic variables in kinetic theory:

$$\begin{aligned} &n = \langle E_k \rangle, \quad \varepsilon = \langle E_k^2 \rangle, \quad p_0 + \Pi = -\frac{1}{3}\langle \Delta_{\alpha\beta} k^\alpha k^\beta \rangle, \\ &n^\mu = \langle k^{\langle \mu \rangle} \rangle, \quad \pi^{\mu\nu} = \langle k^{\langle \mu} k^{\nu \rangle} \rangle, \quad h^\mu = \langle E_k k^{\langle \mu \rangle} \rangle = 0. \end{aligned} \tag{3.12}$$

When the system is in a local thermal equilibrium, it can be shown from the statistical physics that single-particle distribution function f_{0k} gets form [20]

$$f_{0k} = \left(e^{\beta_0 E_k - \alpha_0} + a \right)^{-1}, \tag{3.13}$$

where $a = 1$ corresponds to a Fermi-Dirac statistics for fermions, $a = -1$ corresponds to Bose-Einstein statistics for bosons and $a = 0$ corresponds to Maxwell-Boltzmann statistics for a classical particles. Usually f_{0k} is called local equilibrium distribution function. From previous section we also remember that in local thermal equilibrium all dissipative quantities vanish, and we are left with ideal fluid case. In addition when system is out off equilibrium Landau matching conditions, which were introduced in section 2.3.2, state that our artificial equilibrium state is defined by

$$n = n_0 = \langle E_k \rangle_0, \ \varepsilon = \varepsilon_0 = \langle E_k^2 \rangle_0 \tag{3.14}$$

where we introduced notation

$$\langle \cdots \rangle_0 = \int dK \ \cdots \ f_{0k}. \tag{3.15}$$

Now it is possible to distinguish the pressure p_0 and bulk viscous pressure from each other. This is done by dividing particle distribution function into its equilibrium and off equilibrium parts as $f_k = f_{0k} + \delta f_k$, so that

$$p_0 = -\frac{1}{3}\langle \Delta_{\alpha\beta} k^\alpha k^\beta \rangle_0, \ \ \Pi = -\frac{1}{3}\langle \Delta_{\alpha\beta} k^\alpha k^\beta \rangle_\delta, \tag{3.16}$$

where

$$\langle \cdots \rangle_\delta = \langle \cdots \rangle - \langle \cdots \rangle_0. \tag{3.17}$$

3.2 Expansion of the single-particle distribution function and orthogonal momentum basis

In dissipative hydrodynamics usual assumption is that system is reasonably close to thermal equilibrium. This is why it is convenient expand distribution function f_k around equilibrium distribution f_{0k}:

$$f_k = f_{0k} + \delta f_k, \tag{3.18}$$

where δf_k is correction to the equilibrium distribution, which is usually written as

$$f_k = f_{0k}\tilde{f}_{0k}\phi_k, \tag{3.19}$$

where $\tilde{f}_{0k} = 1 - a f_{0k}$ and ϕ_k contains information about the off-equilibrium correction to the equilibrium distribution. Next we have to expand ϕ_k in terms of a complete set tensors formed by k^μ and E_k. Most natural choice would be to choose momentum basis as:

$$1, k^\mu, k^\mu k^\nu, k^\mu k^\nu k^\lambda, ... \tag{3.20}$$

This was in fact the basis which was used by Israel and Stewart when they derived equations of motion for dissipative currents [28]. However, this basic is not orthogonal, which means that the exact form of expansion coefficients cannot be obtained once the expansion is truncated. In context this thesis this would not be a problem but it is more illustrative to work on orthogonal momentum basis,

$$1, k^{\langle\mu\rangle}, k^{\langle\mu}k^{\nu\rangle}, k^{\langle\mu}k^\nu k^{\lambda\rangle}, ... \tag{3.21}$$

which is used in Refs.[18], [29]. In sake of convenience we also introduced notation for angled brackets

$$A^{\langle\mu_1\cdots\mu_m\rangle} = \Delta^{\mu_1\cdots\mu_m}_{\nu_1\cdots\nu_m} A^{\nu_1\cdots\nu_m}, \tag{3.22}$$

where $\Delta^{\mu_1\cdots\mu_m}_{\nu_1\cdots\nu_m}$ are symmetric, traceless (for $m > 1$) projection operators orthogonal to a 4-velocity. These projection operators are defined using projection $\Delta^{\mu\nu}$ as [30]

$$\Delta^{\mu_1\cdots\mu_\ell\nu_1\cdots\nu_\ell} = \sum_{k=0}^{[\ell/2]} C(\ell,k)\Phi^{\mu_1\cdots\mu_\ell\nu_1\cdots\nu_\ell}_{(\ell k)}, \tag{3.23}$$

where in the summation $[\ell/2]$ denotes the largest integer smaller that $\ell/2$. In addition coefficients $C(\ell,k)$ and tensors $\Phi^{\mu_1\cdots\mu_m\nu_1\cdots\nu_m}_{(\ell k)}$ are defined as

$$C(\ell,k) = (-1)^k \frac{(\ell!)^2}{(2\ell)!}\frac{(2\ell-2k)!}{k!(\ell-k)!(\ell-2k)!}, \tag{3.24}$$

$$\Phi^{\mu_1\cdots\mu_\ell\nu_1\cdots\nu_\ell}_{(\ell k)} = (\ell{-}2k)!\Big(\frac{2^k k!}{\ell!}\Big)^2 \sum_{\mathcal{P}_\mu,\mathcal{P}_\nu} \Delta^{\mu_1\mu_2}\cdots\Delta^{\mu_{2k-1}\mu_{2k}}\Delta^{\nu_1\nu_2}\cdots\Delta^{\nu_{2k-1}\nu_{2k}}\Delta^{\mu_{2k+1}\nu_{2k+1}}\cdots\Delta^{\mu_\ell\nu_\ell}. \tag{3.25}$$

Summation in Eq.(3.25) runs over all permutations of indices μ and ν in such a way that we don't permute indices μ with ν. Construction of these projection operators is done in a such a way that they satisfy following relations when $m > 1$

$$\begin{aligned}
&\Delta^{\mu_1\cdots\mu_\ell}_{\nu_1\cdots\nu_\ell} = \Delta^{(\mu_1\cdots\mu_\ell)}_{(\nu_1\cdots\nu_\ell)},\\
&\Delta^{\mu_1\cdots\mu_\ell}_{\nu_1\cdots\nu_\ell} g_{\mu_i\mu_j} = \Delta^{\mu_1\cdots\mu_\ell}_{\nu_1\cdots\nu_\ell} g^{\nu_i\nu_j} = 0\\
&\Delta^{\mu_1\cdots\mu_\ell}_{\mu_1\cdots\mu_\ell} = 2\ell+1.
\end{aligned} \tag{3.26}$$

As mentioned earlier, basis tensors (3.21) are orthogonal so they obey orthogonality condition,

$$\int dK F_k k^{\langle\mu_1}\cdots k^{\mu_m\rangle} k_{\langle\nu_1}\cdots k_{\nu_n\rangle} = \frac{m!\delta_{mn}}{(2m+1)!!}\Delta^{\mu_1\cdots\mu_m}_{\nu_1\cdots\nu_m}\int dK F_k(\Delta_{\alpha\beta}k^\alpha k^\beta)^m, \tag{3.27}$$

where δ_{mn} is the Kronecker-delta and F_k is an arbitrary function of E_k. Proof of this orthogonality condition is shown in Ref.[31]. Now ϕ_k can be expanded in orthogonal momentum basis (3.21) as

$$\phi_k = \sum_{\ell=0}^{\infty} \lambda_k^{\langle\mu_1\cdots\mu_\ell\rangle} k_{\langle\mu_1}\cdots k_{\mu_\ell\rangle}, \tag{3.28}$$

where the expansion coefficients $\lambda_k^{\langle\mu_1\cdots\mu_\ell\rangle}$ are functions with E_k dependence. In principle, we could expand coefficients $\lambda_k^{\langle\mu_1\cdots\mu_\ell\rangle}$ in terms of orthogonal polynomials of E_k. However, this in not done in here, but we settle to expand $\lambda_k^{\langle\mu_1\cdots\mu_\ell\rangle}$ in the powers of E_k:

$$\lambda_k^{\langle\mu_1\cdots\mu_\ell\rangle} = \sum_{n=0}^{N_\ell} c_n^{\langle\mu_1\cdots\mu_\ell\rangle} E_k^n, \tag{3.29}$$

where N_ℓ is truncation order of power series. In theory parameter N_ℓ should be infinite, but in practice dealing with this kind of infinite series is not possible. Now expansion coefficients can be calculated by matching dissipative currents Π,n^μ,h^μ and $\pi^{\mu\nu}$ with their kinetic definitions in Eqs.(3.12) and (3.16). This is in fact done in case of 14-moment approximation in section 3.4.

3.3 Equations of motion for irreducible moments

In this section we derive equations of motion for the irreducible moments, which are defined as

$$\rho_r^{\mu_1\cdots\mu_\ell} \equiv \langle E_k^r k^{\langle\mu_1}\cdots k^{\mu_\ell\rangle}\rangle_\delta. \tag{3.30}$$

Special cases for these equations will also give us equation of motions for dissipative currents as we can see in section 3.4. In relativistic kinetic theory evolution of single-particle distribution function is determined by the relativistic Boltzmann equation [30]

$$k^\mu\partial_\mu f_k = C[f], \tag{3.31}$$

where $C[f]$ is the collision integral which describes interaction between particles. If we only allow elastic two-to-two collisions with incoming particles having momenta k and k' and outgoing ones having momenta p and p', collision term can be written in form

$$C[f] = \frac{1}{\nu}\int dK'\,dPdP' W_{kk'\to pp'}(f_p f_{p'}\tilde{f}_k\tilde{f}_{k'} - f_k f_{k'}\tilde{f}_p\tilde{f}_{p'}), \tag{3.32}$$

where ν is symmetry factor which is two if particles are identical and otherwise one. In addition, we introduced Lorenz-invariant transition rate $W_{kk'\to pp'}$. Transition rate describes probability of collision to happen and it depends on type of interaction between particles. When deriving equations of motions for irreducible moments it is useful to split distribution function to an equilibrium distribution and to some correction, i.e. $f_k = f_{0k} + \delta f_k$. In addition, when decomposing derivative ∂_μ as $\partial_\mu = u_\mu d/d\tau + \nabla_\mu$ it is possible to write relativistic Boltzmann equation (3.31) in more convenient form,

$$\delta\dot{f}_k = -\dot{f}_{0k} - E_k^{-1}k_\nu\nabla^\nu(f_{0k}+\delta f_k) + E_k^{-1}C[f]. \tag{3.33}$$

Now taking definition of the irreducible moments, Eq.(3.30), and by applying co-moving derivative and projection operator to both sides of this equation we get

$$\dot{\rho}_r^{\langle\mu_1\cdots\mu_\ell\rangle} = \Delta^{\mu_1\cdots\mu_\ell}_{\nu_1\cdots\nu_\ell}\frac{d}{d\tau}\int dK\,E_k^r k^{\langle\mu_1}\cdots k^{\mu_\ell\rangle}\delta f_k. \tag{3.34}$$

As we can see later in section 3.4, we only need these equations up to second rank tensors in order to derive equations of motion for dissipative currents. Let's start with the equation for the scalar ρ_r, which reads

$$\dot{\rho}_r = \frac{d}{d\tau}\int dK\,E_k^r\delta f_k = \int dK\,\frac{d}{d\tau}(E_k^r)\delta f_k + \int dK\,E_k^r\delta\dot{f}_k. \tag{3.35}$$

First term in this equation can be calculated directly:

$$\begin{aligned}\int dK\,\frac{d}{d\tau}(E_k^r)\delta f_k &= r\int dK\,E_k^{r-1}\dot{E}_k\delta f_k = r\dot{u}_\mu\int dK E_k^{r-1}k^\mu\delta f_k \\ &= r\dot{u}_\mu\int dK E_k^{r-1}k^{\langle\mu\rangle}\delta f_k = r\dot{u}_\mu\rho_{r-1}^\mu,\end{aligned} \tag{3.36}$$

where we used the fact that u^μ is orthogonal to $\dot{u}^\mu$ so that $\dot{u}_\mu k^\mu = \dot{u}_\mu k^{\langle\mu\rangle}$. Second term in Eq.(3.35) can be decomposed further by a use of Boltzmann Eq.(3.33),

$$\begin{aligned}\int dK\,E_k^r\delta\dot{f}_k = &-\underbrace{\int dK E_k^r\dot{f}_{0k}}_{A} - \underbrace{\int dK E_k^{r-1}k^\nu\delta\nabla_\nu f_{0k}}_{B} \\ &-\underbrace{\int dK E_k^{r-1}k^\nu\delta\nabla_\nu\delta f_k}_{D} + \underbrace{\int dK E_k^{r-1}C[f]}_{C_{r-1}},\end{aligned} \tag{3.37}$$

where we introduced A,B and D in order to make calculations to look more cleaner. In addition we defined irreducible collision term, which in general can be defined as

$$C_r^{\langle\mu_1\cdots\mu_\ell\rangle} = \int dK E_k^r k^{\langle\mu_1}\cdots k^{\mu_\ell\rangle}C[f]. \tag{3.38}$$

All terms that are proportional to irreducible moments $\rho_r^{\mu_1\cdots\mu_\ell}$ in Eq.(3.37) arise from term D, which can be written as

$$\begin{aligned}D &= \nabla_\nu\int dK E_k^{r-1}k^\nu\delta f_k - \int dK\nabla_\nu(E_k^{r-1})k^\nu\delta f_k \\ &= \nabla_\nu\int dK E_k^{r-1}(E_k u^\nu + k^{\langle\nu\rangle})\delta f_k - (r-1)\nabla_\nu u_\mu\int dK E_k^{r-2}k^\mu k^\nu\delta f_k \\ &= \underbrace{\nabla_v[u^\nu\rho_r]}_{\theta\rho_r} + \nabla_\nu\rho_{r-1}^\nu - \underbrace{(r-1)\nabla_\nu u_\mu\int dK E_k^{r-2}k^{\langle\mu\rangle}k^{\langle\nu\rangle}\delta f_k}_{D_1},\end{aligned} \tag{3.39}$$

where in last step we have used the fact that u^μ and u^ν are orthogonal to $\nabla_\nu u_\mu$. With use of Eq.(3.11), D_1 can be written in terms of irreducible moments:

$$\begin{aligned}D_1 &= (r-1)\nabla_\nu u_\mu\int dK E_k^{r-2}\Big(k^{\langle\mu}k^{\nu\rangle} + \frac{1}{3}\Delta^{\mu\nu}(m^2 - E_k^2)\Big)\delta f_k \\ &= (r-1)\Big([\nabla_\nu u_\mu]\rho_{r-2}^{\mu\nu} + \frac{1}{3}\theta(m^2\rho_{r-2} - \rho_r)\Big).\end{aligned} \tag{3.40}$$

In total, part D is now form of

$$D = \nabla_\nu\rho_{r-1}^\nu - (r-1)\sigma_{\mu\nu}\rho_{r-2}^{\mu\nu} - \frac{1}{3}\Big((r-1)m^2\rho_{r-2} - (r+2)\rho_r\Big). \tag{3.41}$$

Lets next calculate part B in Eq.(3.37):

$$\begin{aligned} B &= \nabla_\nu \int dK E_k^{r-1} k^\nu f_{0k} - (r-1)\nabla_\nu u_\mu \int dK E_k^{r-2} k^\mu k^\nu f_{0k} \\ &= \theta \int dK E_k^r f_{0k} + \nabla_\nu \underbrace{\int dK E_k^{r-1} k^{\langle\nu\rangle} f_{0k}}_{=0} - \underbrace{(r-1)\nabla_\nu u_\mu \int dK E_k^{r-2} k^{\langle\mu\rangle} k^{\langle\nu\rangle} f_{0k}}_{B_1}, \end{aligned} \tag{3.42}$$

where the orthogonality condition (3.27) is used. Last part of this equation B_1 can be calculated even further

$$\begin{aligned} B_1 &= (r-1)\nabla_\nu u_\mu \Big[\underbrace{\int dK E_k^{r-2} k^{\langle\mu} k^{\nu\rangle} f_{0k}}_{=0} + \frac{1}{3} \int dK E_k^{r-2} \Delta^{\mu\nu} (\Delta_{\alpha\beta} k^\alpha k^\beta) f_{0k} \Big] \\ &= \frac{1}{3}(r-1)\theta \int dK E_k^{r-2} (\Delta_{\alpha\beta} k^\alpha k^\beta) f_{0k}. \end{aligned} \tag{3.43}$$

Now it is possible to write B as

$$B = \theta\Big(I_{r0} + (r-1) I_{r1}\Big), \tag{3.44}$$

where we have defined thermodynamic integrals

$$I_{nq} \equiv \frac{1}{(2q+1)!!} \langle E_k^{n-2q} (-\Delta_{\alpha\beta} k^\alpha k^\beta)^q \rangle_0. \tag{3.45}$$

It is important to note that there is couple of special cases where these thermodynamic integrals can be directly identified as thermodynamic variables

$$I_{10} = n, \;\; I_{20} = \varepsilon, \; I_{21} = p_0. \tag{3.46}$$

In order to calculate last term A form Eq.(3.37) we have to first derive some useful relations for comoving derivatives $\dot{\alpha}_0$ and $\dot{\beta}_0$. We start from equations of motion for dissipative energy-momentum tensor and particle 4-current, Eqs. (2.74),

$$\frac{d\varepsilon}{d\tau} = \dot{\alpha_0} \frac{\partial \varepsilon}{\partial \alpha_0} + \dot{\beta}_0 \frac{\partial \varepsilon}{\partial \beta_0} = \pi^{\mu\nu}\sigma_{\mu\nu} - \theta(\varepsilon + p_0 + \Pi), \tag{3.47}$$

$$\frac{dn}{d\tau} = \dot{\alpha_0} \frac{\partial n}{\partial \alpha_0} + \dot{\beta}_0 \frac{\partial n}{\partial \beta_0} = -n\theta - \partial_\mu n^\mu. \tag{3.48}$$

From these equations it possible to solve $\dot{\alpha}_0$ and $\dot{\beta}_0$ in terms of others macroscopic variables and their derivatives. This leads to

$$\dot{\alpha}_0 = \frac{\frac{\partial n}{\partial \beta_0}\Big(\pi^{\mu\nu}\sigma_{\mu\nu} - \theta(\varepsilon + p_0 + \Pi)\Big) + \frac{\partial \varepsilon}{\partial \beta_0}\Big(n\theta + \partial_\mu n^\mu\Big)}{\frac{\partial n}{\partial \beta_0}\frac{\partial \varepsilon}{\partial \alpha_0} - \frac{\partial n}{\partial \alpha_0}\frac{\partial \varepsilon}{\partial \beta_0}}, \tag{3.49}$$

$$\dot{\beta}_0 = \frac{\frac{\partial n}{\partial \alpha_0}\Big(\pi^{\mu\nu}\sigma_{\mu\nu} - \theta(\varepsilon + p_0 + \Pi)\Big) + \frac{\partial \varepsilon}{\partial \alpha_0}\Big(n\theta + \partial_\mu n^\mu\Big)}{\frac{\partial n}{\partial \alpha_0}\frac{\partial \varepsilon}{\partial \beta_0} - \frac{\partial n}{\partial \beta_0}\frac{\partial \varepsilon}{\partial \alpha_0}}. \tag{3.50}$$

Next we need to figure out different derivatives of equilibrium distribution function f_{0k}:

$$\begin{aligned} \frac{\partial f_{0k}}{\partial \beta_0} &= -E_k \frac{\partial f_{0k}}{\partial \alpha_0} = -E_k f_{0k}\tilde{f}_{0k}, \\ \frac{\partial f_{0k}}{\partial E_k} &= -\beta_0 f_{0k}\tilde{f}_{0k}. \end{aligned} \tag{3.51}$$

Now we can see that

$$\frac{\partial I_{nq}}{\partial \beta_0} = -\frac{1}{(2q+1)!!}\int dK E_k^{n+1-2q}(-\Delta_{\alpha\beta}k^\alpha k^\beta)^q \frac{\partial f_{0k}}{\partial \alpha_0} = -\frac{\partial I_{n+1,q}}{\partial \alpha_0} = -J_{n+1,q}, \tag{3.52}$$

where we defined auxiliary thermodynamic integral J_{nq} as

$$J_{nq} \equiv \frac{\partial I_{nq}}{\partial \alpha_0} = \frac{1}{(2q+1)!!}\int dK E_k^{n+1-2q}(-\Delta_{\alpha\beta}k^\alpha k^\beta)^q f_{0k}\tilde{f}_{0k}. \tag{3.53}$$

Especially we notice that the derivatives of pressure, energy density and particle density can be written in terms of these integrals:

$$\frac{\partial n}{\partial \alpha_0} = J_{10}, \;\; \frac{\partial \varepsilon}{\partial \alpha_0} = -\frac{\partial n}{\partial \beta_0} = J_{20}, \;\; \frac{\partial \varepsilon}{\partial \beta_0} = -J_{30}. \tag{3.54}$$

Substituting these relations back to Eqs.(3.49),(3.50) we get following equations for $\dot{\alpha}_0$ and $\dot{\beta}_0$

$$\dot{\alpha}_0 = \frac{1}{D_{20}}\Big(- J_{30}(n\theta + \partial_\mu n^\mu) - J_{20}(\pi^{\mu\nu}\sigma_{\mu\nu} - \theta(\varepsilon + p_0 + \Pi))\Big), \tag{3.55}$$

$$\dot{\beta}_0 = \frac{1}{D_{20}}\Big(- J_{20}(n\theta + \partial_\mu n^\mu) - J_{10}(\pi^{\mu\nu}\sigma_{\mu\nu} - \theta(\varepsilon + p_0 + \Pi))\Big), \tag{3.56}$$

where we defined quantity D_{nq} in terms of thermodynamic auxiliary integrals

$$D_{nq} = J_{n+1,q}J_{n-1,q} - J_{nq}^2. \tag{3.57}$$

Now we are finally in position to calculate A from Eq.(3.37). This is done by using chain rule to comoving time derivative of equilibrium distribution function and

making use of orthogonality condition from Eq.(3.27):

$$\begin{aligned} A &= \int dK E_k^r \dot{f}_{0k} = \int dK E_k^r \Big(\dot{\alpha}_0 \frac{\partial f_{0k}}{\partial \alpha_0} + \dot{\beta}_0 \frac{\partial f_{0k}}{\partial \beta_0} + \dot{E}_k \frac{\partial f_{0k}}{\partial E_k} \Big) \\ &= \dot{\alpha}_0 J_{r0} - \dot{\beta}_0 J_{r+1,0} + \underbrace{\dot{u}_\mu u^\mu}_{=0} \int dK E_k^{r+1} \frac{\partial f_{0k}}{\partial E_k} + \dot{u}^\mu \underbrace{\int dK E_k^r k^{\langle \mu \rangle} \frac{\partial f_{0k}}{\partial E_k}}_{=0} \\ &= -\frac{G_{3r}}{D_{20}} \Big(n\theta + \partial_\mu n^\mu \Big) - \frac{G_{2r}}{D_{20}} \Big(\pi^{\mu\nu} \sigma_{\mu\nu} - \theta(\varepsilon + p_0 + \Pi) \Big), \end{aligned} \tag{3.58}$$

where we introduced one more quantity

$$G_{nq} = J_{n0} J_{q0} - J_{n-1,0} J_{q+1,0}. \tag{3.59}$$

Combining all results from Eqs. (3.36),(3.37),(3.41),(3.44) and (3.58) we can write full scalar equation for irreducible moments

$$\begin{aligned} \dot{\rho}_r - C_{r-1} =& \alpha_r^{(0)} \theta + \frac{G_{2r}}{D_{20}} \Big(\pi^{\mu\nu} \sigma_{\mu\nu} - \theta \Pi \Big) + \frac{G_{3r}}{D_{20}} \partial_\mu n^\mu + r \dot{u}^\mu \rho_{r-1}^\mu - \nabla_\mu \rho_{r-1}^\mu \\ &+ (r-1) \sigma_{\mu\nu} \rho_{r-2}^{\mu\nu} + \frac{1}{3} \theta \Big((r-1) m^2 \rho_{r-2} - (r+2) \rho_r \Big), \end{aligned} \tag{3.60}$$

where coefficient $\alpha_r^{(0)}$ is complicated function temperature and chemical potential defined as

$$\alpha_r^{(0)} = -I_{r0} - (r-1) I_{r1} + \frac{G_{3r}}{D_{20}} n - \frac{G_{2r}}{D_{20}} \Big(\varepsilon + p_0 \Big). \tag{3.61}$$

The equations of motion for irreducible vector moment ρ_r^μ and second rank tensor moment $\rho_r^{\mu\nu}$ can be derived following similar steps and the derivation of these equations is presented in detail in appendix A. The obtained equations of motion are

$$\begin{aligned} \dot{\rho}_r^{\langle \mu \rangle} - C_{r-1}^{\langle \mu \rangle} =& \alpha_r^{(1)} I^\mu + \frac{1}{3} \theta \Big((r-1) m^2 \rho_{r-2}^\mu - (r+3) \rho_r^\mu \Big) + (r-1) \sigma_{\alpha\beta} \rho_{r-2}^{\mu\alpha\beta} \\ &+ \omega_\nu^\mu \rho_r^\nu - \Delta_\nu^\mu \nabla_\alpha \rho_r^{\nu\alpha} + \frac{\beta_0 J_{r+2,1}}{\varepsilon + p_0} \Big(\Pi \dot{u}^\mu - \nabla^\mu \Pi + \Delta_\alpha^\mu \partial_\beta \pi^{\alpha\beta} \Big) \\ &+ r \dot{u}_\nu \rho_{r-1}^{\mu\nu} + \frac{1}{5} \sigma_\beta^\mu \Big(2(r-1) m^2 \rho_{r-2}^\beta - (2r+3) \rho_r^\beta \Big) \\ &- \frac{1}{3} \nabla^\mu (m^2 \rho_{r-1} - \rho_{r+1}) + \frac{1}{3} \dot{u}^\mu \Big(r m^2 \rho_{r-1} + (r+3) \rho_{r+1} \Big), \end{aligned} \tag{3.62}$$

$$\begin{aligned}\dot{\rho}_r^{\langle\mu\nu\rangle} - C_{r-1}^{\langle\mu\nu\rangle} =& 2\alpha_r^{(0)}\sigma^{\mu\nu} + (r-1)\sigma_{\alpha\beta}\rho_{r-2}^{\mu\nu\alpha\beta} - \Delta_{\alpha\beta}^{\mu\nu}\nabla_\lambda\rho_{r-1}^{\alpha\beta\lambda} + 2\omega_\alpha^{\langle\mu}\rho_r^{\nu\rangle\alpha} \\ &- \frac{2}{5}\nabla^{\langle\mu}(m^2\rho_{r-1}^{\nu\rangle} - \rho_{r+1}^{\nu\rangle}) + \frac{2}{5}\Big(rm^2\rho_{r-1}^{\langle\mu} - (r+5)\rho_{r+1}^{\langle\mu}\Big)\dot{u}^{\nu\rangle} \\ &+ \frac{2}{15}\sigma^{\mu\nu}\Big((r-1)m^4\rho_{r-2} - (2r+3)m^2\rho_r + (r+4)\rho_{r+2}\Big) \\ &+ \frac{2}{7}\sigma_\alpha^{\langle\mu}\Big(2(r-1)m^2\rho_{r-2}^{\nu\rangle\alpha} - (2r+5)\rho_r^{\nu\rangle\alpha}\Big) + r\rho_{r-1}^{\mu\nu\lambda}\dot{u}_\lambda \\ &+ \frac{1}{3}\theta\Big((r-1)m^2\rho_{r-2}^{\mu\nu} - (r+4)\rho_r^{\mu\nu}\Big),\end{aligned} \tag{3.63}$$

where we introduce coefficients $\alpha_r^{(1)}$ and $\alpha_r^{(2)}$,

$$\alpha_r^{(1)} = J_{r+1,1} - J_{r+2,1}\frac{n}{\varepsilon + p_0}, \tag{3.64}$$

$$\alpha_r^{(2)} = I_{r+1,1} + (r-1)I_{r+2,2}. \tag{3.65}$$

In addition, we defined vorticity tensor $\omega^{\mu\nu} = (\nabla^\mu u^\nu - \nabla^\nu u^\mu)$ and space-like gradient of the ration between chemical potential and temperature $I^\mu = \nabla^\mu\alpha_0$. It is important to note that these are general equations which can be applied no matter what kind of expansion of distribution function we are using as long as the equilibrium distribution is isotropic distribution described by Eq.(3.13). For anisotropic single-particle distribution function similar kind, but more complicated, equations of motion can also be derived, but that is not done here. More details about anisotropic dissipative fluid dynamics can be found in Ref.[31].

3.4 14-moment approximation

14-moment approximation is maybe the simplest way to handle expansion of single-particle distribution in Eq. (3.28). The idea is to truncate the expansion in such a way that there is equal amount of expansion coefficients and independent macroscopic variables, i.e 14 coefficients. This way it is possible to simply figure out coefficients by matching macroscopic variables to their kinetic definitions. The form of the expansion of ϕ_k in 14-momentum approximation is therefore

$$\phi_k = \lambda_k + \lambda_k^{\langle\mu\rangle}k_{\langle\mu\rangle} + \lambda_k^{\langle\mu\nu\rangle}k_{\langle\mu}k_{\nu\rangle}, \tag{3.66}$$

where expansion coefficients are still expanded in terms of powers of E_k like in Eq.(3.29). Each of these expansions have truncation order N_ℓ indicating highest

power of E_k in expansion. In 14-moment approximation we choose $N_0 = 2, N_1 = 1$ and $N_2 = 0$. This is because there are three independent scalar quantities, ε, n_0, Π, two independent vector quantities n^μ, u^μ and one tensor quantity $\pi^{\mu\nu}$. Expansion coefficient can now simply be written as

$$\lambda_k = c_0 + c_1 E_k + c_2 E_k^2, \quad \lambda_k^{\langle\mu\rangle} = c_0^{\langle\mu\rangle} + c_1^{\langle\mu\rangle} E_k, \quad \lambda_k^{\langle\mu\nu\rangle} = c_0^{\langle\mu\nu\rangle}. \tag{3.67}$$

Now we can solve coefficients $c_n^{\langle\mu_1\cdots\mu_\ell\rangle}$ using kinetic definitions for macroscopic variables from Eqs.(3.12) and (3.16), where we remember that $\delta f_k = \phi_k f_{0k} \tilde{f}_{0k}$. Lets start by writing down definition for shear stress tensor $\pi^{\mu\nu}$:

$$\begin{aligned}
\pi^{\mu\nu} &= \int dK k^{\langle\mu} k^{\nu\rangle} \phi_k f_{0k} \tilde{f}_{0k} = c_0^{\langle\alpha\beta\rangle} \int dK k^{\langle\mu} k^{\nu\rangle} k_{\langle\alpha} k_{\beta\rangle} f_{0k} \tilde{f}_{0k} \\
&= \frac{2}{15} c_0^{\langle\alpha\beta\rangle} \Delta^{\mu\nu}_{\alpha\beta} \int dK (\Delta_{\lambda\sigma} k^\lambda k^\sigma)^2 f_{0k} \tilde{f}_{0k} \\
&= 2 c_0^{\langle\mu\nu\rangle} J_{42},
\end{aligned} \tag{3.68}$$

where we have used orthogonality condition (3.27) in order to get rid off all scalar and vector coefficients. Solving $c_0^{\langle\mu\nu\rangle}$ from this equation we get

$$c_0^{\langle\mu\nu\rangle} = \frac{\pi^{\mu\nu}}{2J_{42}}. \tag{3.69}$$

Now following similar steps than in Eq.(3.68) it is possible get relation between irreducible moment $\rho_r^{\mu\nu}$ and shear stress tensor $\pi^{\mu\nu}$

$$\begin{aligned}
\rho_r^{\mu\nu} &= \int dK E_k^r k^{\langle\mu} k^{\nu\rangle} \phi_k f_{0k} \tilde{f}_{0k} = 2 c_0^{\langle\mu\nu\rangle} J_{r+4,2} \\
&= \gamma_r^{(0)} \pi^{\mu\nu},
\end{aligned} \tag{3.70}$$

where we defined coefficient

$$\gamma_r^{(2)} = \frac{J_{r+4,2}}{J_{42}}. \tag{3.71}$$

When trying to solve coefficients $c_0^{\langle\mu\rangle}$ and $c_1^{\langle\mu\rangle}$ we need two constraints from the kinetic definitions of n^μ and h^μ from which the last one is set to zero because we work in the Landau picture. These definitions read

$$\begin{aligned}
n^\mu &= \int dK k^{\langle\mu\rangle} \phi_k f_{0k} \tilde{f}_{0k} = \int dK k^{\langle\mu\rangle} (c_0^{\langle\nu\rangle} + c_1^{\langle\nu\rangle} E_k) k_{\langle\nu\rangle} f_{0k} \tilde{f}_{0k} \\
&= -\frac{1}{3} \int dK (c_0^{\langle\nu\rangle} + c_1^{\langle\nu\rangle} E_k)(\Delta_{\alpha\beta} k^\alpha k^\beta) f_{0k} \tilde{f}_{0k} \\
&= c_0^{\langle\nu\rangle} J_{21} + c_1^{\langle\nu\rangle} J_{31},
\end{aligned} \tag{3.72}$$

$$
\begin{aligned}
h^\mu &= \int dK E_k k^{\langle\mu\rangle} \phi_k f_{0k} \tilde{f}_{0k} = \int dK E_k k^{\langle\mu\rangle} (c_0^{\langle\nu\rangle} + c_1^{\langle\nu\rangle} E_k) k_{\langle\nu\rangle} f_{0k} \tilde{f}_{0k} \\
&= -\frac{1}{3} \int dK E_k (c_0^{\langle\nu\rangle} + c_1^{\langle\nu\rangle} E_k)(\Delta_{\alpha\beta} k^\alpha k^\beta) f_{0k} \tilde{f}_{0k} \\
&= c_0^{\langle\nu\rangle} J_{31} + c_1^{\langle\nu\rangle} J_{41} = 0,
\end{aligned}
\tag{3.73}
$$

where we have again made use of orthogonality condition (3.27). Solving $c_0^{\langle\mu\rangle}$ and $c_1^{\langle\mu\rangle}$ from Eqs.(3.72) and (3.73) leads to

$$
\begin{aligned}
c_0^{\langle\mu\rangle} &= -\frac{3J_{41}}{D_{31}} n^\mu, \\
c_1^{\langle\mu\rangle} &= \frac{3J_{31}}{D_{31}} n^\mu.
\end{aligned}
\tag{3.74}
$$

Irreducible moments ρ_r^μ can now be written as

$$
\begin{aligned}
\rho_r^\mu &= \int dK E_k^r k^{\langle\mu\rangle} \phi_k f_{0k} \tilde{f}_{0k} = \int dK E_k^r k^{\langle\mu\rangle} (a_0^{\langle\nu\rangle} + a_1^{\langle\nu\rangle} E_k) k_{\langle\nu\rangle} f_{0k} \tilde{f}_{0k} \\
&= c_0^{\langle\nu\rangle} J_{r+2,1} + c_1^{\langle\nu\rangle} J_{r+3,1} = \gamma_r^{(1)} n^\mu,
\end{aligned}
\tag{3.75}
$$

where

$$
\gamma_r^{(1)} = \frac{1}{D_{31}} (J_{41} J_{r+2,1} - J_{31} J_{r+3,1}). \tag{3.76}
$$

Last three scalar coefficients c_0,c_1 and c_2 can be solved from the definition of bulk viscous pressure Π and Landau matching conditions which state that there is no off-equilibrium corrections to energy and particle densities, i.e.

$$
\langle E_k \rangle_\delta = \langle E_k^2 \rangle_\delta = 0. \tag{3.77}
$$

This leads to

$$
\begin{aligned}
\Pi &= -\frac{1}{3} \langle \underbrace{\Delta_{\alpha\beta} k^\alpha k^\beta}_{m^2 - E_k^2} \rangle_\delta = -\frac{m^2}{3} \int dK \phi_k f_{0k} \tilde{f}_{0k} \\
&= -\frac{m^2}{3} (c_0 J_{00} + c_1 J_{10} + c_2 J_{20}),
\end{aligned}
\tag{3.78}
$$

$$
\begin{aligned}
\langle E_k \rangle_\delta &= \int dK E_k \phi_k f_{0k} \tilde{f}_{0k} \\
&= c_0 J_{10} + c_1 J_{20} + c_2 J_{30} = 0,
\end{aligned}
\tag{3.79}
$$

$$\begin{aligned}\langle E_k^2\rangle_\delta &= \int dK E_k \phi_k f_{0k} \tilde{f}_{0k} \\ &= c_0 J_{20} + c_1 J_{30} + c_2 J_{40} = 0,\end{aligned} \tag{3.80}$$

where in the first equation we also used matching conditions to write bulk viscosity in more convenient form. Solution of this group of equations is

$$\begin{aligned}c_0 &= -\frac{3}{m^2}\frac{D_{30}\Pi}{J_{20}D_{20} + J_{30}G_{12} + J_{40}D_{10}}, \\ c_1 &= a_0\frac{G_{23}}{D_{30}}, \\ c_2 &= a_0\frac{D_{20}}{D_{30}}.\end{aligned} \tag{3.81}$$

Like previously, we can now easily derive relation between irreducible moments ρ_r and bulk viscous pressure:

$$\begin{aligned}\rho_r &= \int dK E_k^r \phi_k f_{0k} \tilde{f}_{0k} = c_0 J_{r0} + c_1 J_{r+1,0} + c_2 J_{r+2} \\ &= \gamma_r^{(0)}\Pi,\end{aligned} \tag{3.82}$$

$$\gamma_r^{(0)} = -\frac{3}{m^2}\frac{D_{30}J_{r0} + G_{23}J_{r+1,0} + D_{20}J_{r+2,0}}{J_{20}D_{20} + J_{30}G_{12} + J_{40}D_{10}}. \tag{3.83}$$

Now that we have derived relations between dissipative quantities and irreducible tensors we can write Eqs. (3.60),(3.62) and (3.63) in terms of dissipative quantities. However, because all non-zero irreducible moments are promotional to dissipative quantities, we could use any value of r in Eqs. (3.60),(3.62) and (3.63) to derive equations for dissipative quantities. In this thesis we use $r = 0$, which leads to the following equations:

$$\begin{aligned}-\frac{3}{m^2}\dot{\Pi} - C_{-1} =& \alpha_0^{(0)}\theta + \frac{G_{20}}{D_{20}}\Big(\pi^{\mu\nu}\sigma_{\mu\nu} - \theta\Pi\Big) + \frac{G_{30}}{D_{20}}\partial_\mu n^\mu - \nabla_\mu(\gamma_{-1}^{(1)}n^\mu) \\ &- \gamma_{-2}^{(2)}\sigma_{\mu\nu}\pi^{\mu\nu} + \theta\Pi\Big(2m^{-2} - \frac{1}{3}m^2\gamma_{-2}^{(0)}\Big),\end{aligned} \tag{3.84}$$

$$\begin{aligned}\dot{n}^{\langle\mu\rangle} - C_{-1}^{\langle\mu\rangle} =& \alpha_0^{(1)}I^\mu - \frac{1}{3}\theta n^\mu\Big(m^2\gamma_{-2}^{(1)} + 3\Big) + \omega_\nu^\mu n^\nu - \Delta_\nu^\mu\nabla_\alpha(\gamma_{-1}^{(2)}\pi^{\nu\alpha}) \\ &+ \frac{n}{\varepsilon + p_0}\Big(\Pi\dot{u}^\mu - \nabla^\mu\Pi + \Delta_\alpha^\mu\partial_\beta\pi^{\alpha\beta}\Big) \\ &- \frac{1}{5}\sigma_\beta^\mu n^\beta\Big(2m^2\gamma_{-2}^{(1)} + 3\Big) - \frac{1}{3}\nabla^\mu(m^2\gamma_{-1}^{(0)}\Pi)\end{aligned} \tag{3.85}$$

$$\begin{aligned}\dot{\pi}_r^{\langle\mu\nu\rangle} - C_{r-1}^{\langle\mu\nu\rangle} =& 2\alpha_0^{(0)}\sigma^{\mu\nu} - \frac{2}{15}\sigma^{\mu\nu}\Big(m^4\gamma_{-2}^{(0)}\Pi - 9\Pi\Big) - \frac{2}{5}\nabla^{\langle\mu}(m^2\gamma_{-1}^{(1)}n^{\nu\rangle}) \\ &+ 2\omega_\alpha^{\langle\mu}\pi^{\nu\rangle\alpha} - \frac{2}{7}\sigma_\alpha^{\langle\mu}\Big(2m^2\gamma_{-2}^{(2)}\pi^{\nu\rangle\alpha} + 5\pi^{\nu\rangle\alpha}\Big) \\ &- \frac{1}{3}\theta\Big(m^2\gamma_{-2}^{(2)}\pi^{\mu\nu} + 4\pi^{\mu\nu}\Big),\end{aligned} \tag{3.86}$$

where all the terms with irreducible moments of rank three or higher will vanish because expansion of δf_k contain only momenta up to $k^{\langle\mu}k^{\nu\rangle}$. In addition, we made use of Landau matching conditions, i.e. Eq.(3.77), which state that $\rho_1 = \rho_2 = \rho_1^\mu = 0$. We also note that in derivation of Eq.(3.85) we used the fact that

$$\beta_0 J_{21} = \beta_0 \frac{\partial p_0}{\partial \alpha_0} = \frac{\partial p_0}{\partial \mu_0} = n. \tag{3.87}$$

In order to derive equations of motion for dissipative quantities we still have to deal with the collision terms $C_{r-1}^{\langle\mu_1\cdots\mu_\ell\rangle}$. Perhaps the simplest way to do it is to linearize the collision operator (3.32) in terms of δf_k and then write it in terms of the irreducible moments. How this is done in detail is not addressed in this thesis. However, calculations in Ref.[18] show that this kind of procedure leads to

$$C_{r-1}^{\langle\mu_1\cdots\mu_\ell\rangle} = -\sum_{n=0}^{N_\ell} \mathcal{A}_{rn}^\ell \rho_n^{\mu_1\cdots\mu_\ell}, \tag{3.88}$$

where N_ℓ is order of truncation introduced earlier and $\mathcal{A}_{rn}^\ell$ are complicated coefficients which depend on underlying microscopic theory. In 14-momentum approximation we are left with

$$C_{r-1} = \frac{3}{m^2}\mathcal{A}_{00}^{(0)}\Pi,\ C_{r-1}^{\langle\mu\rangle} = -\mathcal{A}_{00}^{(1)}n^\mu,\ C_{r-1}^{\langle\mu\rangle} = -\mathcal{A}_{00}^{(2)}\pi^{\mu\nu}. \tag{3.89}$$

Now substituting collision terms back to Eqs.(3.84)-(3.86) and rearranging terms we get equations of motion for dissipative quantities,

$$\begin{aligned}\tau_\Pi\dot{\Pi} + \Pi =& -\zeta\theta - \ell_{\Pi n}\nabla_\mu n^\mu - \tau_{\Pi n}F_\mu n^\mu \\ &- \delta_{\Pi\Pi}\Pi\theta - \lambda_{\Pi n}I_\mu n^\mu + \lambda_{\Pi\pi}\pi^{\mu\nu}\sigma_{\mu\nu},\end{aligned} \tag{3.90}$$

$$\begin{aligned}\tau_n\dot{n}^{\langle\mu\rangle} + n^\mu =& \kappa_n I^\mu - \omega_\nu^\mu n^\nu - \delta_{nn}\theta n^\mu - \ell_{n\Pi}\nabla^\mu\Pi + \ell_{n\pi}\Delta_\nu^\mu\nabla_\alpha\pi^{\nu\alpha} \\ &\tau_{n\Pi}\Pi F^\mu - \tau_{n\pi}F_\nu\pi^{\mu\nu} - \lambda_{nn}\sigma_\nu^\mu n^\nu + \lambda_{n\Pi}\Pi I^\mu - \lambda_{n\pi}I_\nu\pi^{\mu\nu},\end{aligned} \tag{3.91}$$

$$\begin{aligned}\tau_\pi \dot{\pi}_r^{\langle\mu\nu\rangle} + \pi^{\mu\nu} =& 2\eta\sigma^{\mu\nu} + 2\omega_\alpha^{\langle\mu}\pi^{\nu\rangle\alpha} - \delta_{\pi\pi}\theta\pi^{\mu\nu} - \ell_{\pi n}\nabla^{\langle\mu}n^{\nu\rangle} - \tau_{\pi\pi}\sigma_\alpha^{\langle\mu}\pi^{\nu\rangle\alpha} \\ & - \tau_{\pi n}F^{\langle\mu}n^{\nu\rangle} + \lambda_{\pi\Pi}\Pi\sigma^{\mu\nu} + \lambda_{\pi n}I^{\langle\mu}n^{\nu\rangle},\end{aligned} \tag{3.92}$$

where we introduced notation $F^\mu = \nabla^\mu p_0$ and ignored terms that are higher than second order in inverse Reynolds or Knudsen numbers. In addition, we used chain rule and Eq.(A.16) from appendix A to write

$$\nabla^\mu \gamma_i^{(\ell)} = \Big(\frac{\partial\gamma_i^{(\ell)}}{\partial\alpha_0} + \frac{n}{\varepsilon + p_0}\frac{\partial\gamma_i^{(\ell)}}{\partial\beta_0}\Big)I^\mu - \frac{1}{\varepsilon + p_0}\frac{\partial\gamma_i^{(\ell)}}{\partial \ln\beta_0}F^\mu. \tag{3.93}$$

As we can now see Eqs.(3.90)-(3.92) are similar to relaxation type equations that were obtained from second law of thermodynamics using general entropy 4-current in section 2.3.5. However, this time around we have also solved exact form of proportionally coefficients, which are presented in appendix B. We also notice that equations of motion derived here have some additional first order terms in dissipative quantities compared to Eqs.(2.82)-(2.84), but they are missing all the second order terms. Terms which are second order in inverse Reynolds number come from non-linear collision term [32]. Terms that are second order in Knudsen number are missing due to the fact that in the 14-moment approximation, the momentum expansion of particle distribution function is truncated and there is not any small parameter, like Knudsen number, in which we could do power counting and therefore improve our approximation by taking higher order terms into account. That is, we have ignored infinite amount of terms that are second order in Knudsen or inverse Reynolds number. Another problem, which is connected to previous one, is that in 14-moment approximation one could use arbitrary value of r in Eqs.(3.60),(3.62) and (3.63) to obtain different transport coefficients for the equations of motion. This is why the 14-moment approximation is presented in this thesis mostly on illustrative purposes. However, the equations of motion for irreducible moments and idea of expanding single-particle distribution function in orthogonal basis are very useful even when doing systematic power counting in terms of Knudsen and inverse Reynolds numbers. More details about how this is done can be found in Refs.[18], [29].

4 Heavy-ion collisions

Modeling heavy ion collisions is a complicated task and there are lots of different methods that try to solve this problem. Most of these methods are based on the hydrodynamics which relies on assumption that strongly interacting matter created in collision has fluid like behavior. However, there are also models which take a slightly different approach to this problem. One of these models is the AMPT-model which uses kinetic theory to solve the evolution of medium formed in collision [33], [34]. This kind of method should in principle be more accurate if the system is far from thermal equilibrium, like in case of Pb-p collisions, but it also has its own problems. For example during its evolution the strongly interacting matter experiences phase transition from the quark-gluon plasma to the hadron gas. In models based on hydrodynamics this phase transition doesn't need any special treatment, but it is already taken account in the equation of state, which describes thermal properties of the medium. In case of models which are based directly on the kinetic theory it is necessary to consider in detail how partons in the quark-gluon plasma hadronize. There are also even some approaches which use hydrodynamics to describe evolution of QGP and switch to kinetic theory after phase transition. This kind of method is used for example in Refs.[12], [35]. Even though both the hydrodynamic and the kinetic theory approaches have their own flaws both of them generate results which seem to agree with the data reasonably well. In this thesis we only focus on the models which use only hydrodynamics.

Even though hydrodynamics is important part of modeling heavy ion collision, it is not enough in itself. The basic structure of models based on hydrodynamics is usually divided into the following steps:

i. Formation of the initial state,

ii. Expansion of the quark-gluon plasma,

iii. Phase transition from the quark-gluon plasma to the hadron gas,

iv. Expansion of the hadron gas,

v. Particle freeze-out,

which are also illustrated in figure 1. From these steps only steps **ii-iv** involve hydrodynamics and even these steps also use equation of state to connect strongly interacting matter to its thermal properties.

There are also some other things that should in principle be taken account when modeling heavy ion collisions. For example when two initial nuclei collide high energy partons, also called jets, are formed together with the QGP. These jets travel through QGP while it is expanding and interact with it. These interactions make simulations of heavy-ion collisions much more complicated. There have even been some discussion that jets traveling through medium could create mach cones, similar to those which are created when velocity of fighter plane exceeds the speed of sound [36]–[38]. Fortunately jets have only slight effect to the expansion of the medium and therefore they are usually ignored when studying properties of QGP and this is also done here. More information about jets in QGP can be found in Refs.[39], [40].

In this section we go through in detail theory behind each step in heavy ion collisions excluding technical discussion about hydrodynamics which is covered in sections 2 and 3. But before that we discuss a little bit about different kind of observables in heavy ion collisions and how these quantities are calculated in theory.

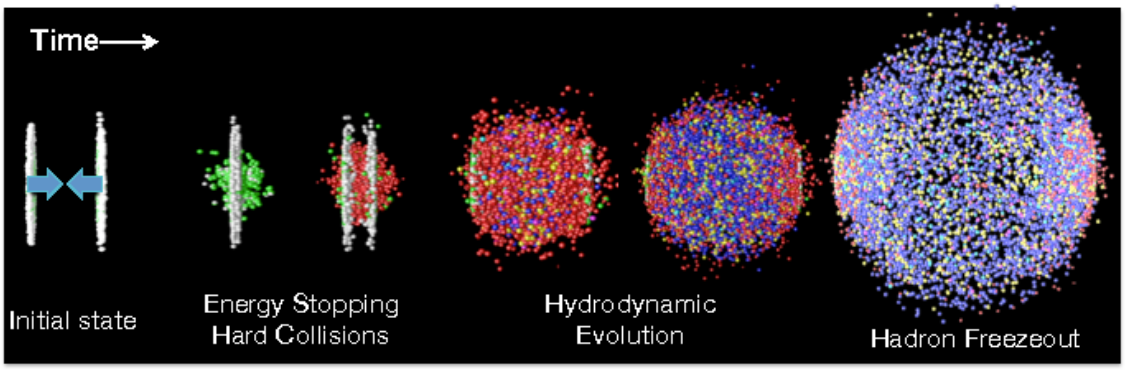

Figure 1. Evolution of a heavy ion collision. Figure from [41].

4.1 Observables

Even though theoretical models predict that existence of QGP is very likely, there is no way to directly observe QGP because of its short lifetime and QCD color confinement. Most of the knowledge about properties of the QGP come through matching theoretical models to the experimental observations.

Most direct measurable observable is the number of hadrons reaching detectors and their energies. Usually particle number is expressed per rapidity y or per pseudorapidity η_s, which are defined as

$$y = \frac{1}{2} \ln \left(\frac{E + p_z}{E - p_z} \right), \tag{4.1}$$

$$\eta_s = -\ln \left[\tan(\theta/2) \right] = \frac{1}{2} \ln \left(\frac{|\mathbf{p}| + p_z}{|\mathbf{p}| - p_z} \right), \tag{4.2}$$

where z-axis is chosen to be the collision beam axis and θ is the angle between particles momentum vector and beam axis. From definitions of y and η we can see that $y = \eta$ if the particles are massless. The reason why we have two different rapidities is that in case of unidentified charged hadrons (not knowledge about hadron masses) one can only measure the number of particles per pseudorapdity $\mathrm{d}N/\mathrm{d}\eta$. In cases when one measures particle number for the specific type of particle, one usually measures the quantity $\mathrm{d}N/\mathrm{d}y$. Commonly in literature either of quantities $\mathrm{d}N/\mathrm{d}y$ or $\mathrm{d}N/\mathrm{d}\eta$ is referred as multiplicity. Usually most accurate measurements are obtained when particles are measured transverse to the beam axis, i.e. $\eta \approx y \approx 0$. This region is called mid-rapidity and it covers rapidity gaps $|\eta| \leq 0.5$ or $|y| \leq 0.5$. This is also the region in which we are focusing on this thesis.

The number of particles created in a collision is also used to categorize events into different percentile bins, which are called centrality classes. These classes are defined such a way that centrality class 0-5% contains all events in which number of produced particles would belong to the highest 5% from all collisions. Similarly centrality class 90-100% would contain events in which number of produced particles would belong to the lowest 10% from all collisions.

In addition of particle number and their rapidities it is also possible to measure particles transverse momentum p_T and the azimuthal angle ϕ, which tells particles direction in a transverse plane. Using these quantities it is then possible to measure $\mathrm{d}N/\mathrm{d}y\mathrm{d}p_T^2\mathrm{d}\phi$ spectrum. However, studying angular dependence this way is not very

practical. Instead, angular dependence is quantified using Fourier coefficients v_n from series:

$$\frac{\mathrm{d}N}{\mathrm{d}y\mathrm{d}p_T^2\mathrm{d}\phi} = \frac{1}{2\pi}\frac{\mathrm{d}N}{\mathrm{d}y\mathrm{d}p_T^2}\Big(1 + \sum_{n=1}^{\infty} v_n(y,p_T)\cos[n(\phi-\psi_n)]\Big), \tag{4.3}$$

where ψ_n is first angle where the n :th harmonic component has its maximum multiplicity and it is called the event plane angle. The Fourier coefficients v_n are often called flow harmonics, and they are defined as

$$v_n(y,p_T) = \Big(\frac{\mathrm{d}N}{\mathrm{d}y\mathrm{d}p_T^2}\Big)^{-1}\int \mathrm{d}\phi\cos[n(\phi-\psi_n)]\frac{\mathrm{d}N}{\mathrm{d}y\mathrm{d}p_T^2\mathrm{d}\phi}. \tag{4.4}$$

Similar coefficients can also be obtained from p_T integrated spectrum $\mathrm{d}N/\mathrm{d}y\mathrm{d}\phi$ and they are given by

$$v_n(y) = \Big(\frac{\mathrm{d}N}{\mathrm{d}y}\Big)^{-1}\int \mathrm{d}\phi\cos[n(\phi-\psi_n)]\frac{\mathrm{d}N}{\mathrm{d}y\mathrm{d}\phi}. \tag{4.5}$$

First order coefficients v_1 describes situations where particles have one preferred direction and for symmetry reasons this coefficient is usually close to zero. One is usually only interested about couple of next coefficients v_2 and v_3 which are called elliptic flow and triangular flow respectively. In last decade also higher order coefficients have been measured, but their contribution to angular distribution is much smaller[42]. In this thesis we use so called averaged initial state (see section 4.2) in which case only v_2 is non-zero. In order to see effects of v_3 or higher order flow harmonics one needs to take account initial state fluctuations. Because the definition of the flow harmonics (4.4) depends on event-plane angles, which are not directly measurable, one usually uses so called cumulants, which don't depend on event-plane. In particular when comparing v_2 using averaged initial state one usually compares them to the 4-particle cumulants defined as [43]

$$v_2\{4\} = \Big(2\langle v_n^2\rangle_{ev})^2 - \langle v_n^4\rangle_{ev}\Big)^{1/4}, \tag{4.6}$$

where averages are taken over all events in given centrality class.

In numerical simulations one usually obtains particle spectrum $\mathrm{d}N/\mathrm{d}y\mathrm{d}p_T^2\mathrm{d}\phi$ for each hadron specie separately. If one then wants to calculate the total multiplicity of charged hadrons it is necessary to write it in terms of η distributions in order to compare results to the data. This kind of transformation can be done using relation [9]

$$\left.\frac{\mathrm{d}N_{ch}}{\mathrm{d}\eta\mathrm{d}p_T^2\mathrm{d}\phi}\right|_{\Delta\eta} = \sum_i \frac{2}{\Delta\eta}\sinh^{-1}\left[\frac{p_T}{m_{T,i}}\sinh\left(\frac{\Delta\eta}{2}\right)\right]\frac{\mathrm{d}N_i}{\mathrm{d}y\mathrm{d}p_T^2\mathrm{d}\phi}, \tag{4.7}$$

where $\Delta\eta$ is pseudorapidity range of interest, $m_{T,i} = \sqrt{m_i^2 + p_T^2}$ and m_i is the mass of hadron i. The sum in Eq.(4.7) is over all the charged hadrons.

4.2 Initial state

When talking about initial state in heavy ion collisions one usually refers to the earliest stages of the collision when QGP is formed and thermalized. Mathematically speaking initial state can be thought as initial values for the components of energy-momentum tensor and particle 4-current. These initial values are necessary when trying to solve hydrodynamic evolution of QGP, because hydrodynamic equations are differential equations which require initial condition. However, usually when collision energies are high enough we can approximate baryon density to be zero so it is enough to give initial values for energy density, pressure, 4-velocity and dissipative currents. In most general case all of these initial state quantities depend from all three spatial coordinates. However, when studying dynamics of the collision in central rapidity region, where particle multiplicity remains constant, one can assume boost invariance to the collisions system and only two spatial dimensions are enough to describe the system. Boost invariance is discussed in more detail in section 4.3.

One of the biggest problem when modeling the heavy ion collisions is the fact that only thing we can measure is the particles which reach the detector. This means that we cannot separately measure things like initial state or viscosity of QGP. In fact there are different kind of initial states that seem to match with the data reasonably well when the viscosity parameters are adjusted accordingly.

Generally speaking initial states can be categorized into two different classes: One where the nucleus is described by its average nuclear density profile and another where the distributions of nucleons inside the nucleus are taken to account. Second choice has obviously more physical grounds. After all, the nuclei consist from many nucleons which will cause some fluctuations to nuclear density. However, this kind of method has one drawback. Because the nucleon positions inside the nucleon has to be sampled randomly according to their position distribution, it is necessary to do thousands of events in order to get averaged results that can be compared to the data. In this sense it reminds real heavy ion collision experiments where it is impossible to study only one collision. Many times these fluctuations in the nucleon positions are called event-by-event (EBYE) fluctuations or just initial state fluctuations. Initial states where we only use average quantities when calculating initial state are often

called averaged initial states.

In this thesis all simulations are done by using averaged initial state obtained from the EKRT model [9]. The EKRT model is also capable of taking account EBYE fluctuations and possible effect of these fluctuations is discussed in section 6. Before going into details of the EKRT model we first discuss about optical Glauber model and how one can use it to determine centrality classes for averaged initial state.

4.2.1 Optical Glauber model

The optical Glauber model is one of the simplest models for initial state and it is mostly based on geometrical arguments. In this section we go through main results of the optical Glauber model without much derivation. More detailed discussion about optical Glauber model can be found in Refs.[44], [45].

In the optical Glauber model colliding nuclei are treated as a round discs moving along straight path such a way that their cross section remains constant even after collision. Geometry of this kind of collision is illustrated in figure 2, where we defined the impact parameter **b** as a difference between transverse coordinates of the two nucleus. We also defined vector **r** as a transverse position vector.

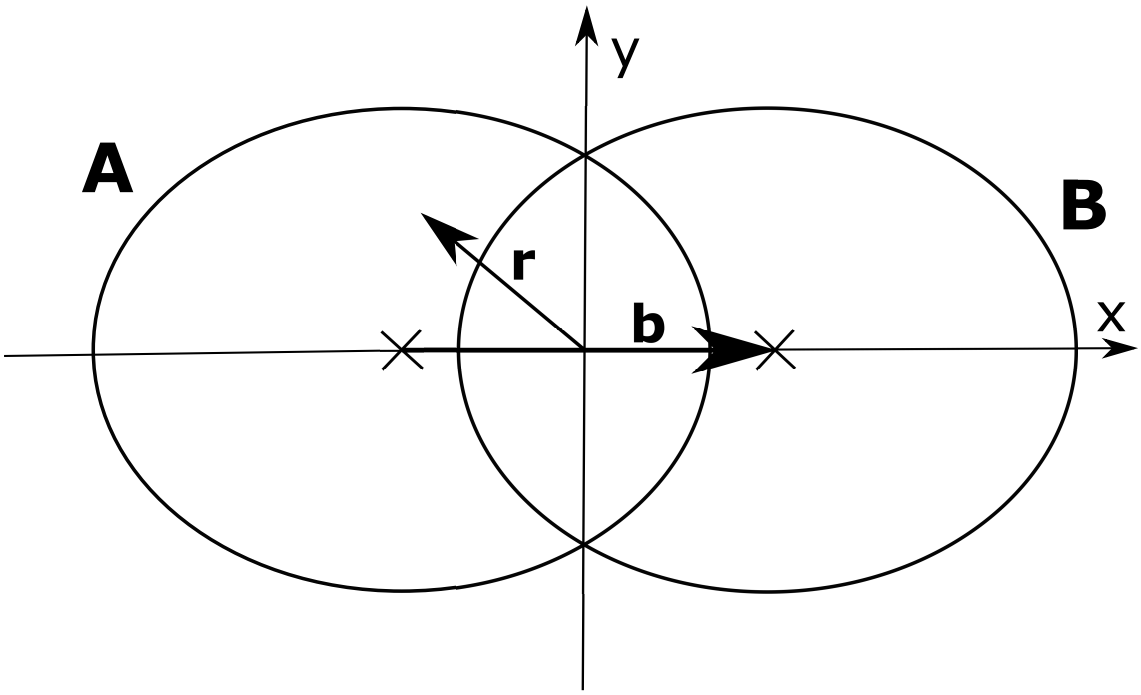

Figure 2. Geometry of the collision system.

Nuclear density of the nucleus with mass number A is given by the Woods-Saxon

parametrization

$$\rho_A(\mathbf{r},z) = \frac{\rho_0}{\exp\Big(\frac{(r^2+z^2)^{1/2}-R_A}{d}\Big)+1}, \tag{4.8}$$

where $d = 0.54$ fm. The nuclear radius R_A can be calculated as

$$R_A = 1.12A^{1/3} - 0.86A^{-1/3}. \tag{4.9}$$

The parameter ρ_0 is obtained by requiring that

$$\int \mathrm{d}^2\mathbf{r}T_A(\mathbf{r}) = \int \mathrm{d}^2\mathbf{r}\mathrm{d}z\rho_A(\mathbf{r},z) = A, \tag{4.10}$$

where we defined nuclear thickness function

$$T_A(\mathbf{r}) = \int dz\rho_A(\mathbf{r},z). \tag{4.11}$$

Typically when $A \sim 200$ we have $\rho_0 \approx 0.17$ fm^{-3}. The optical Glauber model predicts that in A+B collision the total cross section is given by

$$\sigma_{AB} = \int \mathrm{d}^2\mathbf{b}\Big[1 - \Big(1 - \frac{\sigma_{NN}T_{AB}(\mathbf{b})}{AB}\Big)^{AB}\Big] \simeq \int \mathrm{d}^2\mathbf{b}\Big(1 - e^{-\sigma_{NN}T_{AB}(\mathbf{b})}\Big), \tag{4.12}$$

where σ_{NN} is the cross section for inelastic nucleon-nucleon collision and T_{AB} is the nuclear overlap function which is defined as

$$T_{AB}(\mathbf{b}) = \int \mathrm{d}^2\mathbf{r}T_A(\mathbf{r}+\mathbf{b}/2)T_B(\mathbf{r}-\mathbf{b}/2). \tag{4.13}$$

The transverse density of binary nucleon-nucleon collisions can be calculated using optical Glauber model:

$$n_{BC}(\mathbf{r},\mathbf{b}) = \sigma_{NN}T_A(\mathbf{r}+\mathbf{b}/2)T_B(\mathbf{r}-\mathbf{b}/2). \tag{4.14}$$

Glauber model also predicts the transverse density of nucleons participating in nuclear collision, which is often called the wounded nucleon transverse density and it is given by

$$\begin{aligned} n_{WN}(\mathbf{r},\mathbf{b}) = {} & T_A(\mathbf{r}+\mathbf{b}/2)\Big[1 - \Big(1 - \sigma_{NN}\frac{T_B(\mathbf{r}-\mathbf{b}/2)}{B}\Big)^{B}\Big] \\ & + T_B(\mathbf{r}+\mathbf{b}/2)\Big[1 - \Big(1 - \sigma_{NN}\frac{T_A(\mathbf{r}-\mathbf{b}/2)}{A}\Big)^{A}\Big] \end{aligned} \tag{4.15}$$

If the optical Glauber model is used as a initials state for hydrodynamics one assumes that either n_{BC} or n_{WN} is proportional to the energy density (eBC- or eWN-model) or to the entropy density (sBC- or sWB-model) [46]. However in this thesis the energy density is obtained using the EKRT-model and the optical Glauber model is only used in the centrality determination.

Table 1. The averaged values of impact parameter for different centrality classes in $\sqrt{s_{NN}} = 2.76$ TeV Pb+Pb collisions

centrality (%)	b (fm)
0-5	2.32
5-10	4.24
10-20	6.00
20-30	7.76
30-40	9.19
40-50	10.43
50-60	11.53

4.2.2 Centrality determination

Like in a case of Glauber model geometry of averaged initial state is usually controlled by the impact parameter b, which is not observable quantity. Experimentally collisions are categorized to different centrality classes according to amount of particles created in collision. Similar kind of method to determine centrality class can also be used in case of fluctuating initial state where thousands of randomly sampled events are modeled separately. In case of averaged initial states we only want to simulate one event, with specific impact parameter b, for each centrality class. The connection between impact parameter and centrality classes can be found using the optical Glauber model.

In the optical Glauber model collisions are divided into different centrality classes according to their contribution to the total cross section. In this case the $0-5\%$ centrality class would contribute 5% of the total cross section in such a way that impact parameter would range from 0 to some upper limit b_1, i.e.

$$0.05 = \frac{1}{\sigma_{AB}} \int_0^{b_1} \mathrm{d}^2\mathbf{b} \frac{\mathrm{d}\sigma_{AB}}{\mathrm{d}^2\mathbf{b}}, \tag{4.16}$$

where σ_{AB} and $\mathrm{d}\sigma_{AB}/\mathrm{d}^2\mathbf{b}$ are calculated using Eq.(4.12). From this equation we could then determine value b_1. Eq.(4.16) can be also generalized for the centrality

class $c_i - c_{i+1}\%$. In this case

$$c_{i+1} - c_i = \frac{1}{\sigma_{AB}} \int_{b_i}^{b_{i+1}} \mathrm{d}^2\mathbf{b} \frac{\mathrm{d}\sigma_{AB}}{\mathrm{d}^2\mathbf{b}}. \tag{4.17}$$

Now that we know value of b_1 we can use Eq.(4.17) recursively to obtain all values of b_i. Because we only want to use one impact parameter for specific centrality class we calculate averages $\langle b_i \rangle$.

$$\langle b_i \rangle = \frac{1}{\sigma_{c_i}} \int_{b_i}^{b_{i+1}} \mathrm{d}^2\mathbf{b}\, b\, \frac{\mathrm{d}\sigma_{AB}}{\mathrm{d}^2\mathbf{b}}, \tag{4.18}$$

where

$$\sigma_{c_i} = \int_{b_i}^{b_{i+1}} \mathrm{d}^2\mathbf{b} \frac{\mathrm{d}\sigma_{AB}}{\mathrm{d}^2\mathbf{b}}. \tag{4.19}$$

Now doing simulations with the value $\langle b_i \rangle$ (usually denoted as b) would correspond to centrality class $c_i - c_{i+1}\%$. The dependence between centrality classes and averaged values of impact parameter in case of Pb+Pb collision is shown in Table 1

4.2.3 EKRT model

The original EKRT model was introduced by K.J. Eskola, K. Kajantie, P.V.Ruuskanen and K. Tuominen in 2000 and it was aimed to provide initial conditions for central heavy ion collisions [47]. Later, in 2001, the EKRT model was extended for non-central collisions [46]. In both of these cases the EKRT model made use of a leading order (LO) minijet cross section calculations in perturbative QCD (pQCD). Next-to-leading order (NLO) corrections were introduced to the EKRT model in 2013 together with EBYE fluctuations [9], [48]. This version of EKRT model, but without EBYE fluctuations, is also used in this thesis. However in this section we also go though theory behind EBYE version of EKRT model.

The main idea behind EKRT model is that energy density of initial state comes from energies of multiple low-momentum partonic jets, usually referred as a minijets. Because these minijets are mostly dominated by gluons, heavy ion collision in EKRT model is thought to be more like collision between two gluon clouds than collision between two nuclei. Calculating energy of minijets using pQCD is only possible when a QCD coupling constant α_s is much smaller than unity, which corresponds to a condition that a transverse momentum scale of the minijet p_0 is much larger than the QCD scale factor $\Lambda_{QCD} \approx 220$ MeV. This condition would suggest that it is not possible to calculate energy of all minijets only using pQCD. This problem is solved

in the EKRT model by conjecturing that there exists some saturation momentum p_{sat}, which is the lower limit to the minijet transverse momentum. Physical reasoning behind the saturation momentum is that at some point partons with high transverse momentum, which are produced before ones with low transverse momentum, will fill up whole transverse plane. When gluons that have transverse momentum below p_{sat} are produced afterwards there is no enough space in the transverse plane so that these gluons have to fuse together with gluons which have higher transverse momenta. The most natural way to obtain the saturation momentum would be to first calculate a number of produced partons with $p_T \geq p_0$ and then compare it to available transverse area in order to solve saturation momentum. This was in the fact method which was used to calculate saturation scale in original EKRT model which used LO minijet cross section calculations. However, similar kind of method is no longer valid when extending EKRT model to the NLO because number of produced partons is not infrared safe(adding one infinitesimally soft particle does not change the direction or set of jets) and collinearly safe (collinear splitting will not change jets) quantity in NLO pQCD [49]. In the NLO extension of EKRT model saturation is expected to happen when transverse energy E_T production ends. This corresponds to a moment when transverse plane is fully filled and gluon fusions start, i.e. $(3 \to 2)$ processes start to dominate over usual $(2 \to 2)$ processes. Therefore, saturation is set to take place when rapidity densities of the produced transverse energy fulfill the condition

$$\frac{\mathrm{d}E_T}{\mathrm{d}^2\mathbf{r}\mathrm{d}y}(3 \to 2) \sim \frac{\mathrm{d}E_T}{\mathrm{d}^2\mathbf{r}\mathrm{d}y}(2 \to 2). \tag{4.20}$$

We can further write scaling law for the right-hand side of this equation

$$\frac{\mathrm{d}E_T}{\mathrm{d}^2\mathbf{r}\mathrm{d}y}(2 \to 2) \sim (T_A g)^2 \Big(\frac{\alpha_s^2}{p_0^2}\Big) p_0, \tag{4.21}$$

where g denotes gluon parton distribution functions (PDFs) and T_A refers to nuclear thickness function introduced earlier in section 4.2.1. The factor $T_A g$ is assigned for each of the incoming gluons, α_s^2/p_0^2 comes from partonic cross section $\sigma(2 \to 2)$ and p_0 is introduced as cut-off scale for E_T. Similar way it is possible to write left-hand side of the Eq. (4.20) as

$$\frac{\mathrm{d}E_T}{\mathrm{d}^2\mathbf{r}\mathrm{d}y}(3 \to 2) \sim (T_A g)^3 \frac{1}{p_0^2} \Big(\frac{\alpha_s^3}{p_0^2}\Big) p_0, \tag{4.22}$$

where additional factor p_0^{-2} is introduced to compensate dimensions of extra T_A factor. Now substituting Eqs.(4.21) and (4.22) to the saturation condition Eq.(4.20) we obtain

$$T_A g \sim \frac{p_0^2}{\alpha_s}. \tag{4.23}$$

Taking this scaling law and plugging it back to saturation condition Eq.(4.20) and solving $\mathrm{d}E_T/\mathrm{d}^2\mathbf{r}$ leads to the local saturation criterion

$$\frac{\mathrm{d}E_T}{\mathrm{d}^2\mathbf{r}}(p_0, \sqrt{s_{NN}}, A, \mathbf{r},\mathbf{b}; \beta) = \frac{K_{sat}}{\pi} p_0^3 \Delta y, \tag{4.24}$$

where transverse coordinates are denoted as $\mathbf{r} = (x,y)$, A is mass number of colliding nucleon and $\mathbf{b}$ is the impact parameter. In addition $K_{sat} \sim 1$ is introduced as a α_s independent proportionally constant and Δy is mid-rapidity gap in which minijet transverse energy is produced. In Ref.[9] it is chosen that $\Delta y = 1$, i.e. $|y| \leq 0.5$, which is also chose made in this thesis. Exact value of K_{sat} is prior unknown and it has to be determined from the data. We also note that the condition $p_0 \gg \Lambda_{QCD}$ must still hold because left-hand side of Eq.(4.24) has to be calculated perturbatively. This perturbative part describes the total minijet transverse energy produced into a rapidity window Δy in A+A collision when collision energy is $\sqrt{s_{NN}}$ and it can be calculated as [48]

$$\frac{\mathrm{d}E_T}{\mathrm{d}^2\mathbf{r}}(p_0, \sqrt{s_{NN}}, A, \mathbf{r},\mathbf{b}; \beta) = T_A(\mathbf{r_1}) T_A(\mathbf{r_2}) \sigma \langle E_T \rangle_{p_0,\Delta y,\beta}, \tag{4.25}$$

where $\mathbf{r_{1/2}} = \mathbf{r} \pm \mathbf{b}/2$. Last part, $\sigma\langle E_T\rangle_{p_0,\Delta y,\beta}$, is the first E_T-moment of the minijet E_T distribution and it has to be calculated using pQCD and collinear factorization [50]:

$$\sigma \langle E_T \rangle_{p_0,\Delta y,\beta} = \int_0^{\sqrt{s_{NN}}} \mathrm{d}E_T E_T \left.\frac{\mathrm{d}\sigma}{\mathrm{d}E_T}\right|_{p_0,\Delta y,\beta}, \tag{4.26}$$

where the semi-inclusive E_T distribution of minijets is defined as

$$\left.\frac{\mathrm{d}\sigma}{\mathrm{d}E_T}\right|_{p_0,\Delta y,\beta} = \sum_{n=2}^{3} \frac{1}{n!} \int \mathrm{d}[\mathrm{PS}]_n \frac{\mathrm{d}\sigma^{2\to n}}{\mathrm{d}[\mathrm{PS}]_n} \mathcal{S}_n. \tag{4.27}$$

Further, $\mathrm{d}\sigma^{2\to 2}/\mathrm{d}[\mathrm{PS}]_2$ and $\mathrm{d}\sigma^{2\to 3}/\mathrm{d}[\mathrm{PS}]_3$ are defined as a differential NLO partonic cross sections corresponding $(2 \to 2)$ and $(2 \to 3)$ scatterings respectively. More details about computation of these differential cross sections is found in Ref. [49]. Phase-space differentials are notated as $\mathrm{d}[\mathrm{PS}]_n$ and integration is set to take place in $4 - 2\varepsilon$ dimensions in order to handle infrared divergences. The measurement

functions $\mathcal{S}_2$ and $\mathcal{S}_3$ define the total minijet E_T produced into a rapidity window Δy. Because mass of all partons are small compared to their momentum, the minjet E_T produced in Δy can be calculated as a sum of the final state partons transverse momenta whose rapidities are in Δy

$$E_T = \sum_{i=1}^{n=2,3} \theta(y_i \in \Delta y) p_{Ti}, \tag{4.28}$$

where θ is the Heaviside step function which must not to be confused with expansion rate $\theta = \nabla_\mu u^\mu$. In definition of the measurement functions one also must take account that not all scatterings are perturbative. In case of $(2 \to 2)$ processes perturbative scatterings can be chosen to be ones that fulfill

$$p_{T1} + p_{T2} \geq 2p_0, \tag{4.29}$$

where $p_0 \gg \Lambda_{QCD}$. In this case we see that if at least one particle has rapidity in Δy, then $E_T \geq p_0$. Same kind of condition for perturbative scatterings also generalizes to $(2 \to 3)$ processes

$$p_{T1} + p_{T2} + p_{T3} \geq 2p_0. \tag{4.30}$$

In this case however it is possible that two high-p_T partons fall outside Δy range and only one low-p_T parton with $p_T < p_0$ enters Δy. It is shown in Ref.[] that this kind of behavior adds additional freedom when defining measurement function $\mathcal{S}_3$ and it is possible to restrict the minimum E_T even more in infrared and collinearly safe way by applying condition $E_T \geq \beta p_0$, where $0 \leq \beta \leq 1$. Parameter β is called the hardness parameter and it's exact value has to be determined from the data.

Using the definition of minijet E_T and above restrictions it is now possible to write measurement functions as

$$\mathcal{S}_n = \delta\Big(E_T - \Big[\sum_{i=1}^{n=2,3} \theta(y_i \in \Delta y) p_{Ti}\Big]\Big) \times \theta\Big(\sum_{i=1}^{n=2,3} p_{Ti} \geq 2p_0\Big) \times \theta(E_T \geq \beta p_0) \tag{4.31}$$

Plugging measurement functions back to definition (4.26) and integrating over delta functions first E_T-moment minijet E_T distribution can be written as

$$\sigma\langle E_T\rangle_{p_0,\Delta y,\beta} = \sum_{n=2}^{3} \frac{1}{n!} \int \mathrm{d[PS]}_n \frac{\mathrm{d}\sigma^{2\to n}}{\mathrm{d[PS]}_n} \tilde{\mathcal{S}}_n, \tag{4.32}$$

where

$$\tilde{\mathcal{S}}_n = \Big(\sum_{i=1}^{n=2,3} \theta(y_i \in \Delta y) p_{Ti} \Big) \times \theta\Big(\sum_{i=1}^{n=2,3} p_{Ti} \geq 2p_0 \Big) \times \theta\Big(\sum_{i=1}^{n=2,3} \theta(y_i \in \Delta y) p_{Ti} \geq \beta p_0 \Big). \tag{4.33}$$

Now substituting Eq.(4.32) back to saturation criterion (4.24) it is possible to solve numerically saturation momentum $p_{sat}(\mathbf{r}) = p_0(\mathbf{r})$. In order to calculate the initial state energy density we first note that hydrodynamic evolution is done in light-cone coordinates τ and η_s, which are defined as

$$\tau = \sqrt{t^2 - z^2}, \;\; \eta_s = \frac{1}{2} \ln\Big(\frac{t+z}{t-z}\Big) \tag{4.34}$$

so that $t = \tau \cosh(\eta_s)$ and $z = \tau \sinh(\eta_s)$. Coordinate η_s is called the space-time rapidity and τ is the longitudinal proper time. In mid-rapidity, when $y \approx 0$ it can be shown that space-time rapidity is equal to momentum rapidity, i.e. $\eta_s \approx y$. Because we are studying case when $|y| \leq 0.5$ this seems to be a reasonable approximation, and we can write infinitesimal volume element in form

$$\mathrm{d}V = \mathrm{d}^2\mathbf{r}\mathrm{d}z = \mathrm{d}^2\mathbf{r}(\mathrm{d}\tau \sinh(\eta_s) + \mathrm{d}\eta_s \tau \cosh(\eta_s)) \approx \tau \mathrm{d}^2\mathbf{r}\Delta y \tag{4.35}$$

Now using saturation criterion (4.24) energy density at the formation time τ_s can be written as

$$\varepsilon(\mathbf{r}, \tau_s(\mathbf{r})) = \frac{\mathrm{d}E_T}{\mathrm{d}V} = \frac{\mathrm{d}E_T}{\mathrm{d}^2\mathbf{r}} \frac{1}{\tau_s(\mathbf{r})\Delta y} = \frac{K_{sat}}{\pi} (p_{sat}(\mathbf{r}))^4, \tag{4.36}$$

where the formation time of minijet plasma is given by $\tau_s(\mathbf{r}) = 1/p_{sat}(\mathbf{r})$, like in Refs.[9], [51]. Here it is important to note that the formation time depends on spatial coordinates, but initial energy density which is used in a hydrodynamics must be at fixed time. This fixed time is obtained by setting a minimum saturation momentum $p_{sat}^{min} = 1$ GeV for which pQCD calculations are still viable. This minimum saturation momentum then corresponds to a maximum formation time $\tau_0 = 1/p_{sat}^{min} \approx 0.2$ fm. The step which describes evolution between the local formation time $\tau_s(\mathbf{r})$ and the maximum formation time τ_0 is called a pre-thermal evolution. There are two alternative choices how the pre-thermal evolution can be done in EKRT-model. The first way is to use scaling which preserves the transverse energy. In this kind of situation first equality of Eq.(4.36) holds for all times and we can write

$$\varepsilon(\mathbf{r}, \tau_0) = \varepsilon(\mathbf{r}, \tau_s(\mathbf{r})) \Big(\frac{\tau_s(\mathbf{r})}{\tau_0} \Big). \tag{4.37}$$

This kind of scaling is often also called as a free streaming (FS). Another way to handle the pre-thermal evolution is to use the Bjorken hydrodynamic scaling (BJ) [52]

$$\varepsilon(\mathbf{r}, \tau_0) = \varepsilon(\mathbf{r}, \tau_s(\mathbf{r}))\left(\frac{\tau_s(\mathbf{r})}{\tau_0}\right)^{4/3}, \tag{4.38}$$

where work done by a pressure reduces energy almost by a maximum amount. In this thesis all calculations are done by using BJ pre-thermal evolution.

At the some point when trying to calculate saturation momenta in the edges of the system there is the region where solution of the saturation criteria will give momentum smaller than p_{sat}^{min}. In these regions pQCD calculations become questionable and we are no longer able to use Eq.(4.36) to calculate energy densities. This problem is solved by smoothly connecting BJ-evolved energy densities to the binary profile, which is used outside validity of pQCD. In other words when $p_{sat} < p_{sat}^{min}$, the energy density is parameterized as $\varepsilon = C(T_A T_A)^n$ where

$$n = \frac{1}{2}\left[(k+1) + (k-1)\tanh\left(\frac{\sigma_{NN} T_A T_A - g}{\delta}\right)\right]. \tag{4.39}$$

Here σ_{NN} is the total inelastic nucleon-nucleon cross-section and $g = \delta = 0.5$ fm^{-2}. The parameters C and k are adjusted so that the energy density is smooth function when $p_{sat} = p_{sat}^{min}$.

The whole above procedure leads to the energy density profile for the averaged initial state. The figure 3 shows these averaged initial states for 0-5% and 30-40% centrality classes in Pb+Pb collision with $\sqrt{s_{NN}} = 2.76$ TeV and $K_{sat} = 0.52$. The impact parameters corresponding to a different centrality classes were obtained using the optical Glauber model as discussed in section 4.2.2. The initial collision time was set to $\tau_0 = 0.2$ fm and hardness parameter to $\beta = 0.8$ which will remain unchanged for all the simulations done in this thesis. From Fig.3 we can see that energy density profile for 30-40% centrality is narrower and more asymmetrical compared to 0-5% centrality. Maximum value of the energy density is also lower when centrality class is 30-40% . These kinds of results are expected considering that the collision zone gets smaller and more asymmetric when increasing impact parameter, i.e. going to the higher centrality classes.

Even though only the averaged initial states are used in the simulations done in this thesis, it is interesting to see how EBYE fluctuations affect to the initial state. The main reason behind the EBYE fluctuations is that the positions of the nucleons

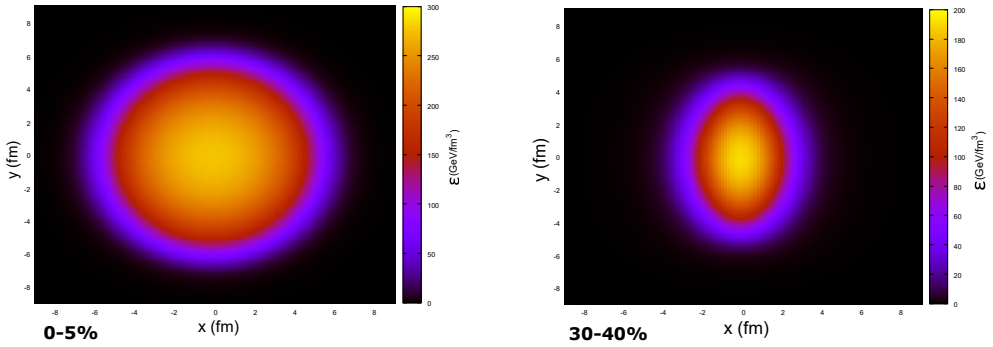

(a) **(b)**

Figure 3. Initial energy densities in $\sqrt{s_{NN}} = 2.76$ TeV Pb+Pb collision at $\tau_0 = 0.2$ fm in the 0-5% (a) and 30-40% (b) centrality classes. The pre-thermal evolution is done using BJ and values of parameters are set to $K_{sat} = 0.52$, $\beta = 0.8$.

randomly fluctuate inside the colliding nuclei. One of the challenges in fluctuating initial state is that nucleons have finite size and finding their distribution inside nuclei is not a trivial task. Fortunately, at least in case of Pb nucleus, standard Woods-Saxon parameterization for charge density is within the error bars of the nucleon distribution and it can be used in practical calculations [53]. The nucleon positions can then be sampled using Woods-Saxon parameterization. In order to get enough statistics for reliable result one needs to sample nucleon positions for around 10000 events. It is also important to note that positions of nucleons are sampled separately for both colliding nuclei. After positions of nucleons are known, it is still necessary to define how these positions correspond to changes in geometry of collision. This is done by defining nuclear thickness function T_A as a sum of the nucleon thickness functions T_n:

$$T_A(\mathbf{r}) = \sum_{i=1}^{A} T_n(|\mathbf{r} - \mathbf{r_i}|), \tag{4.40}$$

where $\mathbf{r_i}$ is the position of nucleon in given nucleus and T_n have been normalized to unity. Because the production of minijets is mostly dominated by gluons, the T_n can be understood as a gluonic thickness function which is given by [9], [54]

$$T_n(r) = \frac{1}{2\pi\sigma^2} e^{-r^2/(2\sigma^2)}, \tag{4.41}$$

where $\sigma \approx 0.43$ fm. Now saturation momentum can again be solved from saturation

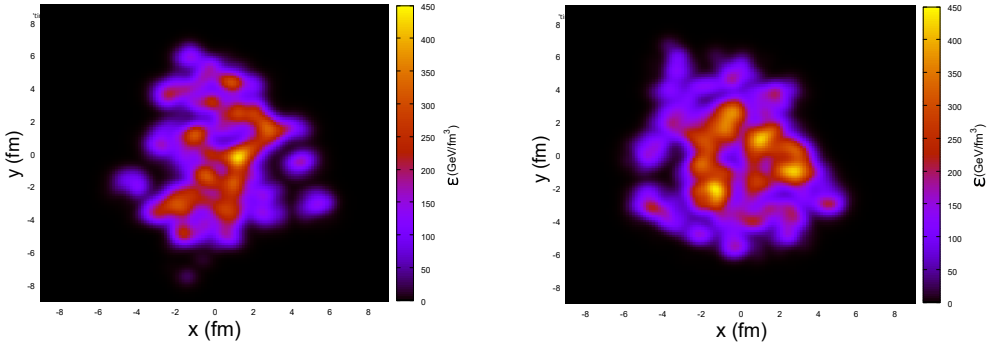

Figure 4. EBYE Initial energy densities in $\sqrt{s_{NN}} = 2.76$ TeV Pb+Pb collision at $\tau_0 = 0.2$ fm for two different nucleon sampling. The pre-thermal evolution is done using BJ and values of parameters are set to $K_{sat} = 0.52$, $\beta = 0.8$.

criteria (4.24) and energy densities can be calculated similarly as in case of averaged initial state. Final BJ-evolved initial state for couple of events is shown in figure 4. We can see that there are multiple peaks at the energy density profile compared to the averaged initial state and the position of these peaks vary greatly event to event. As seen in Refs.[9], [10] EBYE EKRT-model seems to produce data very well in most of the measurements. As a downside computing thousands of events in order to get good statistic is computationally rather expensive.

4.3 Hydrodynamics and boost-invariance

The general structure of hydrodynamics is already derived in section 2 where we discussed about the conservation of the energy-momentum tensor and the particle number. In case of the heavy-ion collisions one typically replaces the particle number with the baryon number, which describes difference between number of quarks and antiquarks. In most of the high energy collisions one usually assumes that baryon density n_B is close to zero and focuses only in the energy momentum tensor. This assumption is also done in this thesis. In this case system is described by equilibrium quantities ε, p_0, u^μ and dissipative quantities $\Pi, \pi^{\mu\nu}$.

The equations of motion for dissipative quantities were derived in section 3.4, but we did not do systematic power counting in terms of Knudsen and inverse Reynolds numbers. In addition we only studied case where $r = 0$ in Eqs.(3.60),(3.62) and (3.63), but in more accurate case one takes account all values of r. More accurate

derivation for equations of motion of dissipative quantities is done in Ref.[29] and when $n_B = 0$ it leads to

$$\tau_\Pi \dot{\Pi} + \Pi = -\zeta\theta - \delta_{\Pi\Pi}\Pi\theta + \lambda_{\Pi\pi}\pi^{\mu\nu}\sigma_{\mu\nu} + \varphi_1\Pi^2 + \varphi_3\pi^{\mu\nu}\pi_{\mu\nu}, \tag{4.42}$$

$$\begin{aligned}\tau_\pi \dot{\pi}_r^{\langle\mu\nu\rangle} + \pi^{\mu\nu} =& 2\eta\sigma^{\mu\nu} + 2\omega_\alpha^{\langle\mu}\pi^{\nu\rangle\alpha} - \delta_{\pi\pi}\theta\pi^{\mu\nu} - \tau_{\pi\pi}\sigma_\alpha^{\langle\mu}\pi^{\nu\rangle\alpha} + \lambda_{\pi\Pi}\Pi\sigma^{\mu\nu} \\ & \varphi_6\Pi\pi^{\mu\nu} + \varphi_7\pi_\alpha^{\langle\mu}\pi^{\nu\rangle\alpha}.\end{aligned} \tag{4.43}$$

The structure of these equations differs from equations (3.90) and (3.92) only by terms which are second power of inverse Reynolds number, i.e. terms with transport coefficients φ_i. However, even all other transport coefficients are not the same than in appendix B. When using these equations of motion, it useful to write all transport coefficients in terms of equilibrium quantities ε and p_0. This can be done in a limit $m \ll T$ in which case transport coefficients for bulk viscous pressure can be written as [55]

$$\begin{aligned}\frac{\zeta}{\tau_\Pi} &= 14.55 \times \left(\frac{1}{3} - c_s^2\right)^2 (\varepsilon + p_0), \\ \frac{\delta_{\Pi\Pi}}{\tau_\Pi} &= \frac{2}{3}, \\ \frac{\lambda_{\Pi\pi}}{\tau_\Pi} &= \frac{8}{5}\left(\frac{1}{3} - c_s^2\right)\end{aligned} \tag{4.44}$$

where c_s is the speed of sound. In similar limit transport coefficients for shear viscosity can also be obtained [32], [55]. These read

$$\begin{aligned}\frac{\eta}{\tau_\pi} &= \frac{\varepsilon + p_0}{5}, \\ \frac{\delta_{\pi\pi}}{\tau_\pi} &= \frac{4}{3}, \\ \frac{\tau_{\pi\pi}}{\tau_\pi} &= \frac{10}{7}, \\ \frac{\lambda_{\pi\Pi}}{\tau_\pi} &= \frac{6}{5}, \\ \varphi_7 &= \frac{9}{70 p_0}.\end{aligned} \tag{4.45}$$

Unfortunately convenient forms for coefficients φ_3 and φ_6 have not yet been obtained and for this reason they are left out when doing hydrodynamic simulations. From Eqs.(4.44) and (4.45) one can see that rest of the transport coefficients can be

expressed either using the bulk viscosity coefficient ζ or the shear viscosity coefficient η. The coefficients ζ and η have to be fitted based on the data.

Generally hydrodynamic equations are solved in 3+1 dimensions, i.e we have 3 spatial and one time coordinate. However, if one assumes longitudinal boost-invariance to the system (system is invariant under Lorentz-boosts in z direction), one can eliminate one of the spatial dimensions and only solve hydrodynamics in 2+1 dimensional system. The idea of boost-invariance, in context of heavy-ion collisions, was first introduced by J.D.Bjorken [52]. The assumption about boost-invariance is based on the experimental fact that in the mid-rapidity region the total particle multiplicity seems to remain constant, as can be seen in figure 5. In case of boost-invariance most natural coordinates for the system are (τ,x,y,η_s) coordinates, where longitudinal proper time τ and spacetime rapidity η_s are defined in Eq.(4.34). The assumption about boost-invariance is then consistent to a definition that the longitudinal flow velocity $u^z = z/t$ and that all hydrodynamic quantities are independent of the spacetime rapidity η_s. As we see in section 4.5.2 choices made above lead eventually to the particle spectrum which is independent of rapidity y.

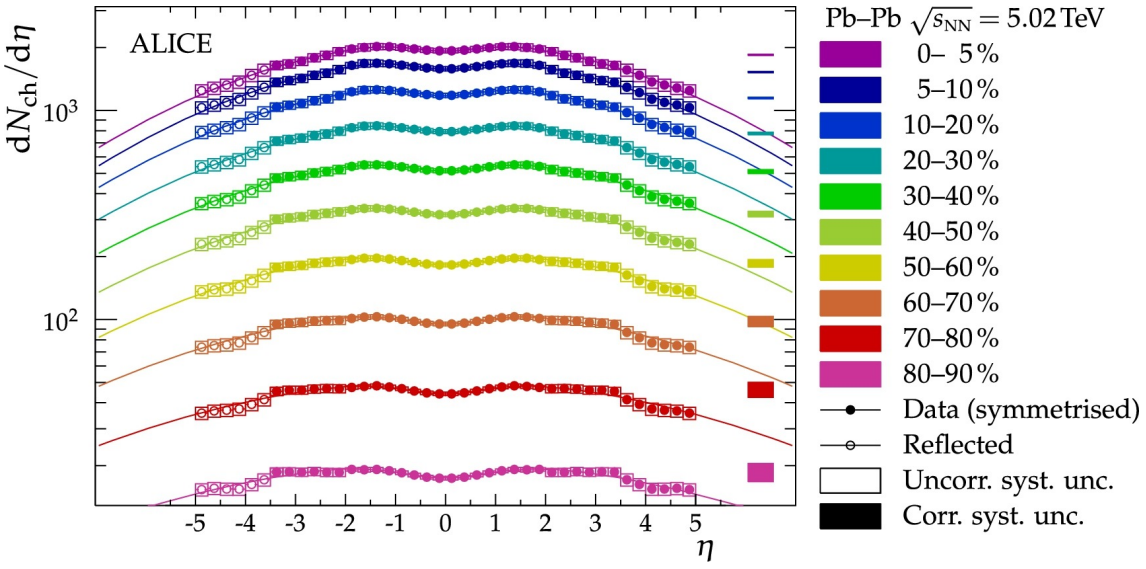

Figure 5. Charged particle pseudorapidity distribution in several centrality classes measured by ALICE for Pb+Pb collisions at $\sqrt{s_{NN}} = 5.02$ TeV. From Ref.[56].

4.4 Equation of state

An equation of state describes thermodynamic properties of the system and it gives relations between various thermodynamic quantities, such as energy density, temperature and pressure. The relation $p = p(\varepsilon, n)$ is in fact necessary to close the system of hydrodynamic conservation equations (2.60).

In case of heavy ion collisions we are interested about behavior of strongly interacting matter which consist two different phases: QGP and hadron gas. Recent lattice QCD calculations have shown that at zero baryon chemical potential the phase transition between these two phases should happen around $T = 154 \pm 9$ MeV [57]. Schematic phase diagram for this kind of matter is presented in figure 6. From this figure we see that at the large collision energies, baryon chemical potential goes close to zero and it can be neglected. This is also why baryon density is usually approximated as a zero and EoS $p = p(\varepsilon)$ is enough when solving equations of motion for the hydrodynamics. At the extremely large chemical potential phase diagram seems to indicate that there exist phase called color superconductor in which quark matter is in condensate state. However, this kind of phase is only theoretical right now and it is thought to only exist in the core of neutron stars.

In this thesis we use the sp95-PCE parameterization for equation of state [58], [59]. This parameterization models hadron gas phase as gas consisting non-interacting hadrons and resonances, which have masses up to 2 GeV. EoS for this so called hadron resonance gas (HRG) can be calculated from thermodynamics and it reads

$$p^{HRG}(T,\mu_i) = \frac{T}{V}\sum_i \ln Z_i(T,V,\mu_i), \tag{4.46}$$

where we sum over all hadrons and resonances. The partition function is defined as

$$\ln Z_i(T,V) = \frac{V g_i}{T}\int_0^\infty \frac{\mathrm{d}^3\mathbf{k}}{(2\pi)^3}\frac{1}{e^{(\mu_i - E_i)/T} \pm 1}, \tag{4.47}$$

where g_i is degeneracy factor and E_i is particles energy. The positive sign in partition function corresponds to fermions and negative sign to bosons. Relation between energy density and pressure can then be obtained using thermodynamic relations (2.24).

Modeling QGP phase is done by using a lattice QCD results from the hotQCD collaboration [60], [61]. In the lattice QCD partition function is expressed as path integral over the classical action and then discretised so that integrals are replaced

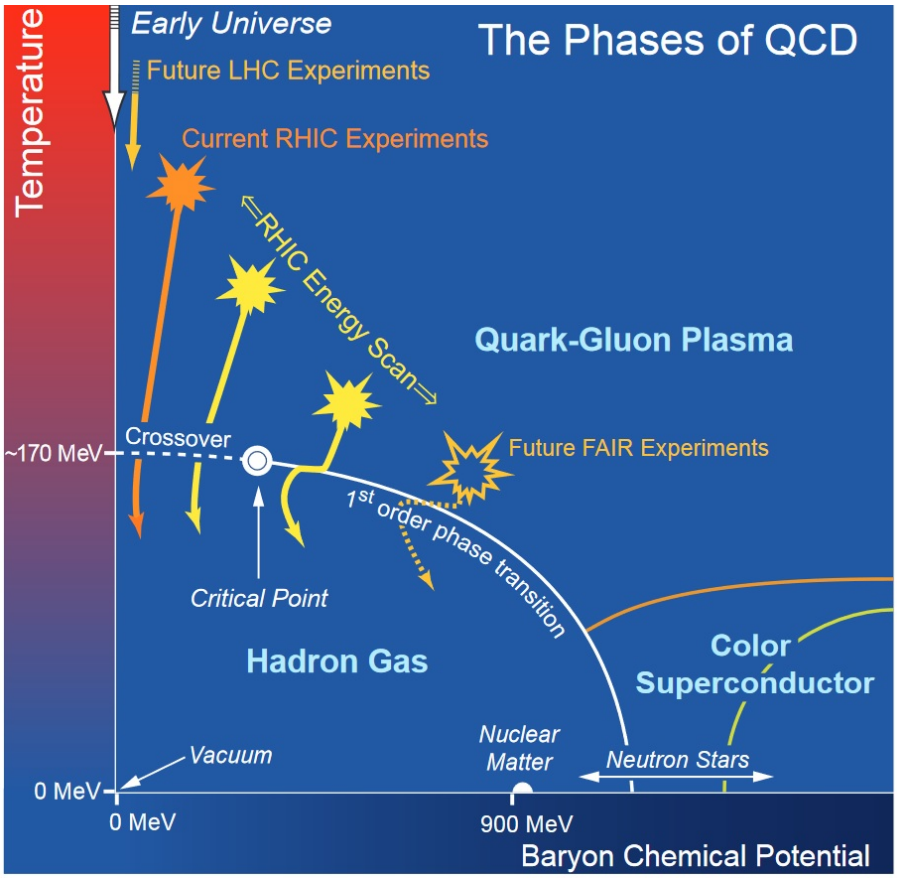

Figure 6. The phase diagram of strongly interacting matter. From Ref.[62].

by sums over fermion fields which occupy nodes in the lattice. These sums are then done in discrete space-time lattice over N_σ^3 spatial and N_τ temporal steps which are related to the systems volume and temperature:

$$V = (aN_\sigma)^3 \;\; T = \frac{1}{aN_\tau}, \tag{4.48}$$

where a is the lattice spacing. Physical continuum and thermodynamic limit is obtained by doing calculation with different lattice sizes keeping ratio N_σ/N_τ constant and then extrapolating to limit $a \to 0, N_\tau \to \infty, V \to \infty$.

After partition function is calculated in lattice, EoS can be computed using trace anomaly [60], [63]

$$\Theta(T) = \varepsilon - 3p = -\frac{T}{V}\frac{\mathrm{d}\ln Z}{\mathrm{d}\ln a}. \tag{4.49}$$

With use of thermodynamic identities (2.24) we can also write

$$\frac{\Theta(T)}{T^5} = \frac{\varepsilon - 3p}{T^5} = \frac{\mathrm{d}}{\mathrm{d}T}\left(\frac{p}{T^4}\right). \tag{4.50}$$

Integrating both sides we obtain

$$\frac{p(T)}{T^4} = \frac{p(T_0)}{T_0^4} + \int_{T_0}^{T} \mathrm{d}T' \frac{\Theta(T')}{T'^5}, \tag{4.51}$$

where T_0 is some reference temperature which can be calculated using HRG model. Again after solving $p = p(T)$ we can easily solve $p = p(\varepsilon)$ with use of thermodynamics.

Connecting lattice QCD calculations to HRG smoothly leads to the equation of state which is demonstrated on Fig.7. Temperature dependence of other thermodynamic quantities is shown in Fig.8. As we can see, there are no discontinuities at the phase transition temperature. This means that strongly interacting matter don't have phase transition in canonical sense, even thought QGP and HRG are clearly different states of matter. This kind of phase transition is usually called crossover phase transition. Even water has this kind phase transition when temperature rises above critical point.

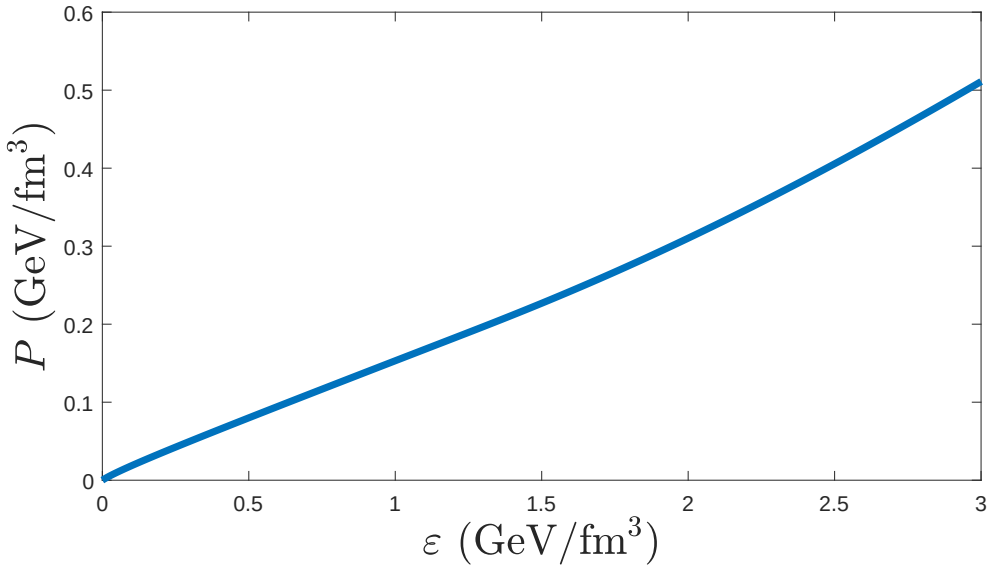

Figure 7. Pressure as a function of energy density at $n_B = 0$.

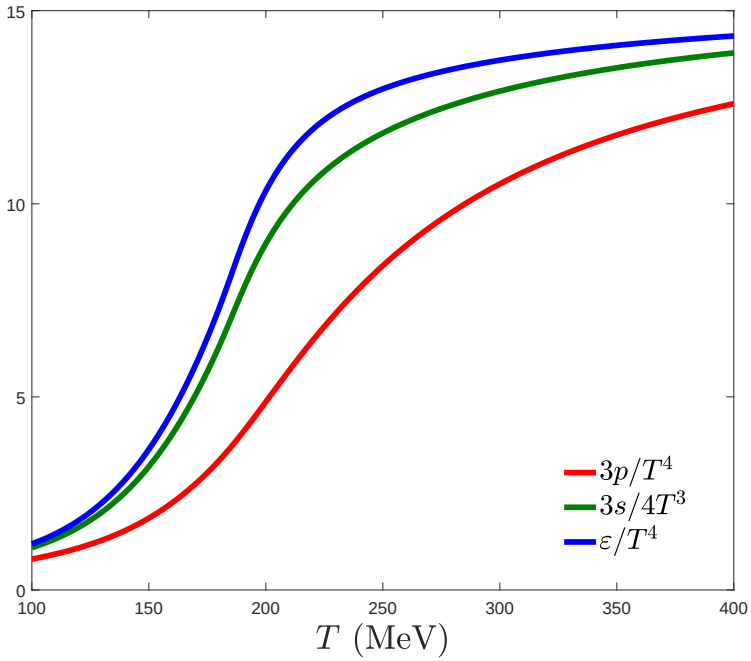

Figure 8. Temperature dependence of different thermodynamic quantities at $n_B = 0$

4.5 Particle freeze-out

In the hydrodynamic phase QGP expands, cools down and experiences phase transition to the hadron gas. This hadron gas keeps expanding until at some point hadrons are so far away from each other that interactions between them stop and freeze-out takes place. Freeze-out stage is divided into two parts: chemical and thermal freeze-out.

4.5.1 Chemical freeze-out

Chemical freeze-out is defined as a point in which all inelastic processes that convert one types of hadrons into a different ones end. Usually one assumes that chemical freeze-out happens when temperature reaches value T_{chem}. If system would evolve according to ideal hydrodynamics this would fix number of hadrons to a constant for each hadron specie separately, i.e. $N_i(T \leq T_{chem}) = N_i(T_{chem})$. This effect is caused by the fact that entropy is conserved in ideal hydrodynamics. In dissipative hydrodynamics entropy is no longer conserved even though there is only small

amount of entropy production bellow $T = 175$ MeV. However, because hadrons cannot change species after chemical freeze-out, the rations between hadrons will remain fixed. Therefore adding chemical freeze-out will add additional constraints to equation of state and slightly change behavior of the hadronic part. In this thesis we use couple of different parametrization which use either 150 MeV or 175 MeV temperature for chemical freeze-out. More details about chemical freeze-out can be found in Refs.[59], [64].

4.5.2 Thermal freeze-out

What we call thermal freeze-out is a moment in which all collision processes that change particles momentum stop. At this stage system is no longer in local thermal equilibrium and hydrodynamics cannot be used to describe the system. On the other hand, only final hadron spectra is observable in experiments, so one needs some method to convert a hydrodynamic quantities into hadrons. Most common way to do this is to use so called Cooper-Frye decoupling procedure [65]. In Cooper-Frye procedure one defines decoupling hypersurface σ^μ in which thermal freeze-out happens. In this thesis decoupling surface is chosen to be constant temperature hypersurface defined by decoupling temperature $T_{dec} = 100$ MeV. Number of specific type of hadrons going through this hypersurface can be calculated as

$$N_i = \int_\sigma \mathrm{d}\sigma_\mu N_i^\mu, \tag{4.52}$$

where index i denotes particles type and $\mathrm{d}\sigma_\mu$ is the normal vector of the surface element, which points outwards of the surface. Using kinetic theory definition of particle 4-current N^μ from Eq. (3.4) leads to a Lorentz-invariant hadron spectrum

$$E\frac{\mathrm{d}^3 N_i}{\mathrm{d}^3\mathbf{p}} = \frac{g_i}{(2\pi)^3}\int_\sigma \mathrm{d}\sigma_\mu p_i^\mu f_i(x,p), \tag{4.53}$$

where p_i^μ is the four-momentum and f_i is hadrons distribution function. Generally surface integral over hypersurface σ contains three integrals. However, in case of boost-invariance one of the integrals can be calculated analytically. Lets see how this is done explicitly. Because we assume that system is boost-invariant, the freeze-out hypersurface is independent of coordinate η_S and we can parameterize it as $\tau = \tau(x,y)$. In this case surface 4-vector in (τ,x,y,η_s) coordinates is given by

$$\sigma^\mu = (\tau(x,y),x,y,0). \tag{4.54}$$

However we want to express this in (t,x,y,z)-coordinates in order to make contraction with p^μ. This kind of transformation from (τ,x,y, η_s)-coordinates to (t,x,y,z)-coordinates is done by a matrix

$$X^\mu_{\nu'} = \frac{\partial x^\mu}{\partial x^{\nu'}} = \begin{pmatrix} \cosh\eta_s & 0 & 0 & \tau\sinh\eta_s \\ 0 & 1 & 0 & 0 \\ 0 & 0 & 1 & 0 \\ \sinh\eta_s & 0 & 0 & \tau\cosh\eta_s \end{pmatrix}. \tag{4.55}$$

Now we can write the surface vector in (t,x,y,z)-coordinates as

$$\sigma^\mu = X^\mu_{\nu'}\sigma^{\nu'} = (\tau(x,y)\cosh\eta_s, x, y, \tau(x,y)\sinh\eta_s). \tag{4.56}$$

In general normal vector $\mathrm{d}\sigma_\mu$ on 3-dimensional hypersurface, which can be parameterized in terms of three parameters u,v and w, is determined by

$$\mathrm{d}\sigma_\mu = \epsilon_{\mu\nu\alpha\beta}\frac{\partial\sigma^\nu}{\partial u}\frac{\partial\sigma^\alpha}{\partial v}\frac{\partial\sigma^\beta}{\partial w}\mathrm{d}u\mathrm{d}v\mathrm{d}w, \tag{4.57}$$

where $\epsilon_{\mu\nu\alpha\beta}$ is totally antisymmetric fourth rank permutation tensor for which $\epsilon_{\mu\nu\alpha\beta} = -1$ for all even permutations of (0,1,2,3). Using this identity it is possible to write normal vector of the hypersurface as

$$\mathrm{d}\sigma_\mu = -[\pm](\cosh\eta_s, -\frac{\partial\tau}{\partial x}, -\frac{\partial\tau}{\partial y}, -\sinh\eta_s)\tau\mathrm{d}x\mathrm{d}y\mathrm{d}\eta_s, \tag{4.58}$$

where additional factor $[\pm]$ =sign($\partial T/\partial\tau$) is added so that normal vector of the surface element points outwards from the surface to the smaller temperature. In (t,x,y,z)-coordinates four-momentum p^μ can be written in terms of rapidity y:

$$p^\mu_i = (m_{T,i}\cosh y, \mathbf{p}_{T,i}, m_{T,i}\sinh y), \tag{4.59}$$

where $\mathbf{p}_{T,i}$ is the transverse momentum vector and $m_{T,i}$ is transverse mass defined as

$$m_{T,i} = \sqrt{m_i^2 + p_{T,i}^2}. \tag{4.60}$$

Combining Eqs.(4.58) and (4.59) we obtain

$$\mathrm{d}\sigma_\mu p^\mu_i = -[\pm]\Big(m_{T,i}\cosh(y-\eta_s) - p^x_i\frac{\partial\tau}{\partial x} - p^y_i\frac{\partial\tau}{\partial y}\Big)\tau\mathrm{d}x\mathrm{d}y\mathrm{d}\eta_s. \tag{4.61}$$

Now that we have written out the surface part $d\sigma_\mu p^\mu_i$ we still must deal with distribution functions $f_i(x,p)$. Like in section 3, we write distribution function as sum of equilibrium part f_{0i} and some correction δf_i:

$$f_i(x,p) = f_{0i} + \delta f_i, \tag{4.62}$$

$$f_{0i} = \Big[\exp\Big(\frac{p_i^\mu u_\mu - \mu_i}{T}\Big) \pm 1\Big]^{-1}. \tag{4.63}$$

Lets first study case where we only have equilibrium distribution. In this case distribution function can be expanded using relation:

$$\frac{1}{e^x \pm 1} = \frac{e^{-x}}{1 \pm e^{-x}} = e^{-x}\sum_{n=0}^{\infty}(\mp 1)^n e^{-nx} = \sum_{n=1}^{\infty}(\mp 1)^{n-1}e^{-nx}, \tag{4.64}$$

where geometrical series is used when expanding $(1 \pm e^{-x})^{-1}$. Now we can write

$$f_{0i} = \sum_{n=1}^{\infty}(\mp 1)^{n-1}\exp\Big(\frac{n\mu_i - np_i^\mu u_\mu}{T}\Big). \tag{4.65}$$

In addition we note that 4-velocity can be written in (t,x,y,z)-coordinates in form of

$$u^\mu = \gamma(1, u^x, u^y, z/t) = \gamma_T(\cosh\eta_s, \mathbf{v_T}, \sinh\eta_s), \tag{4.66}$$

where

$$\mathbf{v_T} = (u^x, u^y)\cosh\eta_s, \quad \gamma_T = (1 - v_T^2)^{-1/2}. \tag{4.67}$$

Contracting this 4-velocity with 4-momentum from Eq.(4.59) we get

$$p_i^\mu u_\mu = \gamma_T(m_{T,i}\cosh(y - \eta_s) - \mathbf{p_{T,i}}\cdot\mathbf{v_T}). \tag{4.68}$$

Now putting Eqs.(4.61),(4.65) and (4.68) back to Cooper-Frye integral formula (4.53) we obtain

$$\begin{aligned} E\frac{\mathrm{d}^3N_i}{\mathrm{d}^3\mathbf{p}} = &-\frac{g_i}{(2\pi)^3}\sum_{n=1}^{\infty}(\mp 1)^{n-1}\int \mathrm{d}x\mathrm{d}y'[\pm]\tau\exp\Big(n\frac{\mu_i + \gamma_T - \mathbf{p_{T,i}}\cdot\mathbf{v_T}}{T}\Big) \\ &\times\int_{-\infty}^{\infty}\mathrm{d}\eta_s\Big[m_{T,i}\cosh(y-\eta_s) - p_i^x\frac{\partial\tau}{\partial x} - p_i^{y'}\frac{\partial\tau}{\partial y'}\Big] \\ &\times\exp\Big(-\frac{\gamma_T m_{T,i}}{T}n\cosh(y-\eta_s)\Big), \end{aligned} \tag{4.69}$$

where we denoted spatial y-coordinate as y' in order to separate it from rapidity y. From this form of the hadron spectrum we can see that all dependence of rapidity y and η_s come through combination $y - \eta_s$. In addition contribution from η_s integral is dominated by region $y \approx \eta_s$ and exponentially suppressed in elsewhere. Now we finally see that assumption made in section 4.3 that hydrodynamic variables are independent of η_s indeed leads to y independent particle spectrum. We also notice that we can do change of variables $\eta' = y - \eta_s$ which leads to y independent hadron

spectrum. In a matter of fact after this kind of change of variables η_s integral can be done analytically and written in terms of modified Bessel functions of the second kind:

$$E\frac{\mathrm{d}^3N_i}{\mathrm{d}^3\mathbf{p}} = -\frac{g_i}{(2\pi)^3}\sum_{n=1}^{\infty}(\mp 1)^{n-1}\int \mathrm{d}x\mathrm{d}y'[\pm]\tau\exp\left(n\frac{\mu_i+\gamma_T-\mathbf{p_T}\cdot\mathbf{v_T}}{T}\right) \times\left[m_{T,i}\mathrm{K}_1\Big(n\frac{\gamma_T m_{T,i}}{T}\Big)-\Big(p_i^x\frac{\partial\tau}{\partial x}-p_i^{y'}\frac{\partial\tau}{\partial y'}\Big)\mathrm{K}_0\Big(n\frac{\gamma_T m_{T,i}}{T}\Big)\right]. \tag{4.70}$$

When comparing results to the data it is useful to write left hand side of Cooper-Frye integral in terms of rapidity y:

$$E\frac{\mathrm{d}^3N_i}{\mathrm{d}^3\mathbf{p}} = 2\frac{\mathrm{d}^3N_i}{\mathrm{d}y\mathrm{d}p_T^2d\phi}, \tag{4.71}$$

where ϕ is the polar coordinate angle of the momentum vector. From this form it then easy to integrate over transverse momentum or angle ϕ to obtain different observable quantities.

Next let's study viscous correction to this equilibrium spectra. We did see in section 3.4 that correction to the equilibrium distribution f_{0i} can be written in form

$$\delta f = f_0\tilde{f}_0\phi = f_0\tilde{f}_0\Big(c_0+c_1E+c_2E^2+c_0^{\langle\mu\nu\rangle}p_{\langle\mu}p_{\nu\rangle}\Big), \tag{4.72}$$

where coefficients c_0,c_1,$c_2 \sim \Pi$ and $c_0^{\langle\mu\nu\rangle} \sim \pi^{\mu\nu}$ are defined in Eqs.(3.69) and (3.81). We also left out index i in order to simplify notation. In this thesis we only consider freeze-out corrections which are caused by shear viscosity. In this case Eq.(4.72) simplifies to

$$\delta f = f_0\tilde{f}_0\frac{p_\mu p_\nu\pi^{\mu\nu}}{2J_{42}}, \tag{4.73}$$

where

$$J_{nq} = \frac{1}{(2q+1)!!}\int dK E_k^{n-2q}(-\Delta_{\alpha\beta}k^\alpha k^\beta)^q f_{0k}\tilde{f}_{0k}, \tag{4.74}$$

and one must remember that $E_k = k^\mu u_\mu \neq E$. Now we can expand $f_0\tilde{f}_0$ similarly than what we did for f_0:

$$f_0\tilde{f}_0 = f_0(1\mp f_0) = \sum_{n=1}^{\infty} n(\pm)^{n+1}\exp\left(\frac{n\mu_i - np_i^\mu u_\mu}{T}\right). \tag{4.75}$$

However in practice we can take only first term from this series because this sum converges quickly and we already study a small correction to the equilibrium hadron

spectra. In this approximation we see that f_0 behaves like the classical Boltzmann gas, so

$$f_0\tilde{f}_0 \approx f_0 = \exp\Big(\frac{\mu - p^\mu u_\mu}{T}\Big). \tag{4.76}$$

For classical Boltzmann gas we can get relations between thermodynamic integrals J_{nq}. This can be most conveniently done by doing partial integration in fluids rest frame where $u^\mu = (1,0,0,0)$, $E_k = k^0$ and $-\Delta_{\alpha\beta}k^\alpha k^\beta = |\mathbf{k}|^2$. In this case:

$$\begin{aligned}
J_{nq} = & I_{nq} = -\frac{T}{(2q+1)!!}\int \underbrace{\frac{dK}{g\mathrm{d}^3k/(2\pi)^3 k_0}} E_k^{n-2q}(-\Delta_{\alpha\beta}k^\alpha k^\beta)^q \underbrace{\frac{\partial|\mathbf{k}|}{\partial E_k}}_{E_k/|\mathbf{k}|}\frac{\partial}{\partial|\mathbf{k}|}f_0 \\
&= \frac{T}{(2q+1)!!}\int \frac{\mathrm{d}\Omega\,\mathrm{d}|\mathbf{k}|}{(2\pi)^3}\frac{\partial}{\partial|\mathbf{k}|}\Big(g|\mathbf{k}|^{2q+1}E_k^{n-2q}\Big)f_0 \\
&= \frac{T}{(2q+1)!!}\int \frac{\mathrm{d}\Omega\,\mathrm{d}|\mathbf{k}|}{(2\pi)^3} g\Big((2q+1)|\mathbf{k}|^{2q}E_k^{n-2q} \\
&+ (n-2q)|\mathbf{k}|^{2q+1}E_k^{n-2q-1}\frac{|\mathbf{k}|}{E_k}\Big)f_0 \\
&= \frac{T}{(2q+1)!!}\int dK\Big((2q+1)(-\Delta_{\alpha\beta}k^\alpha k^\beta)^{q-1}E_k^{n-1-2q} \\
&+ (n-2q)(-\Delta_{\alpha\beta}k^\alpha k^\beta)^q E_k^{n-2q-1}\frac{|\mathbf{k}|}{E_k}\Big)f_0 \\
&= T\Big(I_{n-1,q-1} + (n-2q)I_{n-1,q}\Big),
\end{aligned} \tag{4.77}$$

where we neglected surface term because f_0 vanishes exponentially when $|\mathbf{k}| \to \infty$. Using this relation two times for J_{42} we obtain

$$J_{42} = T^2(\varepsilon + p_0), \tag{4.78}$$

where we used kinetic theory definitions for $\varepsilon = I_{20}$ and $p_0 = I_{21}$. Now we can write viscous correction in simple form

$$\delta f = f_0\frac{p_\mu p_\nu \pi^{\mu\nu}}{T^2(\varepsilon + p_0)}. \tag{4.79}$$

Hydrodynamic evolution is done in (τ,x,y,η) coordinates so all components of $\pi^{\mu\nu}$ should be expressed in this basic. However we have to calculate contraction $p_\mu p_\nu \pi^{\mu\nu}$ and we only know p^μ in (t,x,y,z) coordinates. p^μ in (τ,x,y,η) coordinates can be obtained by using inverse of transformation (4.55):

$$p^{\mu'} = \Big(X^{\mu'}_\nu\Big)^{-1}p^\nu = (m_T\cosh(y-\eta_s), \mathbf{p_T}, \frac{m_T}{\tau}\sinh(y-\eta_s)). \tag{4.80}$$

Using inverse of transformation (4.55) we can also calculate metric $g^{\mu\nu}$ in these new coordinates and it is

$$g_{\mu\nu} = \mathrm{Diag}(1, -1, -1, -\tau^2). \tag{4.81}$$

After these transformations obtaining $p_\mu p_\nu \pi^{\mu\nu}$ is straightforward calculation. Final answer reads:

$$\begin{aligned} p_\mu p_\nu \pi^{\mu\nu} &= m_T^2 \cosh^2(y-\eta_s)\pi^{\tau\tau} + (p^x)^2\pi^{xx} + (p^y)^2\pi^{yy} + \tau^2 m_T^2 \sinh^2(y-\eta_s)\pi^{\eta\eta} \\ &- 2m_T \cosh(y-\eta_s)\Big(p^x\pi^{\tau x} + p^y\pi^{\tau y}\Big) - 2\tau m_T^2 \cosh(y-\eta_s)\sinh(y-\eta_s)\pi^{\tau\eta} \\ &+ 2p_x p_y \pi^{xy} + 2\tau m_T \sinh(y-\eta_s)\Big(p^x\pi^{\eta x} + p^y\pi^{\eta y}\Big) \end{aligned} \tag{4.82}$$

Finally we are in position to calculate viscous correction to hadron spectra. This is done by substituting Eqs.(4.61), (4.79) and (4.82) to Cooper-Frye integral. Like in case of equilibrium spectrum η_s integral can be done analytically. After little bit of manipulation of hyperbolic functions we arrive to the final result:

$$\begin{aligned} E\frac{\mathrm{d}^3N_{visc}}{\mathrm{d}^3\mathbf{p}} &= -\frac{g_i}{T^2(\varepsilon+p_0)(2\pi)^3}\int \mathrm{d}x\mathrm{d}y[\pm]\tau \exp\left(\frac{\mu+\gamma_T - \mathbf{p_T}\cdot\mathbf{v_T}}{T}\right) \\ &\times \Bigg[\Big((p^x)^2\pi^{xx} + (p^y)^2 + p^x p^y \pi^{xy}\Big)\Big(m_T \mathrm{K}_1 - \Big(p^x\frac{\partial\tau}{\partial x} + p^y\frac{\partial\tau}{\partial y}\Big)\mathrm{K}_0\Big) \\ &+ m_T^2\pi^{\tau\tau}\Big(\frac{1}{4}m_T\Big(\mathrm{K}_3 + 3\mathrm{K}_1\Big) - \frac{1}{2}\Big(p^x\frac{\partial\tau}{\partial x} + p^y\frac{\partial\tau}{\partial y}\Big)\Big(\mathrm{K}_2 + \mathrm{K}_0\Big)\Big) \\ &+ \tau^2 m_T^2\pi^{\eta\eta}\Big(\frac{1}{4}m_T\Big(\mathrm{K}_3 - \mathrm{K}_1\Big) - \frac{1}{2}\Big(p^x\frac{\partial\tau}{\partial x} + p^y\frac{\partial\tau}{\partial y}\Big)\Big(\mathrm{K}_2 - \mathrm{K}_0\Big)\Big) \\ &- 2m_T\Big(p^x\pi^{\tau x} + p^y\pi^{\tau y}\Big)\Big(\frac{1}{2}m_T\Big(\mathrm{K}_2 - \mathrm{K}_0\Big) - \Big(p^x\frac{\partial\tau}{\partial x} + p^y\frac{\partial\tau}{\partial y}\Big)\mathrm{K}_1\Big)\Bigg], \end{aligned} \tag{4.83}$$

where each modified Bessel function has an argument $\gamma_T m_T/T$. The total hadron spectra can be obtained by summing viscous correction to result from equilibrium calculation Eq.(4.70).

Even though bulk viscosity is taken account in hydrodynamic evolution we do not take it account when calculating viscous correction to hadron spectra. The main reason for this is that theory behind bulk viscous corrections is not yet well established. However, there has been some researches which use bulk viscosity

correction to the distribution function, which is calculated using Chapman-Enskog expansion [66], [67]. In these cases the correction is form of

$$\delta f_{bulk} = -f_0(1 \pm f_0)\frac{C_{bulk}}{T}\left[\frac{m^2}{3p_\mu u^\mu} - \left(\frac{1}{3} - c_s^2\right)p_\mu u^\mu\right]\Pi, \tag{4.84}$$

where c_s is the speed of sound and

$$\frac{1}{C_{bulk}} = \frac{1}{3T}\sum_i g_i m_i^2 \int \frac{\mathrm{d}^3\mathbf{k}}{(2\pi)^3 E_k} f_{0i}(1 \pm f_{0i})\left[\frac{m_i^2}{3E_k} - \left(\frac{1}{3} - c_s^2\right)E_k\right]. \tag{4.85}$$

Unfortunately in this case one cannot integrate one integral analytically when calculating Cooper-Frye integral (4.53), which makes numerical calculations a bit more expensive. In theory ignoring bulk viscosity in freeze-out could be problematic. Nevertheless, at least when $T_{dec} = 100$ MeV, effect of bulk viscosity is very small compared to shear viscosity at the freeze-out. This is demonstrated in figure 9 where we present quantities $|\Pi|/p_0$ and $\sqrt{\pi^{\mu\nu}\pi_{\mu\nu}}/p_0$ averaged over the freeze-out surface in function of centrality. From this figure we can see that in most central collisions bulk viscosity is around one fourth of the shear viscosity at the freeze-out surface. The difference between shear and bulk viscosity gets only larger when going to a larger centrality classes. From this we can conclude that at least in context of this thesis it is justified to ignore bulk viscous correction at the freeze-out.

After calculating particle spectra at the thermal freeze-out, one still needs to take account possible decays of the unstable particles before they reach detectors. The Cooper-Frye integral is calculated for all particles included in the HRG part of the EoS. This consists in total several hundreds of particles which each can decay to other particles through multiple decay channels. In this thesis we take account all 2- and 3-particle decays. However, we don't go through how these decays are calculated in practice. Interested reader can find more details about calculating these particle decays in Refs.[68], [69].

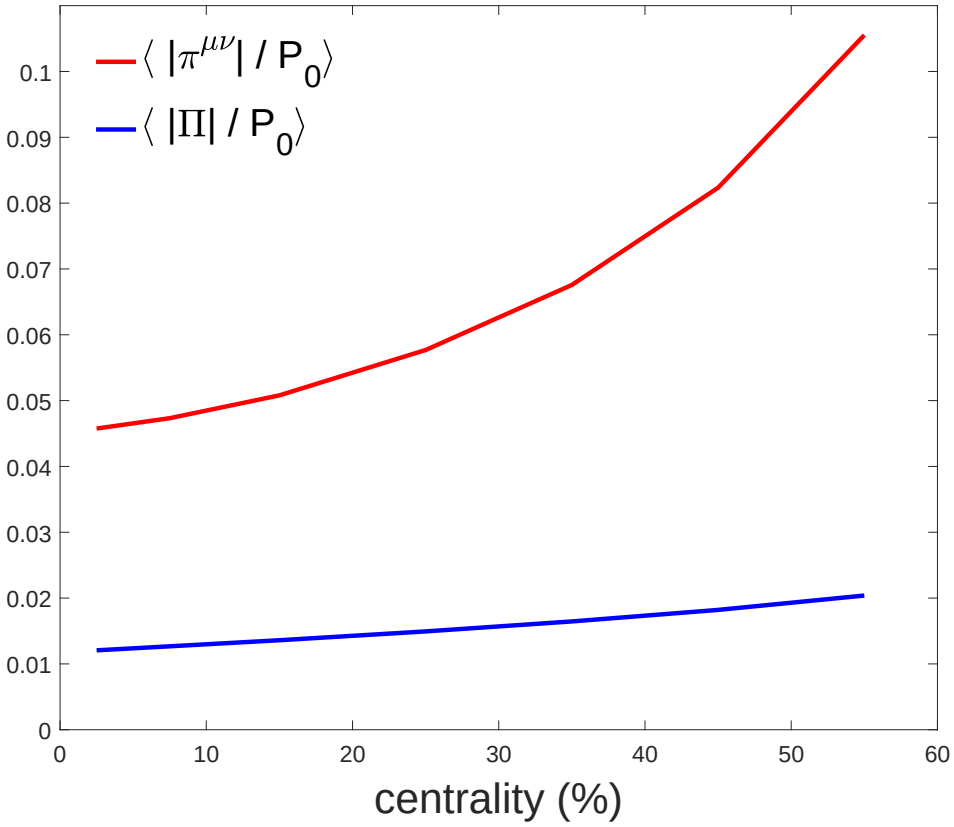

Figure 9. Quantities $\langle|\Pi|/p_0\rangle$ and $\langle|\pi^{\mu\nu}|/p_0\rangle = \langle|\sqrt{\pi^{\mu\nu}\pi_{\mu\nu}}/p_0\rangle$ as function of centrality. Averages are over 100 MeV constant temperature freeze-out surface.

5 Numerical methods

5.1 Equations of motion

In section 2 we derived equations of motion for hydrodynamics in terms of different equilibrium and dissipative quantities. However it is numerically more convenient to solve components of the energy-momentum tensor from the conservation law

$$\partial_\mu T^{\mu\nu} = 0. \tag{5.1}$$

We also use boost-invariant approximation where the natural choice of coordinates is (τ,x,y,η_s). When changing coordinates we have to replace derivatives ∂_μ with the covariant derivatives D_μ [70]. This leads to

$$D_\mu T^{\mu\nu} = \partial_\mu T^{\mu\nu} + \Gamma^\mu_{\mu\lambda} T^{\lambda\nu} + \Gamma^\nu_{\mu\lambda} T^{\mu\lambda} = 0, \tag{5.2}$$

where

$$\Gamma^\mu_{\nu\lambda} = \frac{1}{2} g^{\mu\sigma} \Big(\partial_\nu g_{\lambda\sigma} - \partial_\sigma g_{\nu\lambda} + \partial_\lambda g_{\sigma\nu} \Big) \tag{5.3}$$

are the Chritoffel symbols. We already calculated metric $g_{\mu\nu}$ in (τ,x,y,η_s) coordinates in section 4.5.2 and it reads

$$g_{\mu\nu} = \mathrm{Diag}(1, -1, -1, -\tau^2). \tag{5.4}$$

Using this form of the metric it is easy to see that only non-zero Chirstoffel symbols are

$$\Gamma^\tau_{\eta\eta} = \tau, \qquad \Gamma^\eta_{\eta\tau} = \Gamma^\eta_{\tau\eta} = \frac{1}{\tau}. \tag{5.5}$$

Now we can write Eqs.(5.2) in form

$$\begin{aligned} &\partial_\mu T^{\mu\tau} + \frac{1}{\tau} T^{\tau\tau} + \tau T^{\eta\eta} = 0, \\ &\partial_\mu T^{\mu x} + \frac{1}{\tau} T^{\tau x} = 0, \\ &\partial_\mu T^{\mu y} + \frac{1}{\tau} T^{\tau y} = 0, \\ &\partial_\mu T^{\mu\eta} + \frac{3}{\tau} T^{\tau\eta} = 0. \end{aligned} \tag{5.6}$$

These equations can be further simplified because all components of $T^{\mu\nu}$ are not independent. In order to do so, we first need to know form of fluid's 4-velocity in these new coordinates. This is done by applying inverse of transformation (4.55) to the 4-velocity in Eq.(4.66):

$$u^{\mu'} = \left(X^{\mu'}_{\nu}\right)^{-1} u^{\nu} = \gamma_T(1, \mathbf{v_T}, 0). \tag{5.7}$$

Now using definition (2.56) we can write following relations for the components of the energy-momentum tensor

$$\begin{aligned} T^{xx} &= v_x T^{\tau x} + (p_0 + \Pi) + \pi^{xx} - v_x \pi^{\tau x}, \\ T^{\tau x} &= v_x T^{\tau\tau} + v_x(p_0 + \Pi) + \pi^{\tau x} - v_x \pi^{\tau\tau}, \\ T^{xy} &= v_y T^{\tau x} + \pi^{xy} - v_y \pi^{\tau x}, \\ T^{\eta\eta} &= \frac{1}{\tau^2}(p_0 + \Pi) + \pi^{\eta\eta}, \end{aligned} \tag{5.8}$$

where indices x and y are interchangeable. We also note that $T^{\eta\mu} = \pi^{\eta\mu}$ when $\mu \neq \eta$. In the boost-invariant approximation all derivatives of η vanish in which case we can eliminate last equation from Eqs. (5.6), because it does not provide any addition information. The rest of equations of motion (5.6) can be simplified using relations (5.8) to a form

$$\begin{aligned} &\partial_\tau T^{\tau\tau} + \partial_x(v_x T^{\tau\tau}) + \partial_y(v_y T^{\tau\tau}) = -\partial_x\Big(v_x(p_0 + \Pi - \pi^{\tau\tau}) + \pi^{\tau x}\Big) \\ &- \partial_y\Big(v_y(p_0 + \Pi - \pi^{\tau\tau}) + \pi^{\tau y}\Big) - \frac{1}{\tau}(T^{\tau\tau} + p_0 + \Pi) - \tau\pi^{\eta\eta} \end{aligned} \tag{5.9}$$

$$\begin{aligned} &\partial_\tau T^{\tau x} + \partial_x(v_x T^{\tau x}) + \partial_y(v_y T^{\tau x}) = -\frac{1}{\tau} T^{\tau x} - \partial_y(\pi^{xy} - v_y \pi^{\tau x}) \\ &- \partial_x(p_0 + \Pi + \pi^{xx} - v_x \pi^{\tau x}), \end{aligned} \tag{5.10}$$

$$\begin{aligned} &\partial_\tau T^{\tau y} + \partial_x(v_x T^{\tau y}) + \partial_y(v_y T^{\tau y}) = -\frac{1}{\tau} T^{\tau y} - \partial_x(\pi^{xy} - v_x \pi^{\tau x}) \\ &- \partial_y(p_0 + \Pi + \pi^{yy} - v_y \pi^{\tau y}). \end{aligned} \tag{5.11}$$

Finally equations of motion (5.9)-(5.11) are in a form where they can be solved numerically using the SHASTA algorithm, which is introduced in section 5.2. The equations of motion for dissipative quantities (4.42) and (4.43) can also be written in form which can be numerically solved using the SHASTA algorithm:

$$\partial_\tau \Pi + \partial_x(v_x \Pi) + \partial_y(v_y \Pi) = \Pi\Big(\partial_x v_x + \partial_y v_y\Big) + \frac{1}{\tau\gamma_T}\Big(- \zeta\theta + ...\Big) \tag{5.12}$$

$$\partial_\tau \pi^{\mu\nu} + \partial_x(v_x \pi^{\mu\nu}) + \partial_y(v_y \pi^{\mu\nu}) = \pi^{\mu\nu}\Big(\partial_x v_x + \partial_y v_y\Big) + \frac{1}{\tau\gamma_T}\Big(2\eta\sigma^{\mu\nu} + ...\Big), \quad (5.13)$$

where we didn't explicitly write all terms from the right-hand side of Eqs.(4.42) and (4.43). In dissipative equations we have quantities $\theta, \sigma^{\mu\nu}$ and $\omega^{\mu\nu}$, which all have to be written in terms of velocity. This is already done in Ref.[71] and not repeated here.

5.2 SHASTA

The SHASTA (SHArp and Smooth Transport Algorithm) was introduced by Jay P. Boris and David L. Book in 1971 [72] and it is used to numerically solve equations which are of the form

$$\partial_t \rho(x,t) + \sum_{i=1}^{3} \partial_i(v_i \rho(\mathbf{x},t)) = C, \quad (5.14)$$

where v is local flow velocity and C includes all possible source terms. Without the source terms this equation expresses local conservation of quantity

$$m = \int_V \mathrm{d}^3 x \rho(\mathbf{x},t). \quad (5.15)$$

This is why quantity ρ can be considered as a density and m as a mass. Lets first study how SHASTA works in one dimension and then generalize algorithm into two dimensions.

5.2.1 SHASTA in one dimension

In one dimension Eq.(5.14) simplifies to

$$\partial_t \rho(x,t) + \partial_x(v_x \rho(x,t)) = C. \quad (5.16)$$

The SHASTA algorithm consists of two major stages, a transport stage which is followed by an antidiffusive stage. Both of these stages are executed in a cell grid, where all variables are known at the node points which typically locate at the center of the cell. In transport stage the density distribution between two node points is approximated by linear distribution like in figure 10. Mass between two node points is

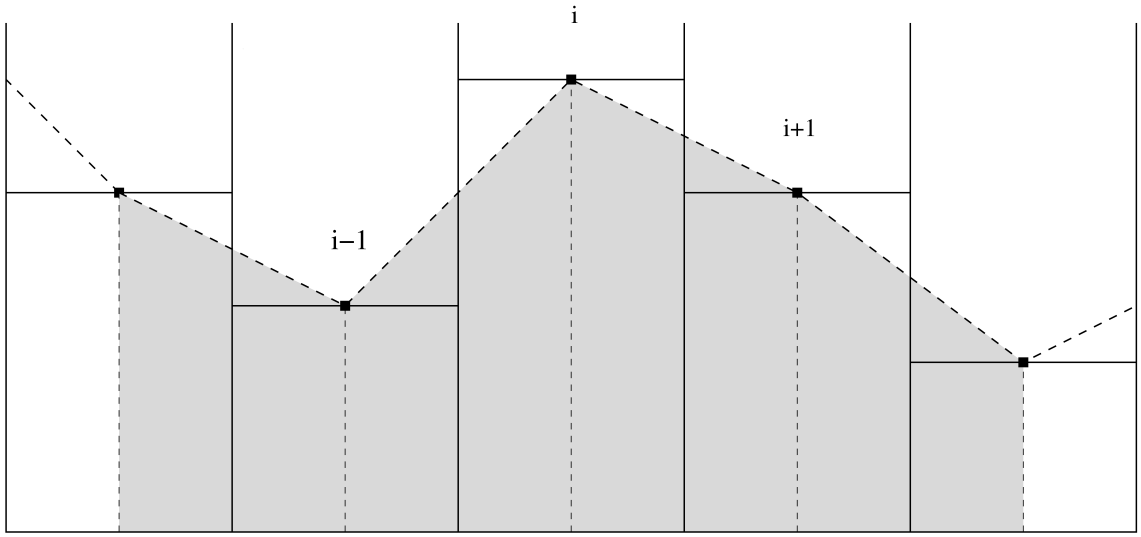

Figure 10. The SHASTA transport stage 1. Picture from Harri Niemi [69].

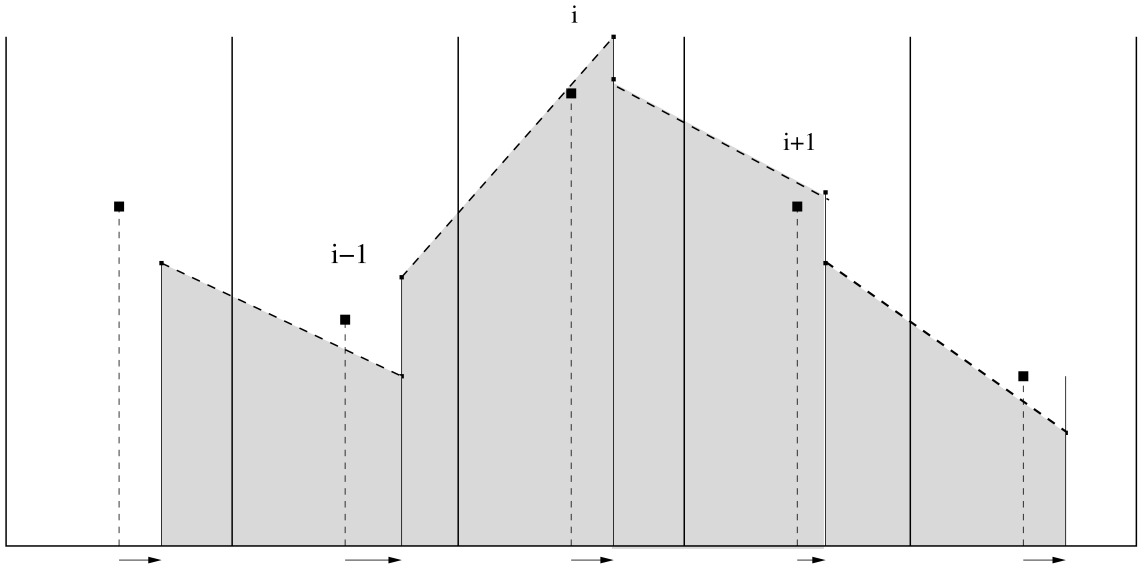

Figure 11. The SHASTA transport stage 2. Picture from Harri Niemi [69].

$$m = \frac{1}{2}(\rho_j^n + \rho_{j+1}^n)\Delta x, \tag{5.17}$$

where upper index indicates time steps and lower index position of node point. Now we transfer node points by a distance $v_j \Delta t$. This is illustrated in figure 11 Mass between node points must be conserved so we define new densities ρ'_j and ρ'_{j+1} so

that

$$m' = \frac{1}{2}(\rho'_j + \rho'_{j+1})(\Delta x - v_j \Delta t + v_{j+1}\Delta t) = \frac{1}{2}(\rho^n_j + \rho^n_{j+1})\Delta x = m. \tag{5.18}$$

Now we can choose

$$\rho'_j = \frac{\Delta x}{\Delta x'}\rho^n_j, \tag{5.19}$$

where $\Delta x'$ is the new distance between node points defined as

$$\Delta x' = \Delta x - v_j \Delta t + v_{j+1}\Delta t. \tag{5.20}$$

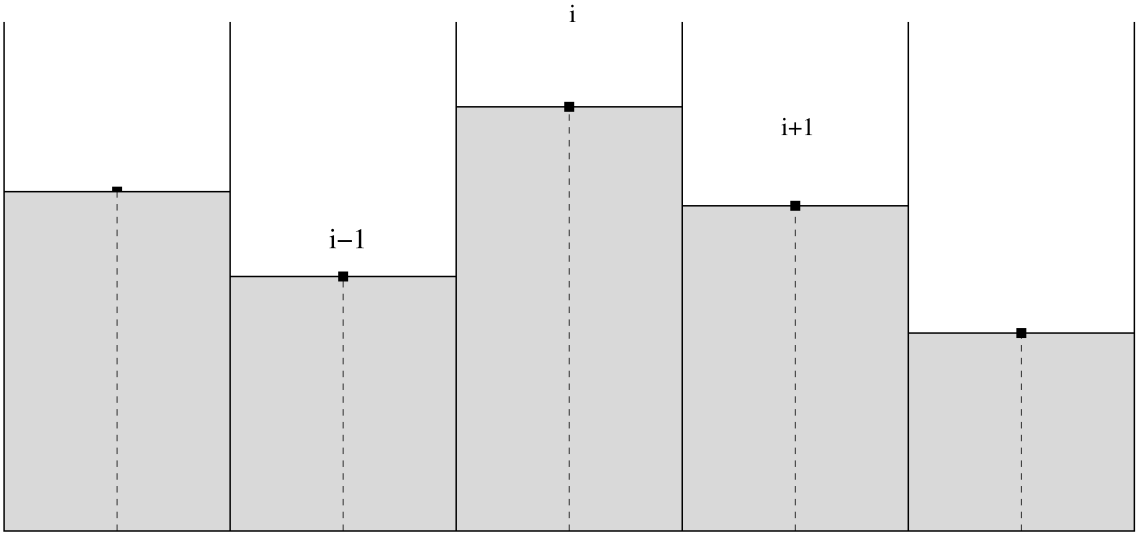

Figure 12. The SHASTA transport stage 3. Picture from Harri Niemi [69].

To get density ρ^{n+1}_j we must calculate average density on the original cell to obtain a piecewise-constant mass distribution like in figure 12. With this kind of method we can write the updated density in terms of the original quantities

$$\rho^{n+1}_j = \frac{1}{2}Q^2_-(\rho^n_{j-1} - \rho^n_j) + \frac{1}{2}Q^2_+(\rho^n_{j+1} - \rho^n_j) + (Q_+ + Q_-)\rho^n_j, \tag{5.21}$$

where

$$Q_\pm = \frac{1/2 \mp \epsilon_j}{1 \pm (v_{j\pm1} - v_j)\frac{\Delta t}{\Delta x}}, \tag{5.22}$$

$$\epsilon_j = v_j \frac{\Delta t}{\Delta x}. \tag{5.23}$$

In order to make this method work one must demand that

$$|\epsilon_j| = |v_j \frac{\Delta t}{\Delta x}| < \frac{1}{2}, \tag{5.24}$$

because otherwise the node point would move out of the cell. Much artificial diffusion is created during this transport phase. That's why there is antidiffusion stage where the generated diffusion is compensated with antidiffusion. One advantage of SHASTA is that explicit form of the diffusion can be obtained. When velocity is constant everywhere equation (5.21) takes form

$$\rho_j^{n+1} = \rho_j^n + \frac{1}{2}\epsilon_j(\rho_{j+1}^n - \rho_{j-1}^n) + \Big(\frac{1}{8} + \frac{\epsilon_j^2}{2}\Big)(\rho_{j+1}^n - 2\rho_j^n + \rho_{j-1}^n), \tag{5.25}$$

where final term tells amount of diffusion. In this work $\frac{\Delta t}{\Delta x} = 0.2$ is used so that $\epsilon < 0.02$ and velocity independent part of diffusion dominates. If we add antidiffusion to density which fully compensates diffusion in equation (5.25) we get

$$\bar{\rho}_j^{n+1} = \rho_j^{n+1} - f_{j+1/2} + f_{j-1/2}, \tag{5.26}$$

where

$$f_{j\pm1/2} = \pm\Big(\frac{1}{8} + \frac{\epsilon^2}{2}\Big)(\rho_{j\pm1}^n - \rho_j^n). \tag{5.27}$$

Unfortunately using this kind of antidiffusion directly generates unphysical ripples in to the solutions. This problem can be solved by requiring that no new maxima or minima is generated in the antidiffusion stage. To guarantee this the antidiffusion flux is defined as

$$f_{j+1/2}^c = S\text{max}(0,\text{min}(S\Delta_{j-1/2}, D|\Delta_{j+1/2}|, S\Delta_{j+3/2}))), \tag{5.28}$$

where

$$S = \text{sign}(\Delta_{j+1/2}), \tag{5.29}$$

$$\Delta_{j+1/2} = \rho_{j+1}^n - \rho_j \tag{5.30}$$

and D is antidiffusion coefficient. According to equation (5.25) this coefficient should have numerical value of $1/8 + \epsilon^2/2$, but in practice this value seems to produce unstable solutions so smaller values are used. Typically diffusion coefficient is set somewhere between $0.10 - 0.11$. Now the density after the antidiffusion stage is

$$\bar{\rho}_j^{n+1} = \rho_j^{n+1} - f_{j+1/2}^c + f_{j-1/2}^c, \tag{5.31}$$

There are still source terms C that need to be added to the solution. This is simply done by following way

$$\tilde{\rho}_j^{n+1} = \bar{\rho}_j^{n+1} - C\Delta t. \tag{5.32}$$

After the source terms are added we can recursively use SHASTA algorithm to get solution for Eq.(5.16) at arbitrary time. More details in implementing one dimensional SHASTA can be found from Ref.[73].

5.2.2 SHASTA in two dimensions

The transport stage of the two-dimensional SHASTA algorithm can be done by applying Eq.(5.21) in both spatial dimensions separately. However, the antidiffusion stage has to be modified in order to prevent existence of new minima or maxima. Modification to the antidiffusion stage was done by Zalesak in 1979 [74]. In two dimensions, where node points are denoted by (i,j), numerical diffusion flux is defined as:

$$f_{i+1/2,j} = D(\rho_{i+1,j}^{n+1} - \rho_{i,j}^{n+1}), \tag{5.33}$$

where $\rho_{i,j}^{n+1}$ is the density after the transport stage. Next we want to find some limiting densities $\rho_{i,j}^{min}$ and $\rho_{i,j}^{max}$ so that when $\rho_{i,j}^{min} < \rho_{i,j} < \rho_{i,j}^{max}$ there is no new minima or maxima that are created. Zalesak defines these densities as

$$\begin{aligned}
\rho_{i,j}^{max} &= \max(\rho_{i-1,j}^{a},\rho_{i,j}^{a},\rho_{i+1,j}^{a},\rho_{i,j-1}^{a},\rho_{i,j+1}^{a}),\\
\rho_{i,j}^{a} &= \max(\rho_{i,j}^{n},\bar{\rho}_{i,j}^{n+1}),\\
\rho_{i,j}^{min} &= \min(\rho_{i-1,j}^{b},\rho_{i,j}^{b},\rho_{i+1,j}^{b},\rho_{i,j-1}^{b},\rho_{i,j+1}^{b}),\\
\rho_{i,j}^{b} &= \min(\rho_{i,j}^{n},\bar{\rho}_{i,j}^{n+1}),
\end{aligned} \tag{5.34}$$

where ρ^n is the density in previous time step and $\bar{\rho}$ is density after the transport stage which includes the pressure gradient source terms. When doing antidiffusion using the Zalesak algorithm, the first step is to set numerical diffusion flux to zero in directions of pressure gradients. This is done because pressure gradients will enhance

minima and maxima. Therefore we have to set restrictions

$$\begin{aligned} f_{i+1/2,j} = 0, \text{if } & f_{i+1/2,j}(\bar{\rho}^{n+1}_{i+1,j} - \bar{\rho}^{n+1}_{i,j}) < 0 \\ \text{and either } & f_{i+1/2,j}(\bar{\rho}^{n+1}_{i+2,j} - \bar{\rho}^{n+1}_{i+1,j}) < 0 \\ \text{or } & f_{i+1/2,j}(\bar{\rho}^{n+1}_{i,j} - \bar{\rho}^{n+1}_{i-1,j}) < 0, \\ f_{i,j+1/2} = 0, \text{if } & f_{i,j+1/2}(\bar{\rho}^{n+1}_{i,j+1} - \bar{\rho}^{n+1}_{i,j}) < 0 \\ \text{and either } & f_{i,j+1/2}(\bar{\rho}^{n+1}_{i,j+2} - \bar{\rho}^{n+1}_{i,j+1}) < 0 \\ \text{or } & f_{i,j+1/2}(\bar{\rho}^{n+1}_{i,j} - \bar{\rho}^{n+1}_{i,j-1}) < 0. \end{aligned} \tag{5.35}$$

In the Zelasek algorithm one also has to define following flux related quantities:

$$R^+_{i,j} = \begin{cases} \min(1, O^+_{i,j}/P^+_{i,j}), & \text{if } P^+_{i,j} > 0 \\ 0, & \text{if } P^+_{i,j} = 0 \end{cases}, \tag{5.36}$$

$$R^-_{i,j} = \begin{cases} \min(1, O^-_{i,j}/P^-_{i,j}), & \text{if } P^-_{i,j} > 0 \\ 0, & \text{if } P^-_{i,j} = 0 \end{cases}, \tag{5.37}$$

where

$$\begin{aligned} P^+_{i,j} &= \sum(\text{all flux into cell (i,j)}) \\ &= \max(0, f_{i-1/2,j}) - \min(0, f_{i+1/2,j}) + \max(0, f_{i,j-1/2}) - \min(0, f_{i,j+1/2}), \\ O^+_{i,j} &= \rho^{max}_{i,j} - \bar{\rho}^{n+1}_{i,j}, \\ P^-_{i,j} &= \sum(\text{all flux out from cell (i,j)}) \\ &= \max(0, f_{i+1/2,j}) - \min(0, f_{i-1/2,j}) + \max(0, f_{i,j+1/2}) - \min(0, f_{i,j-1/2}), \\ O^-_{i,j} &= \bar{\rho}^{n+1}_{i,j} - \rho^{min}_{i,j}. \end{aligned} \tag{5.38}$$

Using these quantities one can then obtain final form of antidiffusion fluxes:

$$\begin{aligned} f^c_{i+1/2,j} &= C_{i+1/2,j} A_{i+1/2,j}, \\ f^c_{i,j+1/2} &= C_{i,j+1/2} A_{i,j+1/2}, \end{aligned} \tag{5.39}$$

where

$$C_{i+1/2,j} = \begin{cases} \min(R^+_{i+1,j}, R^-_{i,j}), & \text{if } f_{i+1/2,j} > 0 \\ \min(R^+_{i,j}, R^-_{i+1,j}), & \text{if } f_{i+1/2,j} < 0 \end{cases}, \tag{5.40}$$

$$C_{i,j+1/2} = \begin{cases} \min(R^+_{i,j+1}, R^-_{i,j}), & \text{if } f_{i,j+1/2} > 0 \\ \min(R^+_{i,j}, R^-_{i,j+1}), & \text{if } f_{i,j+1/2} < 0 \end{cases}. \tag{5.41}$$

The final updated density can then be obtained by adding these antidiffusions to transport stage similar manner that was done in one-dimensional case:

$$\tilde{\rho}_{i,j}^{n+1} = \rho_{i,j}^{n+1} - f_{i+1/2,j}^{c} + f_{i-1/2,j}^{c} - f_{i,j+1/2}^{c} + f_{i,j-1/2}^{c} - \Delta t C, \tag{5.42}$$

where we also included the effect of the source terms.

5.3 Structure of the code

The basic of numerical calculations done in this thesis was already existing numerical code, which was first tested in Ref.[71] and then successfully applied in the context of heavy-ion collisions in Refs.[7], [9], [10], [75]. However, these studies only included shear viscosity to the evolution of the system. As a part of this thesis, bulk viscosity was also included to this existing numerical code.

The used code consist from two major parts: one which calculates hydrodynamic evolution and another which calculates final particle spectrum using methods discussed in section 4.5.2. The hydrodynamic evolution is mostly solved using the SHASTA algorithm but it can only solve evolution of components energy momentum tensor and dissipative quantities from one time-step to next one. Because source terms of Eqs.(5.9)-(5.13) contain also pressures and velocities it is necessary to have some method how to extract these quantities between time-steps. This can be done by noticing that energy density and transverse components of velocity can be written as:

$$\begin{aligned} \varepsilon &= T^{\tau\tau} - \pi^{\tau\tau} - v_x\Big(T^{\tau x} - \pi^{\tau x}\Big) - v_y\Big(T^{\tau y} - \pi^{\tau y}\Big), \\ v_i &= \frac{T^{\tau i} - \pi^{\tau i}}{T^{\tau\tau} - \pi^{\tau\tau} + \Big(p_0(\varepsilon) + \Pi\Big)}, \end{aligned} \tag{5.43}$$

where $i = x,y$. So we have group of equations which can be solved numerically when we know equation of state $p_0 = p_0(\varepsilon)$. After velocity and pressure are known, we could use SHASTA recursively to obtain the full time evolution. However, better accuracy is achieved when first calculating velocity and pressure using half time-step from t_i to $t_i + \Delta t/2$ and then doing complete time-step from t_i to $t_i + \Delta t$ using half time-step values for velocity and pressure in source terms.

The hydrodynamic evolution has to calculated to the point in which whole thermal freeze-out surface is inside our (τ,x,y) space, i.e. if freeze-out surface is defined by

$\tau_{surf} = \tau_{surf}(x,y)$ hydrodynamic evolution must be continued until $\tau > \tau_{surf}(x,y)$ for all x,y. Of course one cannot prior know the parametrization of freeze-out surface, so its not so obvious when to stop hydrodynamic evolution. However we chose freeze-out surface as a constant temperature hypersurface with $T = 100$ MeV. With this choice one can at each time step check the temperature in every grid point and then stop evolution when temperature drops below 100 MeV everywhere. The freeze-out surface is then found from full evolution space by using the Cornelius algorithm [76].

In the second part of the code, integrals (4.70) and (4.83) are calculated numerically for each hadron species separately to obtain hadron spectra at the freeze-out. After that 2- and 3-particle decays are calculated. This leads to the final hadron spectra from which one can calculate the observable quantities that can be compared with the data.

6 Results

The simulations of this thesis were done to study effect of bulk viscosity in case of a Pb+Pb collisions with a center of mass energy $\sqrt{s_{NN}} = 2.760$ TeV. This was done by using three different parametrizations: one with the bulk viscosity and two without it. The initial state parameters and the chemical freeze-out temperatures for all parametrizations are shown in table 2. Values for K_{sat} parameter were chosen such a way that total charged particle multiplicity would match with the data in 0-5% centrality class. All parametrizations included constant shear viscosity with no temperature dependence. For bulk viscosity, temperature dependence was taken account with similar parametrizations that was used in Refs.[12], [35]:

$$\zeta/s(T) = \frac{(\zeta/s)_{max}}{1 + \left(\frac{T-(\zeta/s)_{T_0}}{(\zeta/s)_{width}}\right)}, \tag{6.1}$$

where values $(\zeta/s)_{max} = 0.062$, $(\zeta/s)_{T_0} = 180$ MeV and $(\zeta/s)_{width} = 0.019$ were used. Temperature dependence of bulk viscosity is also shown in figure 13 from where on can see that bulk viscosity peaks at the QCD phase transition temperature $T = 180$ MeV. This kind of behavior is expected based on calculations in Refs.[77]–[79].

	K_{sat}	β	T_{chem} (MeV)
PCE150+bulk, $\eta/s = 0.1$	0.56	0.8	150
PCE150, η/s =0.15	0.60	0.8	150
PCE175, η/s =0.15	0.52	0.8	175

Table 2. The initial state parameters and the chemical freeze-out temperatures for different parametrizations.

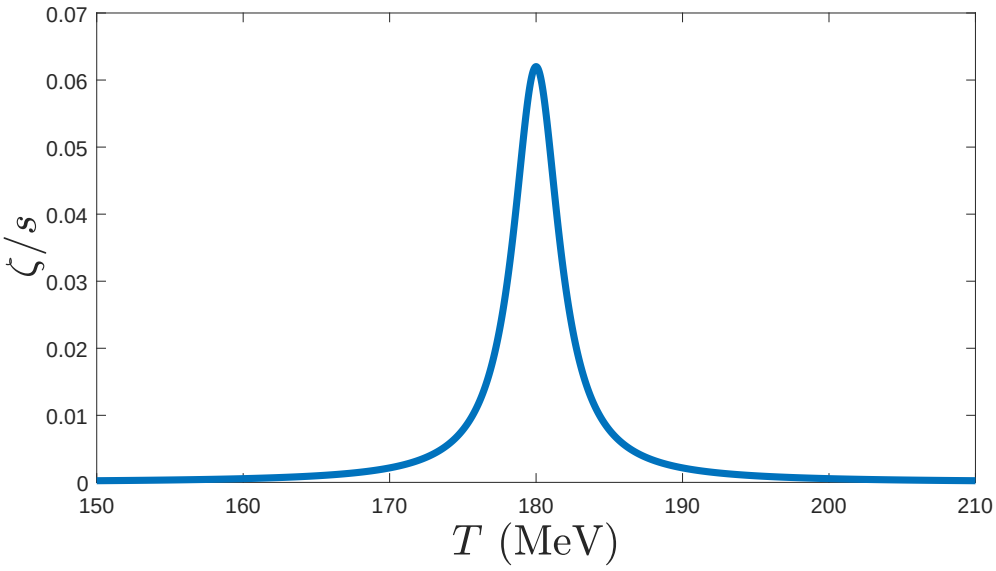

Figure 13. Temperature dependence of the bulk viscosity.

6.1 Hydrodynamic evolution

The hydrodynamic evolution were done in a grid with $N_x = N_y = 220$ grid points in both x, y directions. The distance between each grid point was set to $\Delta x = \Delta y = 0.15$ fm and time between each time step to $\Delta t = 0.06$ fm.

The expansion of the medium during the hydrodynamic evolution is caused by the pressure gradients. The effect of these gradients can be seen in figure 14, which shows transverse velocity as a function of radius in most central $0 - 5\%$ collisions. At the initial state biggest pressure gradients are around $r = 6$ fm (check Fig.3), which generates peak in the velocity profile at the early times $\tau = 1.4$ fm. The similar kind of behavior can be seen with all parametrizations even though adding bulk viscosity will reduce the height of the peak when temperature is close to 180 MeV. This is not a surprise since bulk viscosity is supposed to resist the expansion of the fluid and 180 MeV is the same temperature in which $\zeta/s(T)$ gets its maximum value. We also notice that at the edges of the grid, when $r \geq 16$ fm, velocity seems to remain constant and mostly depend on chemical freeze-out temperature. However, this behavior should not have impact on measurable quantities since there is almost no material (i.e. energy density is close to zero) when $r \geq 16$ fm. At the time $\tau = 7.4$ fm transverse velocity has increased significantly. The effect of bulk viscosity at early times can be still seen as a small dip in the transverse velocity profile around $r = 8$

fm but other than that all parametrizations have similar behavior.

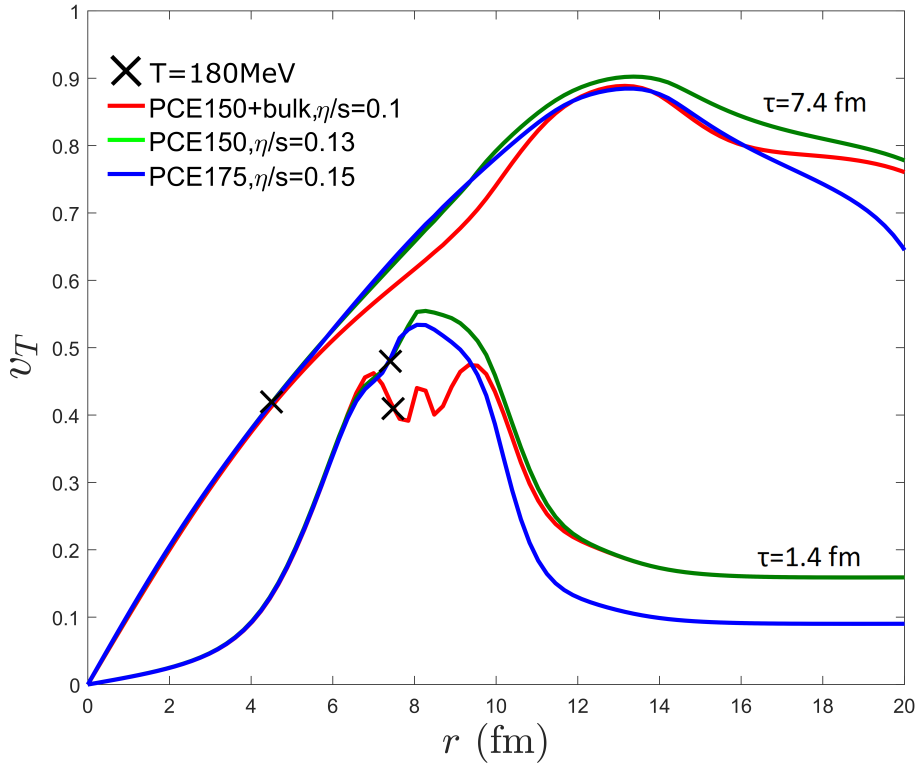

Figure 14. Transverse velocity as a function of radius at times $\tau = 1.3, 7{,}4$ fm in most central 0-5% collisions.

The entropy production during hydrodynamic evolution for centrality classes 0-5% and 30-40% is illustrated in figures 15 and 16. In case of 0-5% centrality class the most of the entropy is produced within first couple of fm. The initial production of entropy seems to heavily depend on chemical freeze out-temperature and value of η/s. At the times 3 fm $\leq \tau \leq$ 12 fm, only parametrization with bulk viscosity have noticeable increase in entropy, which indicates that the bulk viscosity produces entropy constantly throughout the evolution while the shear viscosity produces lots of entropy, but only at the early times. After the time $\tau = 12$ fm total entropy seems to be decreasing, which would violate the second law of thermodynamics. Of course this is not the case and the decrease of entropy is caused by the fact that at the late times part of the fluid is already gone outside the grid, which decreases the entropy. This doesn't have any effect on final observables because temperature of this escaping fluid is already below the freeze-out temperature 100 MeV. The entropy seems to be produced similar manner also in case of 30-40% centrality class. The

biggest difference is that the values of $\mathrm{d}S/\mathrm{d}y$ are around three times smaller than in previous case. The bulk viscosity also seems to have bigger impact on entropy production, which translates to bigger values of entropy at the late times.

Figures 15 and 16 also show points in which center of the system reaches freeze-out temperature. After this point the whole system has decoupled and the hydrodynamic evolution will no longer have any impact on observable quantities. In 0-5% centrality class this freeze-out point seems mostly depend on chemical freeze-out temperature, while in $30-40\%$ centrality class also viscosities seem to have an impact.

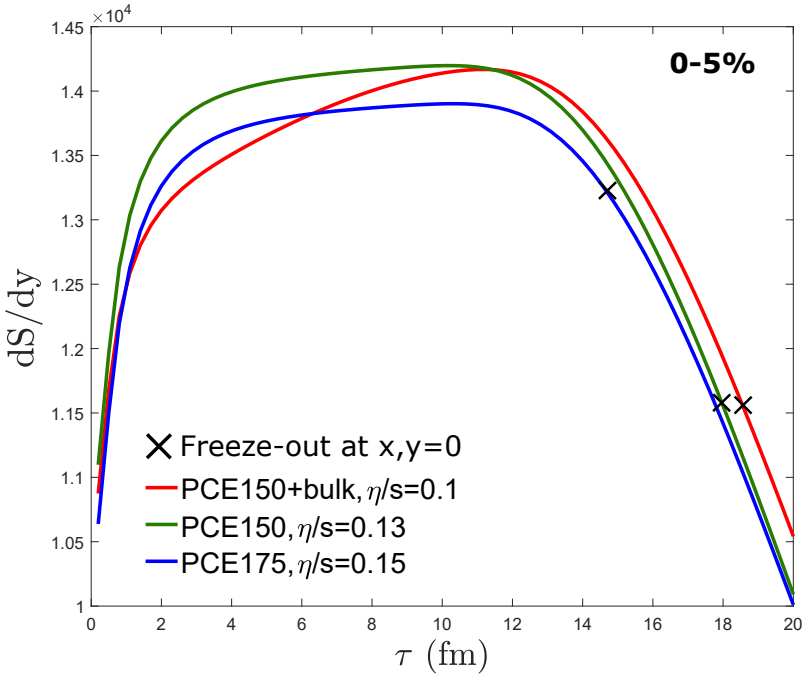

Figure 15. The rapidity density of entropy as a function of longitudinal proper time in 0-5% centrality class.

The systems anisotropy during hydrodynamic evolution was also studied. The anisotropy of system can be characterized by the momentum space eccentricity defined as [80]:

$$\varepsilon_p = \frac{\int \mathrm{d}x\mathrm{d}y(T^{xx} - T^{yy})}{\int \mathrm{d}x\mathrm{d}y(T^{xx} + T^{yy})}. \tag{6.2}$$

Momentum eccentricity is closely related to elliptical flow coefficient v_2 obtained from hadron spectra. The momentum eccentricities as function of longitudinal proper time for 0-5% and 30-40% centrality classes are shown in figures 17 and 18. With both centralities the system starts initially from value $\varepsilon_p = 0$. This is because we have set

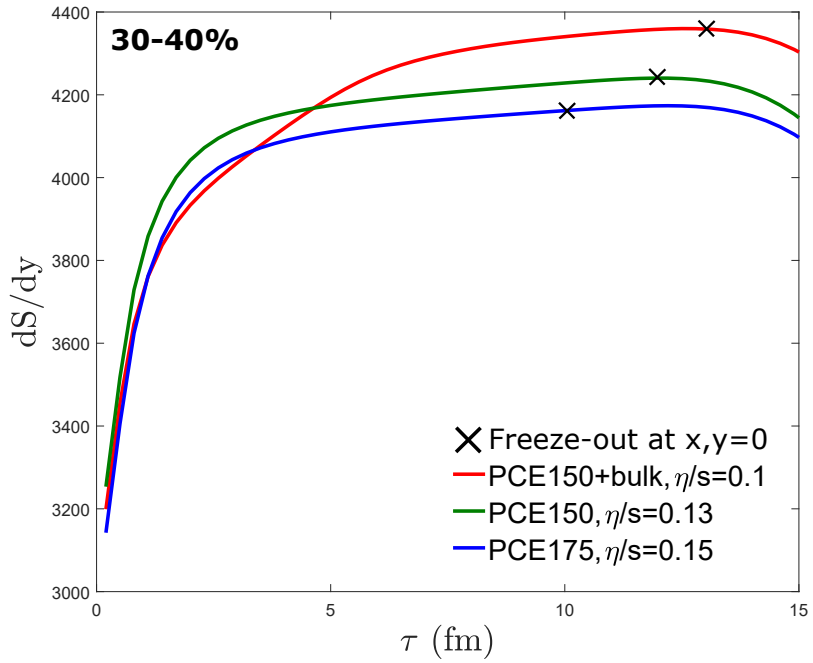

Figure 16. The rapidity density of entropy as a function of longitudinal proper time in 30-40% centrality class.

initial velocity to zero so $T^{xx} = T^{yy}$. When system is not completely cylindrically symmetric pressure gradients start to generate difference between velocities v_x and v_y. Collision systems with centrality $0-5\%$ are almost cylindrically symmetric, so $v_x \sim v_y$. This is why values eccentricities in fig.17 are much smaller when compared to eccentricities in fig.18, where initial state geometry is more ellipsoidal (see Fig.3). In case of 0-5% centrality class we see that viscosity only has small impact on eccentricities at least in the late times. At the times 4 fm $\leq \tau \leq$11 fm there is slight deviation between different parametrizastions which follows general trend that smaller values of η/s correspond to larger eccentricities. The bulk viscosity seems also have small impact in this region based on differences between different parametrizations. For centrality 30-40% behavior seem pretty similar, except the fact that effects of viscosity are little bit more apparent. The bulk viscosity in this case seem to create clear peak at the time $\tau = 5$ fm which was not so apparent with centrality 0-5%.

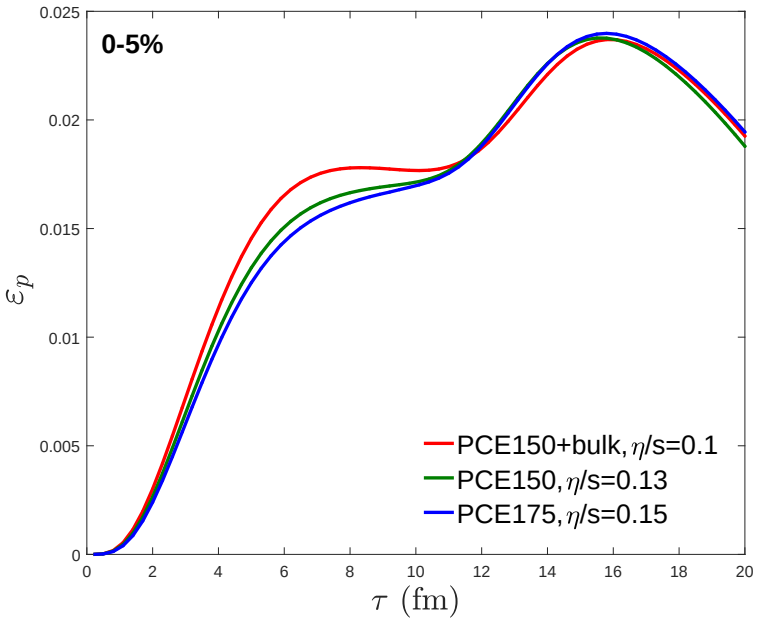

Figure 17. Momentum eccentricity as function of longitudinal proper time in the 0-5% centrality class.

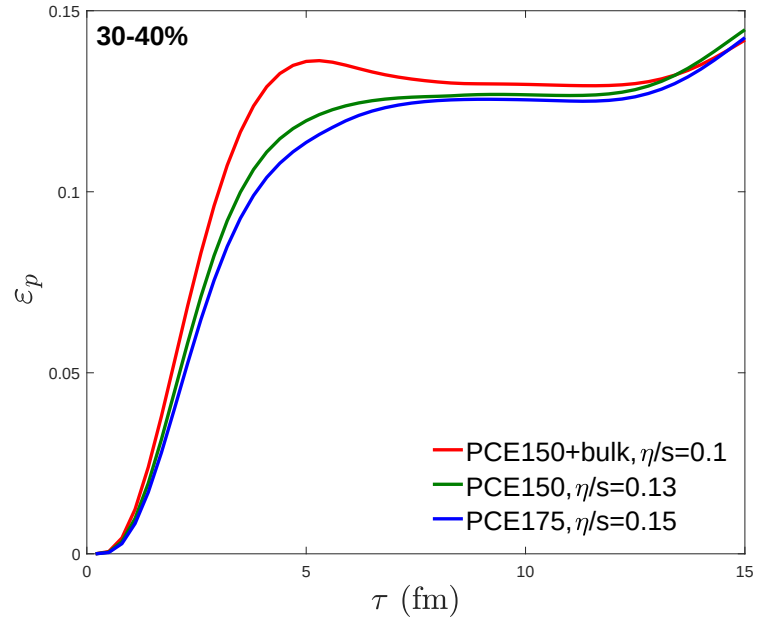

Figure 18. Momentum eccentricity as function of longitudinal proper time in the 30-40% centrality class.

6.2 Multiplicities, average p_T and flow harmonics

The Cooper-Frye integrals (4.70) and (4.83) were calculated numerically for different values of transverse momentum p_T and azimuthal angle ϕ. In simulations 51 evenly distributed transverse momentum points, with $\Delta p_T = 0.2$ GeV, ranging from 0 GeV to 10 GeV were used. Azimuthal angle was calculated in 24 points that cover all values of ϕ, i.e $\Delta\phi = \pi/12$. It was noticed that higher transverse momentum resolution slightly increased multiplicities, but difference was insignificant in context of this thesis. However, in future higher resolution should be used.

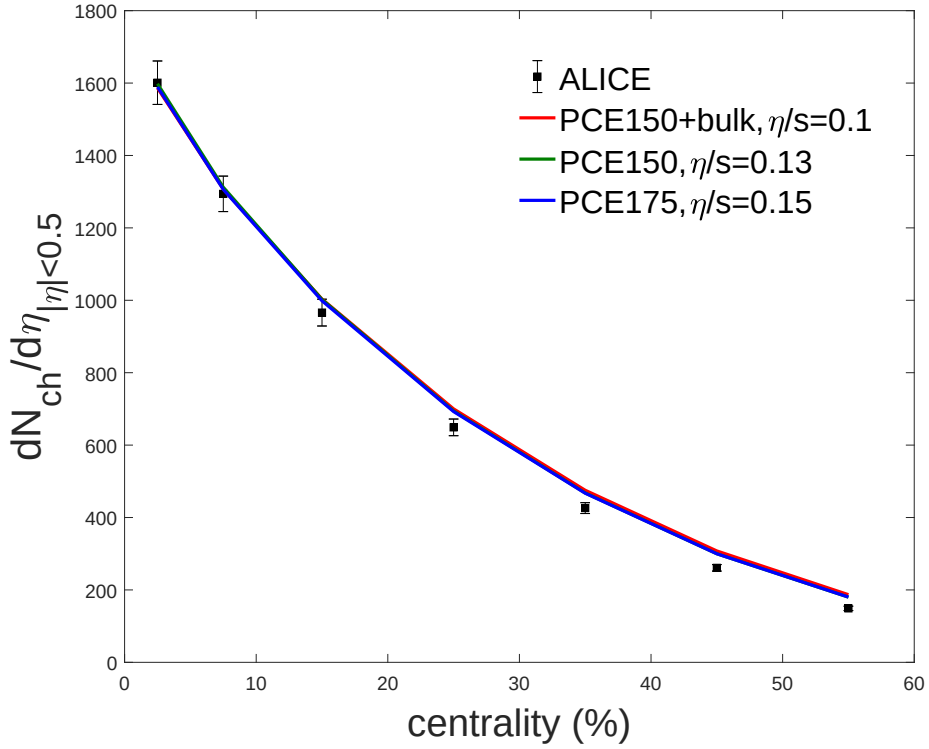

Figure 19. Centrality dependence of the total charged hadron multiplicity for different parametrizations. Experimental data is taken from ALICE [81].

The calculated total charged hadron multiplicities for different centrality classes are shown in Fig, 19 and compared to the ALICE measurements [81]. As we see all different paramerizations produce almost identical results and match with the data in couple of most central centrality bin. However, at the larger centralities all paramerizations overshoot the data quite considerably. This problem is caused by the fact that we used averaged initial states that do not take account initial state

fluctuations. Calculations that take account these fluctuations are done in Refs.[9], [10] where the charged hadron multiplicity matches nicely with the data.

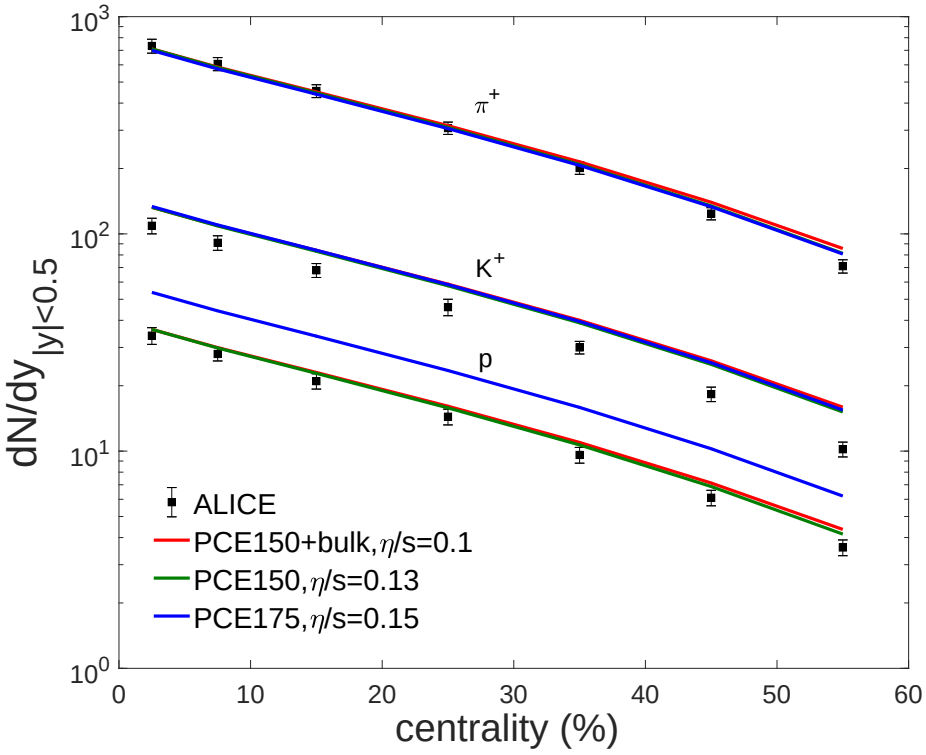

Figure 20. Multiplicities of pions, kaons and protons as function of centrality for different parametrizations. Experimental data is taken from ALICE [82].

The multiplicities of identified hadrons, were also calculated and they are shown in figure 20 against the ALICE measurements [82]. Pion multiplicity matches well with the data for all parametrizations even though centrality dependence is not quite right. This is excepted since the centrality dependence of the total charged hadron multiplicity was not perfect either. In case of kaons, multiplicities are constantly too large no matter what parametrization is used. Unfortunately this cannot be completely fixed by taking account the initial state fluctuations, but would most likely require some changes in the equation of state. For protons, parametrizations that use chemical freeze-out temperature T_{chem} =150 MeV fit well to the data while parametrization using T_{chem} = 175 MeV overshoots the data by a large margin.

Figure 21 presents calculated values of elliptic flow coefficients v_2 compared against ALICE measurements of 4-particle cumulant $v_2\{4\}$ [83]. As can be seen from the figure all parametrizations give similar values and match with the data very well

except in the first 0-5% centrality bin. This again caused by the fact that we did not take account initial state fluctuations which are the main source of anisotropy in case of most central collisions. There is also some small deviations between different parametrizations at large centralities, but even these could be mostly removed by fine tuning the viscosity parameters.

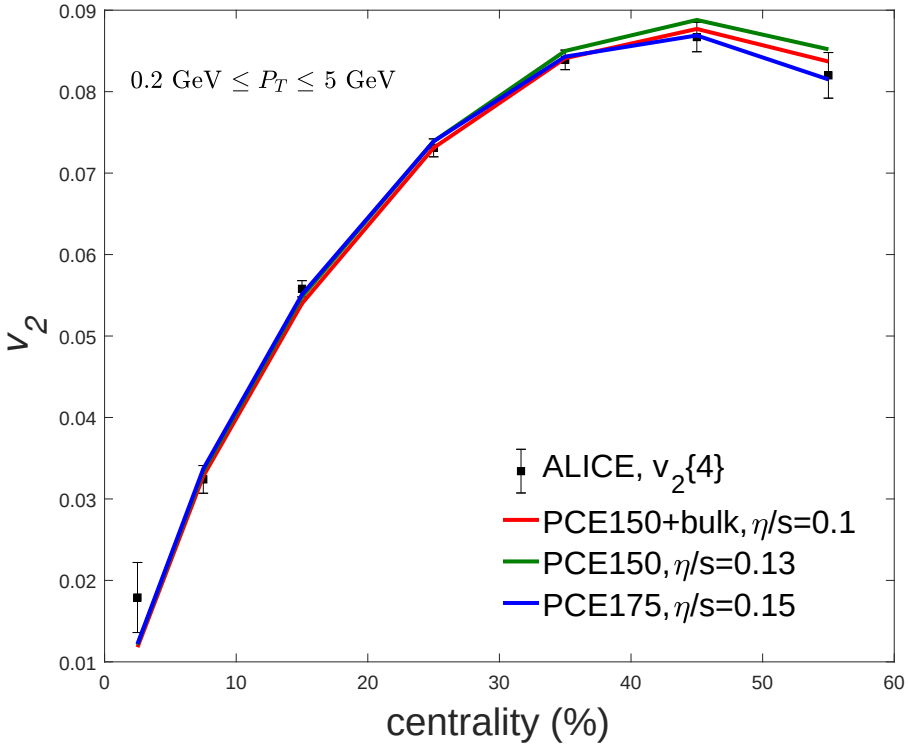

Figure 21. Centrality dependence of elliptic flow coefficient v_2 for different parametrizations. Calculations were compared to the ALICE measurements of the 4-particle cumulant $v_2\{4\}$ [83].

The most important effect of the bulk viscosity can be seen from the centrality dependence of the averaged transverse momentum, which is presented in Fig.22. The PCE175, $\eta/s = 0.15$ -parametrization gives too small averaged p_T values for all studied hadrons while the PCE150, $\eta/s = 0.13$ -parametrization gives mostly too large values, only exceptions being large centralities for pions and kaons. Adding bulk viscosity reduces average p_T of particles giving more accurate results at least in small centralities. Nevertheless, even parametrization with bulk viscosity struggles to give correct centrality dependence. Better centrality dependence could be obtained by taking account initial state fluctuations [9]. Adding initial state fluctuations would

also increase average p_T to a such a level that using $T_{chem} = 175$ MeV, without bulk viscosity, would give good agreement with the data. In this case all parametrizations that have $T_{chem} = 150$ MeV but do not have bulk viscosity would produce way too large values for average p_T. This indicates that using bulk viscosity would be necessary in order to produce good results for the identified hadron multiplicities and for the average transverse momentum. However, detailed studies using bulk viscosity together with EBYE EKRT initial state have not yet been done, so exact effects of bulk viscosity in this situation are still unknown.

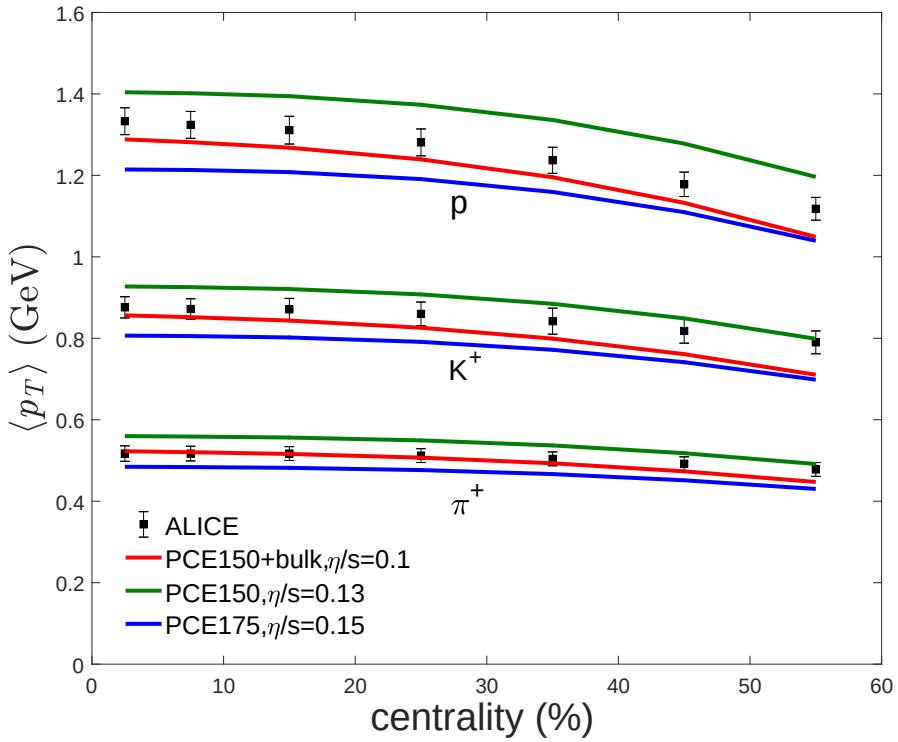

Figure 22. Averaged transverse momentum of pions, kaons and protons as function of centrality for different parametrizations. Experimental data is taken from ALICE [82].

7 Conclusion

In this thesis ultra relativistic heavy-ion collisions were modeled using the viscous hydrodynamics and averaged initial state obtained from the EKRT-model. The equation of state used was based on lattice QCD calculations and thermal freeze-out was done using Cooper-Frye procedure, where only shear viscous correction was taken account.

The main goal of this thesis was to study effects of bulk viscosity and provide some theoretical background behind relativistic hydrodynamics and heavy ion collisions in general. During hydrodynamic evolution bulk viscosity slowed down expansion of the strongly interacting matter and produced some entropy at the later stages of evolution. From the observable quantities, the bulk viscosity mainly affected to the averaged transverse momenta, which was decreased in presence of bulk viscosity. Even though parametrization that used bulk viscosity produced data reasonably well there is still some room for improvements.

There are multiple ways to improve the accuracy of the simulations in a future. First and foremost, the initial state fluctuations should be taken account in order to get better centrality dependence for multiplicities. Taking account initial state fluctuations would also make possible to compare higher order flow harmonics to the data. Secondly bulk viscous correction at thermal freeze-out should also be taken account. In addition, adding temperature dependence for shear viscosity and fine-tuning all parameters could also improve the results.

In the future one could also start expanding simulations outside mid-rapidity region. This would require tweaking the initial state and also modifying hydrodynamic code to work in 3+1 dimensions. In addition, baryon density could no longer be ignored and this should be taken account in EoS. However, all these additions will cost lots of computation power and doing this kind of simulations with the fluctuating initial state might not even be possible on modern hardware.

References

[1] W. Busza, K. Rajagopal, and W. van der Schee, "Heavy Ion Collisions: The Big Picture, and the Big Questions", *Ann. Rev. Nucl. Part. Sci.*, vol. 68, pp. 339–376, 2018. DOI: 10.1146/annurev-nucl-101917-020852. arXiv: 1802.04801 [hep-ph].

[2] R. K. Ellis, W. J. Stirling, and B. R. Webber, *QCD and collider physics*. Cambridge Univ. Press, 2004, ISBN: 0-521-54589-7.

[3] A. K. Chaudhuri, *A short course on Relativistic Heavy Ion Collisions*. IOPP, 2014, ISBN: 9780750310611. DOI: 10.1088/978-0-750-31060-4. arXiv: 1207.7028 [nucl-th]. [Online]. Available: http://inspirehep.net/record/1124193/files/arXiv:1207.7028.pdf.

[4] R. Stock, "Relativistic nucleus–nucleus collisions: From the bevalac to rhic", *Journal of Physics G: Nuclear and Particle Physics*, vol. 30, no. 8, S633–S648, Jul. 2004, ISSN: 1361-6471. DOI: 10.1088/0954-3899/30/8/001. [Online]. Available: http://dx.doi.org/10.1088/0954-3899/30/8/001.

[5] A. Bilandzic, "Recent results on anisotropic flow and related phenomena in ALICE", in *Proceedings, 51st Rencontres de Moriond on QCD and High Energy Interactions: La Thuile, Italy, March 19-26, 2016*, 2016, pp. 281–284. arXiv: 1605.06160 [nucl-ex].

[6] R. Schicker, "Overview of ALICE results in pp, pA and AA collisions", *EPJ Web Conf.*, vol. 138, p. 01 021, 2017. DOI: 10.1051/epjconf/201713801021. arXiv: 1701.04810 [nucl-ex].

[7] H. Niemi *et al.*, "Influence of the shear viscosity of the quark-gluon plasma on elliptic flow in ultrarelativistic heavy-ion collisions", *Phys. Rev. Lett.*, vol. 106, p. 212 302, 2011. DOI: 10.1103/PhysRevLett.106.212302. arXiv: 1101.2442 [nucl-th].

[8] U. Heinz and R. Snellings, "Collective flow and viscosity in relativistic heavy-ion collisions", *Ann. Rev. Nucl. Part. Sci.*, vol. 63, pp. 123–151, 2013. DOI: 10.1146/annurev-nucl-102212-170540. arXiv: 1301.2826 [nucl-th].

[9] H. Niemi, K. J. Eskola, and R. Paatelainen, "Event-by-event fluctuations in a perturbative QCD + saturation + hydrodynamics model: Determining QCD matter shear viscosity in ultrarelativistic heavy-ion collisions", *Phys. Rev.*, vol. C93, no. 2, p. 024 907, 2016. DOI: 10.1103/PhysRevC.93.024907. arXiv: 1505.02677 [hep-ph].

[10] K. J. Eskola *et al.*, "Latest results from the EbyE NLO EKRT model", *Nucl. Phys.*, vol. A967, pp. 313–316, 2017. DOI: 10.1016/j.nuclphysa.2017.04.038. arXiv: 1704.04060 [hep-ph].

[11] S. Ryu *et al.*, "Importance of the Bulk Viscosity of QCD in Ultrarelativistic Heavy-Ion Collisions", *Phys. Rev. Lett.*, vol. 115, no. 13, p. 132 301, 2015. DOI: 10.1103/PhysRevLett.115.132301. arXiv: 1502.01675 [nucl-th].

[12] J. E. Bernhard, "Bayesian parameter estimation for relativistic heavy-ion collisions", PhD thesis, Duke U., 2018-04-19. arXiv: 1804.06469 [nucl-th].

[13] J. Noronha-Hostler *et al.*, "Bulk viscosity effects in event-by-event relativistic hydrodynamics", *Physical Review C*, vol. 88, no. 4, Oct. 2013, ISSN: 1089-490X. DOI: 10.1103/physrevc.88.044916. [Online]. Available: http://dx.doi.org/10.1103/PhysRevC.88.044916.

[14] P. Bożek, "Bulk and shear viscosities of matter created in relativistic heavy-ion collisions", *Physical Review C*, vol. 81, no. 3, Mar. 2010, ISSN: 1089-490X. DOI: 10.1103/physrevc.81.034909. [Online]. Available: http://dx.doi.org/10.1103/PhysRevC.81.034909.

[15] J. L. Nagle and W. A. Zajc, "Small System Collectivity in Relativistic Hadronic and Nuclear Collisions", *Ann. Rev. Nucl. Part. Sci.*, vol. 68, pp. 211–235, 2018. DOI: 10.1146/annurev-nucl-101916-123209. arXiv: 1801.03477 [nucl-ex].

[16] P. Romatschke, "Do nuclear collisions create a locally equilibrated quark–gluon plasma?", *Eur. Phys. J.*, vol. C77, no. 1, p. 21, 2017. DOI: 10.1140/epjc/s10052-016-4567-x. arXiv: 1609.02820 [nucl-th].

[17] P. Bozek, "Collective flow in p-Pb and d-Pd collisions at TeV energies", *Phys. Rev.*, vol. C85, p. 014 911, 2012. DOI: 10.1103/PhysRevC.85.014911. arXiv: 1112.0915 [hep-ph].

[18] G. S. Denicol, "Microscopic foundations of relativisticdissipative fluid dynamics", PhD thesis, Johann Wolfgang Goethe-Universität Frankfurt am Main, 2012.

[19] J.-Y. Ollitrault, "Relativistic hydrodynamics for heavy-ion collisions", *Eur. J. Phys.*, vol. 29, pp. 275–302, 2008. DOI: 10.1088/0143-0807/29/2/010. arXiv: 0708.2433 [nucl-th].

[20] R. Bowley and M. Sanchez, *Introductory statistical mechanics*. Clarendon Press, 1999, ISBN: 978-0198505761.

[21] L. D. Landau and L. E. M., *Fluid dynamics*. Pergamon, 1987.

[22] W. A. Hiscock and L. Lindblom, "Stability and causality in dissipative relativistic fluids", *Annals of Physics*, vol. 151, no. 2, pp. 466–496, 1983, ISSN: 0003-4916. DOI: https://doi.org/10.1016/0003-4916(83)90288-9. [Online]. Available: http://www.sciencedirect.com/science/article/pii/0003491683902889.

[23] W. A. Hiscock and L. Lindblom, "Generic instabilities in first-order dissipative relativistic fluid theories", *Phys. Rev. D*, vol. 31, pp. 725–733, 4 Feb. 1985. DOI: 10.1103/PhysRevD.31.725. [Online]. Available: https://link.aps.org/doi/10.1103/PhysRevD.31.725.

[24] S. Pu, T. Koide, and D. H. Rischke, "Does stability of relativistic dissipative fluid dynamics imply causality?", *Physical Review D*, vol. 81, no. 11, Jun. 2010, ISSN: 1550-2368. DOI: 10.1103/physrevd.81.114039. [Online]. Available: http://dx.doi.org/10.1103/PhysRevD.81.114039.

[25] W. Israel, "Nonstationary irreversible thermodynamics: A causal relativistic theory", *Annals of Physics*, vol. 100, no. 1, pp. 310–331, 1976, ISSN: 0003-4916. DOI: https://doi.org/10.1016/0003-4916(76)90064-6. [Online]. Available: http://www.sciencedirect.com/science/article/pii/0003491676900646.

[26] H. Niemi and G. S. Denicol, "How large is the Knudsen number reached in fluid dynamical simulations of ultrarelativistic heavy ion collisions?", 2014. arXiv: 1404.7327 [nucl-th].

[27] K. Gallmeister *et al.*, "Exploring the applicability of dissipative fluid dynamics to small systems by comparison to the Boltzmann equation", *Phys. Rev.*, vol. C98, no. 2, p. 024 912, 2018. DOI: 10.1103/PhysRevC.98.024912. arXiv: 1804.09512 [nucl-th].

[28] W. Israel and J. M. Stewart, "Transient relativistic thermodynamics and kinetic theory", *Annals Phys.*, vol. 118, pp. 341–372, 1979. DOI: 10.1016/0003-4916(79)90130-1.

[29] G. S. Denicol *et al.*, "Derivation of transient relativistic fluid dynamics from the Boltzmann equation", *Phys. Rev.*, vol. D85, p. 114 047, 2012, [Erratum: Phys. Rev.D91,no.3,039902(2015)]. DOI: 10.1103/PhysRevD.85.114047,10.1103/PhysRevD.91.039902. arXiv: 1202.4551 [nucl-th].

[30] S. R. De Groot, *Relativistic Kinetic Theory. Principles and Applications*, W. A. Van Leeuwen and C. G. Van Weert, Eds. 1980.

[31] E. Molnar, H. Niemi, and D. H. Rischke, "Derivation of anisotropic dissipative fluid dynamics from the Boltzmann equation", *Phys. Rev.*, vol. D93, no. 11, p. 114 025, 2016. DOI: 10.1103/PhysRevD.93.114025. arXiv: 1602.00573 [nucl-th].

[32] E. Molnár *et al.*, "Relative importance of second-order terms in relativistic dissipative fluid dynamics", *Physical Review D*, vol. 89, no. 7, Apr. 2014, ISSN: 1550-2368. DOI: 10.1103/physrevd.89.074010. [Online]. Available: http://dx.doi.org/10.1103/PhysRevD.89.074010.

[33] Z.-W. Lin *et al.*, "A Multi-phase transport model for relativistic heavy ion collisions", *Phys. Rev.*, vol. C72, p. 064 901, 2005. DOI: 10.1103/PhysRevC.72.064901. arXiv: nucl-th/0411110 [nucl-th].

[34] C. Zhang *et al.*, "Update of a multiphase transport model with modern parton distribution functions and nuclear shadowing", *Phys. Rev.*, vol. C99, no. 6, p. 064 906, 2019. DOI: 10.1103/PhysRevC.99.064906. arXiv: 1903.03292 [nucl-th].

[35] J. S. Moreland, J. E. Bernhard, and S. A. Bass, "Estimating initial state and quark-gluon plasma medium properties using a hybrid model with nucleon substructure calibrated to p-Pb and Pb-Pb collisions at $\sqrt{s_{\mathrm{NN}}} = 5.02$ TeV", 2018. arXiv: 1808.02106 [nucl-th].

[36] G. Torrieri *et al.*, "Mach cones in heavy ion collisions", *Acta Phys. Polon.*, vol. B39, pp. 3281–3308, 2008. arXiv: 0901.0230 [nucl-th].

[37] Y. Tachibana and T. Hirano, "Interplay between Mach cone and radial expansion and its signal in γ-jet events", *Phys. Rev.*, vol. C93, no. 5, p. 054 907, 2016. DOI: 10.1103/PhysRevC.93.054907. arXiv: 1510.06966 [nucl-th].

[38] H. Stöcker, "Collective flow signals the quark–gluon plasma", *Nuclear Physics A*, vol. 750, no. 1, pp. 121–147, Mar. 2005, ISSN: 0375-9474. DOI: 10.1016/j.nuclphysa.2004.12.074. [Online]. Available: http://dx.doi.org/10.1016/j.nuclphysa.2004.12.074.

[39] Y. Mehtar-Tani, J. G. Milhano, and K. Tywoniuk, "Jet physics in heavy-ion collisions", *Int. J. Mod. Phys.*, vol. A28, p. 1 340 013, 2013. DOI: 10.1142/S0217751X13400137. arXiv: 1302.2579 [hep-ph].

[40] C. Nattrass, "Measurements of jets in heavy ion collisions", *EPJ Web Conf.*, vol. 172, p. 05 010, 2018. DOI: 10.1051/epjconf/201817205010. arXiv: 1810.04721 [nucl-ex].

[41] T. K. Nayak, "Heavy Ions: Results from the Large Hadron Collider", *Pramana*, vol. 79, pp. 719–735, 2012. DOI: 10.1007/s12043-012-0373-7. arXiv: 1201.4264 [nucl-ex].

[42] S. Acharya *et al.*, "Systematic studies of correlations between different order flow harmonics in Pb-Pb collisions at $\sqrt{s_{\mathrm{NN}}} = 2.76$ TeV", *Phys. Rev.*, vol. C97, no. 2, p. 024 906, 2018. DOI: 10.1103/PhysRevC.97.024906. arXiv: 1709.01127 [nucl-ex].

[43] N. Borghini, P. M. Dinh, and J.-Y. Ollitrault, "Flow analysis from multiparticle azimuthal correlations", *Phys. Rev.*, vol. C64, p. 054 901, 2001. DOI: 10.1103/PhysRevC.64.054901. arXiv: nucl-th/0105040 [nucl-th].

[44] R. Vogt, "Relation of hard and total cross-sections to centrality", *Acta Phys. Hung.*, vol. A9, pp. 339–348, 1999. arXiv: nucl-th/9903051 [nucl-th].

[45] D. G. d'Enterria, "Hard scattering cross-sections at LHC in the Glauber approach: From pp to pA and AA collisions", 2003. arXiv: nucl-ex/0302016 [nucl-ex].

[46] P. F. Kolb *et al.*, "Centrality dependence of multiplicity, transverse energy, and elliptic flow from hydrodynamics", *Nucl. Phys.*, vol. A696, pp. 197–215, 2001. DOI: 10.1016/S0375-9474(01)01114-9. arXiv: hep-ph/0103234 [hep-ph].

[47] K. Eskola *et al.*, "Scaling of transverse energies and multiplicities with atomic number and energy in ultrarelativistic nuclear collisions", *Nuclear Physics B*, vol. 570, no. 1-2, pp. 379–389, Mar. 2000, ISSN: 0550-3213. DOI: 10.1016/s0550-3213(99)00720-8. [Online]. Available: http://dx.doi.org/10.1016/S0550-3213(99)00720-8.

[48] R. Paatelainen *et al.*, "Multiplicities andptspectra in ultrarelativistic heavy ion collisions from a next-to-leading order improved perturbative qcd+saturation+hydrodynamics model", *Physical Review C*, vol. 87, no. 4, Apr. 2013, ISSN: 1089-490X. DOI: 10.1103/physrevc.87.044904. [Online]. Available: http://dx.doi.org/10.1103/PhysRevC.87.044904.

[49] R. Paatelainen, *Minijet initial state of heavy-ion collisions from next-to-leading order perturbative qcd*, 2014. arXiv: 1409.3508 [hep-ph].

[50] K. J. Eskola and K. Tuominen, "Transverse energy from minijets in ultrarelativistic nuclear collisions: A next-to-leading order analysis", *Physical Review D*, vol. 63, no. 11, Apr. 2001, ISSN: 1089-4918. DOI: 10.1103/physrevd.63.114006. [Online]. Available: http://dx.doi.org/10.1103/PhysRevD.63.114006.

[51] R. Paatelainen *et al.*, "Fluid dynamics with saturated minijet initial conditions in ultrarelativistic heavy-ion collisions", *Physics Letters B*, vol. 731, pp. 126–130, Apr. 2014, ISSN: 0370-2693. DOI: 10.1016/j.physletb.2014.02.018. [Online]. Available: http://dx.doi.org/10.1016/j.physletb.2014.02.018.

[52] J. D. Bjorken, "Highly Relativistic Nucleus-Nucleus Collisions: The Central Rapidity Region", *Phys. Rev.*, vol. D27, pp. 140–151, 1983. DOI: 10.1103/PhysRevD.27.140.

[53] H. D. Vries, C. D. Jager, and C. D. Vries, "Nuclear charge-density-distribution parameters from elastic electron scattering", *Atomic Data and Nuclear Data Tables*, vol. 36, no. 3, pp. 495–536, 1987, ISSN: 0092-640X. DOI: https://

doi.org/10.1016/0092-640X(87)90013-1. [Online]. Available: http://www.sciencedirect.com/science/article/pii/0092640X87900131.

[54] S. Chekanov *et al.*, "Exclusive electroproduction of J/Ψ mesons at HERA", *Nuclear Physics B*, vol. 695, no. 1-2, pp. 3–37, Sep. 2004, ISSN: 0550-3213. DOI: 10.1016/j.nuclphysb.2004.06.034. [Online]. Available: http://dx.doi.org/10.1016/j.nuclphysb.2004.06.034.

[55] G. S. Denicol, S. Jeon, and C. Gale, "Transport coefficients of bulk viscous pressure in the 14-moment approximation", *Physical Review C*, vol. 90, no. 2, Aug. 2014, ISSN: 1089-490X. DOI: 10.1103/physrevc.90.024912. [Online]. Available: http://dx.doi.org/10.1103/PhysRevC.90.024912.

[56] J. Adam *et al.*, "Centrality dependence of the pseudorapidity density distribution for charged particles in Pb-Pb collisions at $\sqrt{s_{\mathrm{NN}}} = 5.02$ TeV", *Phys. Lett.*, vol. B772, pp. 567–577, 2017. DOI: 10.1016/j.physletb.2017.07.017. arXiv: 1612.08966 [nucl-ex].

[57] A. Bazavov *et al.*, "Equation of state in (2+1)-flavor qcd", *Physical Review D*, vol. 90, no. 9, Nov. 2014, ISSN: 1550-2368. DOI: 10.1103/physrevd.90.094503. [Online]. Available: http://dx.doi.org/10.1103/PhysRevD.90.094503.

[58] P. Huovinen and P. Petreczky, "Qcd equation of state and hadron resonance gas", *Nuclear Physics A*, vol. 837, no. 1-2, pp. 26–53, Jun. 2010, ISSN: 0375-9474. DOI: 10.1016/j.nuclphysa.2010.02.015. [Online]. Available: http://dx.doi.org/10.1016/j.nuclphysa.2010.02.015.

[59] P. Huovinen, "Chemical freeze-out temperature in the hydrodynamical description of Au + Au collisions at $\sqrt{s_{\mathrm{NN}}} = 200$ GeV ", *The European Physical Journal A*, vol. 37, no. 1, pp. 121–128, Jul. 2008, ISSN: 1434-601X. DOI: 10.1140/epja/i2007-10611-3. [Online]. Available: http://dx.doi.org/10.1140/epja/i2007-10611-3.

[60] M. Cheng *et al.*, "Qcd equation of state with almost physical quark masses", *Physical Review D*, vol. 77, no. 1, Jan. 2008, ISSN: 1550-2368. DOI: 10.1103/physrevd.77.014511. [Online]. Available: http://dx.doi.org/10.1103/PhysRevD.77.014511.

[61] A. Bazavov *et al.*, "Equation of state and qcd transition at finite temperature", *Physical Review D*, vol. 80, no. 1, Jul. 2009, ISSN: 1550-2368. DOI: 10.1103/physrevd.80.014504. [Online]. Available: http://dx.doi.org/10.1103/PhysRevD.80.014504.

[62] T. D. N. S. A. Committee, *The frontiers of nuclear science, a long range plan*, 2008. arXiv: 0809.3137 [nucl-ex].

[63] R. Soltz *et al.*, "Lattice qcd thermodynamics with physical quark masses", *Annual Review of Nuclear and Particle Science*, vol. 65, no. 1, pp. 379–402, Oct. 2015, ISSN: 1545-4134. DOI: 10.1146/annurev-nucl-102014-022157. [Online]. Available: http://dx.doi.org/10.1146/annurev-nucl-102014-022157.

[64] D. Teaney, *Chemical freezeout in heavy ion collisions*, 2002. arXiv: nucl-th/0204023 [nucl-th].

[65] F. Cooper and G. Frye, "Single-particle distribution in the hydrodynamic and statistical thermodynamic models of multiparticle production", *Phys. Rev. D*, vol. 10, pp. 186–189, 1 Jul. 1974. DOI: 10.1103/PhysRevD.10.186. [Online]. Available: https://link.aps.org/doi/10.1103/PhysRevD.10.186.

[66] J.-F. Paquet *et al.*, "Production of photons in relativistic heavy-ion collisions", *Physical Review C*, vol. 93, no. 4, Apr. 2016, ISSN: 2469-9993. DOI: 10.1103/physrevc.93.044906. [Online]. Available: http://dx.doi.org/10.1103/PhysRevC.93.044906.

[67] S. Ryu *et al.*, "Effects of bulk viscosity and hadronic rescattering in heavy ion collisions at energies available at the bnl relativistic heavy ion collider and at the cern large hadron collider", *Physical Review C*, vol. 97, no. 3, Mar. 2018, ISSN: 2469-9993. DOI: 10.1103/physrevc.97.034910. [Online]. Available: http://dx.doi.org/10.1103/PhysRevC.97.034910.

[68] J. Sollfrank, P. Koch, and U. Heinz, "Is there a low-pt"anomaly" in the pion momentum spectra from relativistic nuclear collisions?", *Zeitschrift für Physik C Particles and Fields*, vol. 52, no. 4, pp. 593–609, Dec. 1991. DOI: 10.1007/BF01562334. [Online]. Available: https://doi.org/10.1007/BF01562334.

[69] H. Niemi, "Hydrodynamical flow and hadron spectra in ultrarelativistic heavy ion collisions at rhic and the lhc", PhD thesis, Jyväskylän yliopisto fysiikan laitos, 2008.

[70] S. M. Carroll, *Spacetime and geometry: an introduction to general relativity*. Pearson, 2014, ISBN: 9781292039015.

[71] E. Molnar, H. Niemi, and D. H. Rischke, "Numerical tests of causal relativistic dissipative fluid dynamics", *Eur. Phys. J.*, vol. C65, pp. 615–635, 2010. DOI: 10.1140/epjc/s10052-009-1194-9. arXiv: 0907.2583 [nucl-th].

[72] J. P. Boris and D. L. Book, "Flux-corrected transport. I. SHASTA, a fluid transport algorithm that works", *J. Comput. Phys.*, vol. 11, no. 1, pp. 38–69, 1973. DOI: 10.1016/0021-9991(73)90147-2.

[73] H. Hirvonen, "Numerical methods to solve 1+1 dimensional hydrodynamical equations", Research training thesis, Jyväskylän yliopisto fysiikan laitos, 2018.

[74] S. T. Zalesak, "Fully multidimensional flux-corrected transport algorithms for fluids", *Journal of Computational Physics*, vol. 31, no. 3, pp. 335–362, 1979, ISSN: 0021-9991. DOI: https://doi.org/10.1016/0021-9991(79)90051-2. [Online]. Available: http://www.sciencedirect.com/science/article/pii/0021999179900512.

[75] H. Niemi *et al.*, "Influence of a temperature-dependent shear viscosity on the azimuthal asymmetries of transverse momentum spectra in ultrarelativistic heavy-ion collisions", *Phys. Rev.*, vol. C86, p. 014 909, 2012. DOI: 10.1103/PhysRevC.86.014909. arXiv: 1203.2452 [nucl-th].

[76] P. Huovinen and H. Petersen, "Particlization in hybrid models", *The European Physical Journal A*, vol. 48, no. 11, Nov. 2012, ISSN: 1434-601X. DOI: 10.1140/epja/i2012-12171-9. [Online]. Available: http://dx.doi.org/10.1140/epja/i2012-12171-9.

[77] J. Noronha-Hostler, J. Noronha, and C. Greiner, "Transport coefficients of hadronic matter neartc", *Physical Review Letters*, vol. 103, no. 17, Oct. 2009, ISSN: 1079-7114. DOI: 10.1103/physrevlett.103.172302. [Online]. Available: http://dx.doi.org/10.1103/PhysRevLett.103.172302.

[78] F. Karsch, D. Kharzeev, and K. Tuchin, "Universal properties of bulk viscosity near the qcd phase transition", *Physics Letters B*, vol. 663, no. 3, pp. 217–221, May 2008, ISSN: 0370-2693. DOI: 10.1016/j.physletb.2008.01.080. [Online]. Available: http://dx.doi.org/10.1016/j.physletb.2008.01.080.

[79] P. Arnold, Ç. Doğan, and G. D. Moore, "Bulk viscosity of high-temperature qcd", *Physical Review D*, vol. 74, no. 8, Oct. 2006, ISSN: 1550-2368. DOI: 10.1103/physrevd.74.085021. [Online]. Available: http://dx.doi.org/10.1103/PhysRevD.74.085021.

[80] P. F. Kolb, J. Sollfrank, and U. Heinz, "Anisotropic transverse flow and the quark-hadron phase transition", *Physical Review C*, vol. 62, no. 5, Oct. 2000, ISSN: 1089-490X. DOI: 10.1103/physrevc.62.054909. [Online]. Available: http://dx.doi.org/10.1103/PhysRevC.62.054909.

[81] K. Aamodt *et al.*, "Centrality Dependence of the Charged-Particle Multiplicity Density at Midrapidity in Pb-Pb Collisions at $\sqrt{s_{NN}} = 2.76$ TeV", *Physical Review Letters*, vol. 106, no. 3, Jan. 2011, ISSN: 1079-7114. DOI: 10.1103/physrevlett.106.032301. [Online]. Available: http://dx.doi.org/10.1103/PhysRevLett.106.032301.

[82] B. Abelev *et al.*, "Centrality dependence of π, K, p production in Pb-Pb collisions at $\sqrt{s_{NN}} = 2.76$ TeV", *Phys. Rev.*, vol. C88, p. 044 910, 2013. DOI: 10.1103/PhysRevC.88.044910. arXiv: 1303.0737 [hep-ex].

[83] K. Aamodt *et al.*, "Elliptic flow of charged particles in Pb-Pb collisions at 2.76 TeV", *Phys. Rev. Lett.*, vol. 105, p. 252 302, 2010. DOI: 10.1103/PhysRevLett.105.252302. arXiv: 1011.3914 [nucl-ex].

Appendices

A Derivation of equations of motions for irreducible vector and tensor moments

Equations of motion for irreducible vector and tensor moments (3.62) and (3.63) are derived in this appendix. Lets start by writing general Eq.(3.30) in case of vector moments:

$$\dot{\rho}_r^{\langle\mu\rangle} = \Delta^\mu_\nu \frac{d}{d\tau}\int dK E_k^r k^{\langle\nu\rangle}\delta f_k = \underbrace{\Delta^\mu_\nu \int dK \frac{d}{d\tau}(E_k^r \Delta^\nu_\alpha)k^\alpha \delta f_k}_{A^\mu} + \int dK E_k^r k^{\langle\nu\rangle}\delta\dot{f}_k \quad \text{(A.1)}$$

The first part A^μ can be written as

$$\begin{aligned} A^\mu &= r\dot{u}_\alpha \int dK E_k^{r-1} k^{\langle\alpha\rangle}k^{\langle\mu\rangle}\delta f_k - \Delta^\mu_\nu \int dK E_k^r (u^\nu \dot{u}_\alpha) + \dot{u}^\nu u_\alpha) k^\alpha \delta f_k \\ &= r\dot{u}_\alpha \Delta^\mu_\nu \int dK E_k^{r-1}\Big(k^{\langle\alpha}k^{\nu\rangle} + \frac{1}{3}\Delta^{\alpha\nu}(m^2 - E_k^2)\Big) - \dot{u}^\mu \int dK E_k^{r+1}\delta f_k \\ &= r\dot{u}_\alpha \rho_{r-1}^{\alpha\mu} + \frac{1}{3}r\dot{u}^\mu(m^2\rho_{r-1} - \rho_{r+1}) - \dot{u}^\mu \rho_{r+1}. \end{aligned} \quad \text{(A.2)}$$

The second term can be opened up using Boltzmann equation (3.31):

$$\begin{aligned} \int dK E_k^r k^{\langle\nu\rangle}\delta\dot{f}_k = &- \underbrace{\int dK E_k^{r-1}k^{\langle\mu\rangle}k^\alpha \nabla_\alpha \delta f_k}_{B^\mu} + \underbrace{\int dK E_k^{r-1}k^{\langle\mu\rangle}C[f]}_{=C_{r-1}^{\langle\mu\rangle}} \\ &- \underbrace{\int dK E_k^{r-1}k^{\langle\mu\rangle}k^\alpha \nabla_\alpha f_{0k}}_{D^\mu} - \underbrace{\int dK E_k^r k^{\langle\mu\rangle}\dot{f}_{0k}}_{G^\mu}, \end{aligned} \quad \text{(A.3)}$$

where $C_{r-1}^{\langle\mu\rangle}$ is collision term defined by Eq.(3.38). Only term B^μ is containing δf_k which leads to irreducible moments. This term can be written as

$$\begin{aligned} B^\mu &= \nabla_\alpha \int dK E_k^{r-1}k^{\langle\mu\rangle}k^\alpha \delta f_k - \int dK \nabla_\alpha (E_k^{r-1}\Delta^\mu_\nu)k^\nu k^\alpha \\ &= \underbrace{\nabla_\alpha \int dK E_k^{r-1}k^{\langle\mu\rangle}(E_k u^\alpha + k^{\langle\alpha\rangle})}_{B_1^\mu} - \underbrace{(r-1)\nabla_\alpha u_\beta \int dK E_k^{r-2}k^{\langle\mu\rangle}k^{\langle\alpha\rangle}k^{\langle\beta\rangle}\delta f_k}_{B_2^\mu} \\ &- \underbrace{\int dK E_k^{r-1}\nabla_\alpha(\Delta^\mu_\nu)k^\nu k^\alpha \delta f_k}_{B_3^\mu}, \end{aligned} \quad \text{(A.4)}$$

where in the second term we used fact that $\nabla_\alpha u_\beta$ is orthogonal to u^α and u^β. With use of Eq.(3.11), term B_1^μ can be calculated and written in terms of irreducible moments:

$$\begin{aligned} B_1^\mu &= \nabla_\alpha\Big[u^\alpha \int dK E_k^r k^{\langle\mu} k^{\alpha\rangle}\delta f_k + \int dK E_k^{r-1}\Big(k^{\langle\mu}k^{\alpha\rangle} + \frac{1}{3}\Delta^{\mu\alpha}(m^2 - E_k^2)\Big)\delta f_k\Big] \\ &= \theta\rho_r^\mu + \nabla_\alpha\rho_{r-1}^{\mu\alpha} + \frac{1}{3}\nabla^\mu(m^2\rho_{r-1} - \rho_{r+1}) - \frac{1}{3}u^\mu\theta(m^2\rho_{r-1} - \rho_{r+1}). \end{aligned} \tag{A.5}$$

In case of B_2^μ we need to use definition of the projection operator (3.23) to write

$$\Delta^{\mu_1\mu_2\mu_3}_{\nu_1\nu_2\nu_3} = \frac{1}{6}\sum_{\mathcal{P}_\mu,\mathcal{P}_\nu}\Delta^{\mu_1}_{\nu_1}\Delta^{\mu_2}_{\nu_2}\Delta^{\mu_3}_{\nu_3} - \frac{1}{15}\sum_{\mathcal{P}_\mu,\mathcal{P}_\nu}\Delta^{\mu_1\mu_2}\Delta_{\nu_1\nu_2}\Delta^{\mu_3}_{\nu_3}, \tag{A.6}$$

so we can notice that

$$\begin{aligned} k^{\langle\mu}k^\alpha k^{\beta\rangle} &= k^{\langle\mu\rangle}k^{\langle\alpha\rangle}k^{\langle\beta\rangle} - \frac{3}{5}\Delta^{(\mu\alpha}k^{\langle\beta\rangle)}\Delta_{\lambda\sigma}k^\lambda k^\sigma \\ &= k^{\langle\mu\rangle}k^{\langle\alpha\rangle}k^{\langle\beta\rangle} - \frac{3}{5}\Delta^{(\mu\alpha}k^{\langle\beta\rangle)}(m^2 - E_k^2), \end{aligned} \tag{A.7}$$

where ()- brackets denote symmetrization over all different indices. Now B_2^μ can be written as:

$$\begin{aligned} B_2^\mu &= (r-1)\nabla_\alpha u_\beta\rho_{r-2}^{\mu\alpha\beta} + \frac{1}{5}(r-1)(\nabla^\mu u_\beta + \nabla_\beta u^\mu)\int dK E_k^{r-2}k^{\langle\beta\rangle}(m^2 - E_k^2)\delta f_k \\ &+ \frac{1}{5}(r-1)\theta\int dK E_k^{r-2}k^{\langle\mu\rangle}(m^2 - E_k^2)\delta f_k \\ &= (r-1)\sigma_{\alpha\beta}\rho_{r-2}^{\mu\alpha\beta} + \frac{2}{5}(r-1)\sigma_\beta^\mu(m^2\rho_{r-2}^\beta - \rho_r^\beta) + \frac{1}{3}(r-1)\theta(m^2\rho_{r-2}^\mu - \rho_r^\mu). \end{aligned} \tag{A.8}$$

With a little bit of manipulation B_3^μ can also be written in more convenient form

$$\begin{aligned} B_3^\mu &= -\int dK E_k^{r-1}(u^\mu\nabla_\alpha u_\beta + u_\beta\nabla_\alpha u^\mu)k^\beta k^\alpha\delta f_k \\ &= u^\mu u_\beta\nabla_\alpha\int dK E_k^{r-1}k^{\langle\beta\rangle}k^{\langle\alpha\rangle}\delta f_k - \nabla_\alpha u^\mu\rho_r^\alpha \\ &= -u^\mu u_\beta\nabla_\alpha\rho_{r-1}^{\alpha\beta} - \frac{1}{3}u^\mu\theta(m^2\rho_{r-1} - \rho_{r+1}) + (\omega_\alpha^\mu - \sigma_\alpha^\mu)\rho_r^\alpha - \frac{1}{3}\theta\rho_r^\mu, \end{aligned} \tag{A.9}$$

where $\omega_\alpha^\mu = (\nabla^\mu u_\alpha - \nabla_\alpha u^\mu)/2$ is vorticity tensor introduced in the main text. Putting Eqs.(A.5), (A.8) and (A.9) back together we can write B^μ in terms of irreducible moments

$$\begin{aligned} B^\mu &= \Delta_\nu^\mu\nabla_\alpha\rho_r^{\nu\alpha} - \omega_\alpha^\mu\rho_r^\alpha + \frac{1}{3}\nabla^\mu(m^2\rho_{r-1} - \rho_{r+1}) - (r-1)\sigma_{\alpha\beta}\rho_{r-2}^{\mu\alpha\beta} \\ &- \frac{1}{5}\sigma_\beta^\mu\Big(2(r-1)m^2\rho_{r-2}^\beta - (2r+3)\rho_r^\beta\Big) - \frac{1}{3}\theta\Big((r-1)m^2\rho_r^\mu - (r+3)\rho_{r+2}^\mu\Big). \end{aligned} \tag{A.10}$$

Now we still have to calculate equilibrium terms D^μ and G^μ. Lets start with D^μ which can be written as

$$D^\mu = \Delta^\mu_\nu \nabla_\alpha \underbrace{\int dK E_k^{r-1} k^\nu k^\alpha f_{0k}}_{D_1^{\nu\alpha}} - (r-1)\Delta^\mu_\nu \nabla_\alpha u_\beta \underbrace{\int dK E_k^{r-2} k^\nu k^\alpha k^\beta f_{0k}}_{D_2^{\nu\alpha\beta}}, \tag{A.11}$$

where $D_1^{\nu\alpha}$ can be decomposed to parts which are parallel or orthogonal to 4-velocity:

$$D_1^{\nu\alpha} = I_{r+1,0} u^\nu u^\alpha - I_{r+1,1}\Delta^{\nu\alpha}. \tag{A.12}$$

Here $I_{r+1,1}$ is defined similarly than in Eq.(3.45) which can be seen by contracting Eq.(A.12) with $\Delta_{\nu\alpha}$:

$$I_{r+1,1} = -\frac{1}{3}\Delta_{\nu\alpha} D_1^{\mu\alpha} = -\frac{1}{3}\langle E_k^{r-1}(\Delta_{\alpha\beta} k^\alpha k^\beta)\rangle_0, \tag{A.13}$$

where we remembered that $\Delta^\mu_\mu = 3$. Now we can write

$$\begin{aligned}
\Delta^\mu_\nu \nabla_\alpha D_1^{\nu\alpha} &= -\Delta^\mu_\nu \nabla_\alpha (\Delta^{\nu\alpha} I_{r+1,1}) = -\nabla^\mu I_{r+1,1} \\
&= -\nabla^\mu(\alpha_0)\frac{\partial}{\partial\alpha_0} I_{r+1,1} - \nabla^\mu(\beta_0)\frac{\partial}{\partial\beta_0} I_{r+1,1} \\
&= -J_{r+1,1} I^\mu + J_{r+2,1}\nabla^\mu\beta_0,
\end{aligned} \tag{A.14}$$

where $J_{mn} = \partial I_{mn}/\partial\alpha$. Using thermodynamic relations (2.24), we can derive relation between $\nabla^\mu\beta_0$ and other thermodynamic quantities:

$$\nabla^\mu p_0 = s\nabla^\mu(\beta_0^{-1}) + n\nabla^\mu(\mu) = -\nabla^\mu\beta_0\Big(\frac{s}{\beta_0^2} + \frac{n\mu}{\beta_0}\Big) + \frac{n}{\beta_0} I^\mu. \tag{A.15}$$

Solving $\nabla^\mu\beta_0$ leads to

$$\nabla^\mu\beta_0 = \frac{nI^\mu - \beta_0\nabla^\mu p_0}{s\beta^1 + n\mu} = \frac{nI^\mu - \beta_0\nabla^\mu p_0}{\varepsilon + p_0}, \tag{A.16}$$

where we again used relations 2.24. We can also decompose $D_2^{\nu\alpha}$ similarly to what we did for $D_1^{\nu\alpha}$:

$$D_2^{\nu\alpha\beta} = I_{r+2,0} u^\nu u^\alpha u^\beta - 3I_{r+2,1} u^{(\nu}\Delta^{\alpha\beta)}. \tag{A.17}$$

In this case we are not interested from exact form of coefficients $I_{r+2,0}$ and $I_{r+2,1}$, because both of these parts vanish when calculating D^μ, i.e.

$$(r-1)\Delta^\mu_\nu \nabla_\alpha u_\beta D_2^{\nu\alpha\beta} = 3(r-1) I_{r+2,1}\Delta^\mu_\nu \nabla_\alpha u_\beta u^{(\nu}\Delta^{\alpha\beta)} = 0. \tag{A.18}$$

Now putting Eqs.(A.14) and (A.16) back to Eq.(A.11) we get

$$D^{\mu} = J_{r+2,1}\frac{nI^{\mu} - \beta_0\nabla^{\mu}p_0}{\varepsilon + p_0} - J_{r+1,1}I^{\mu}. \tag{A.19}$$

The last part G^{μ} can be massaged a bit by using chain rule and equation of motion (2.60):

$$\begin{aligned} G^{\mu} &= \int dK E_k^r k^{\langle\mu\rangle}\dot{f}_{0k} = \int dK E_k^r k^{\langle\mu\rangle}\Big(\dot{\alpha_0}\frac{\partial f_{0k}}{\partial\alpha_0} + \dot{\beta}_0\frac{\partial f_{0k}}{\partial\beta_0} + \dot{E}_k\frac{\partial f_{0k}}{\partial E_k}\Big) \\ &= -\dot{u}_{\nu}\beta_0\int dK E_k^r k^{\langle\mu\rangle}k^{\langle\nu\rangle}f_{0k}\tilde{f}_{0k} \\ &= -\dot{u}_{\nu}\beta_0\Big[\underbrace{\int dK E_k^r k^{\langle\mu}k^{\nu\rangle}f_{0k}\tilde{f}_{0k}}_{=0} + \frac{1}{3}\int dK E_k^r\Delta^{\mu\nu}(\Delta_{\alpha\beta}k^{\alpha}k^{\beta})f_{0k}\tilde{f}_{0k}\Big] \\ &= -\beta_0\dot{u}^{\mu}J_{r+2,1} = \frac{\beta_0 J_{r+2,1}}{\varepsilon + p_0}\Big(\nabla^{\mu}p_0 - \Pi\dot{u}^{\mu} + \nabla^{\mu}\Pi - \Delta^{\mu}_{\alpha}\partial_{\beta}\pi^{\alpha\beta}\Big), \end{aligned} \tag{A.20}$$

where we also used orthogonality condition (3.27). Now finally we are in position to put all different terms from Eqs. (A.2),(A.19),(A.19) and (A.20) back to Eq.(A.1). This way we can write equations of motion for irreducible vector moment in following form

$$\begin{aligned} \dot{\rho}_r^{\langle\mu\rangle} - C_{r-1}^{\langle\mu\rangle} =& \alpha_r^{(1)}I^{\mu} + \frac{1}{3}\theta\Big((r-1)m^2\rho_r^{\mu} - (r+3)\rho_{r+2}^{\mu}\Big) + (r-1)\sigma_{\alpha\beta}\rho_{r-2}^{\mu\alpha\beta} \\ &+ \omega_{\nu}^{\mu}\rho_r^{\nu} - \Delta_{\nu}^{\mu}\nabla_{\alpha}\rho_r^{\nu\alpha} + \frac{\beta_0 J_{r+2,1}}{\varepsilon + p_0}\Big(\Pi\dot{u}^{\mu} - \nabla^{\mu}\Pi + \Delta^{\mu}_{\alpha}\partial_{\beta}\pi^{\alpha\beta}\Big) \\ &+ r\dot{u}_{\nu}\rho_{r-1}^{\mu\nu} + \frac{1}{5}\sigma_{\beta}^{\mu}\Big(2(r-1)m^2\rho_{r-2}^{\beta} - (2r+3)\rho_r^{\beta}\Big) \\ &- \frac{1}{3}\nabla^{\mu}(m^2\rho_{r-1} - \rho_{r+1}) + \frac{1}{3}\dot{u}^{\mu}\Big(rm^2\rho_{r-1} + (r+3)\rho_{r+1}\Big), \end{aligned} \tag{A.21}$$

where we defined

$$\alpha_r^{(1)} = J_{r+1,1} - J_{r+2,1}\frac{n}{\varepsilon + p_0}. \tag{A.22}$$

Next lets write Eq.(3.30) for tensor moments:

$$\begin{aligned} \dot{\rho}_r^{\langle\mu\nu\rangle} =& \Delta_{\alpha\beta}^{\mu\nu}\frac{d}{d\tau}\int dK E_k^r k^{\langle\alpha}k^{\beta\rangle}\delta f_k = \underbrace{\Delta_{\alpha\beta}^{\mu\nu}\int dK E_k^r\frac{d}{d\tau}(\Delta_{\lambda\sigma}^{\alpha\beta})k^{\lambda}k^{\sigma}\delta f_k}_{A_1^{\mu\nu}} \\ &+ \underbrace{\Delta_{\alpha\beta}^{\mu\nu}\int dK\frac{d}{d\tau}(E_k^r)k^{\langle\alpha}k^{\beta\rangle}\delta f_k}_{A_2^{\mu\nu}} + \Delta_{\alpha\beta}^{\mu\nu}\int dK E_k^r k^{\langle\alpha}k^{\beta\rangle}\delta\dot{f}_k. \end{aligned} \tag{A.23}$$

First term $A_1^{\mu\nu}$ can be directly calculated:

$$\begin{aligned} A_1^{\mu\nu} &= \Delta^{\mu\nu}_{\alpha\beta}\int dK(2\Delta^{\alpha}_{\lambda}\frac{d}{d\tau}\Delta^{\beta}_{\sigma} - \frac{1}{3}\Delta_{\lambda\sigma}\frac{d}{d\tau}\Delta^{\alpha\beta})k^{\lambda}k^{\sigma}\delta f_k \\ &= -2\Delta^{\mu\nu}_{\alpha\beta}\dot{u}^{\beta}\int dK E_k^{r+1}k^{\langle\alpha\rangle}\delta f_k = -2\dot{u}^{\langle\mu}\rho^{\nu\rangle}_{r+1} \end{aligned} \tag{A.24}$$

In term $A_2^{\mu\nu}$ we need to use relation (A.7) to obtain

$$\begin{aligned} A_2^{\mu\nu} &= r\Delta^{\mu\nu}_{\alpha\beta}\dot{u}_{\lambda}\int dK E_k^{r-1}k^{\langle\alpha}k^{\beta\rangle}k^{\lambda}\delta f_k = r\Delta^{\mu\nu}_{\alpha\beta}\dot{u}_{\lambda}\int dK E_k^{r-1}k^{\langle\alpha\rangle}k^{\langle\beta\rangle}k^{\langle\lambda\rangle}\delta f_k \\ &= r\Delta^{\mu\nu}_{\alpha\beta}\dot{u}_{\lambda}\int dK E_k^{r-1}\Big(k^{\langle\alpha}k^{\beta}k^{\lambda\rangle} + \frac{3}{5}\Delta^{(\alpha\beta}k^{\langle\lambda\rangle)}(m^2 - E_k^2)\Big)\delta f_k \\ &= r\dot{u}_{\lambda}\rho^{\mu\nu\lambda}_{r-1} + \frac{2}{5}r\dot{u}^{\langle\mu}\Big(m^2\rho^{\nu\rangle}_{r-1} - \rho^{\nu\rangle}_{r+1}\Big). \end{aligned} \tag{A.25}$$

The last term from Eq.(A.23) can be opened up using Boltzmann Eq.(3.31):

$$\begin{aligned} \Delta^{\mu\nu}_{\alpha\beta}\int dK E_k^{r}k^{\langle\alpha}k^{\beta\rangle}\delta\dot{f}_k = &-\underbrace{\Delta^{\mu\nu}_{\alpha\beta}\int dK E_k^{r-1}k^{\langle\alpha}k^{\beta\rangle}k^{\lambda}\nabla_{\lambda}\delta f_k}_{B^{\mu\nu}} \\ &+\underbrace{\int dK E_k^{r-1}k^{\langle\mu}k^{\nu\rangle}C[f]}_{=C^{\langle\mu\nu\rangle}_{r-1}} - \underbrace{\Delta^{\mu\nu}_{\alpha\beta}\int dK E_k^{r-1}k^{\langle\alpha}k^{\beta\rangle}k^{\lambda}\nabla_{\lambda}f_{0k}}_{D^{\mu\nu}} \\ &-\underbrace{\int dK E_k^{r}k^{\langle\mu}k^{\nu\rangle}\dot{f}_{0k}}_{G^{\mu\nu}}, \end{aligned} \tag{A.26}$$

where $C^{\langle\mu\nu\rangle}_{r-1}$ is again the same collision term which is defined in Eq.(3.38). In addition $G^{\mu\nu} = 0$, because of the orthogonality condition (3.27). The term $B^{\mu\nu}$ can be divided into couple of smaller pieces:

$$\begin{aligned} B^{\mu\nu} = &\underbrace{\Delta^{\mu\nu}_{\alpha\beta}\nabla_{\lambda}\int dK E_k^{r-1}k^{\langle\alpha}k^{\beta\rangle}k^{\lambda}\delta f_k}_{B_1^{\mu\nu}} \\ &-\underbrace{(r-1)\Delta^{\mu\nu}_{\alpha\beta}\nabla_{\lambda}u_{\sigma}\int dK E_k^{r-2}k^{\langle\alpha}k^{\beta\rangle}k^{\lambda}k^{\sigma}\delta f_k}_{B_2^{\mu\nu}} \\ &-\underbrace{\Delta^{\mu\nu}_{\alpha\beta}\int dK E_k^{r-1}\nabla_{\lambda}(\Delta^{\alpha\beta}_{\sigma\gamma})k^{\sigma}k^{\gamma}k^{\lambda}\delta f_k}_{B_3^{\mu\nu}}. \end{aligned} \tag{A.27}$$

First piece $B_1^{\mu\nu}$ can be easily calculated using earlier relations

$$\begin{aligned} B_1^{\mu\nu} &= \Delta^{\mu\nu}_{\alpha\beta}\nabla_\lambda \int dK E_k^{r-1}\Big(k^{\langle\alpha\rangle}k^{\langle\beta\rangle} - \frac{1}{3}\Delta^{\alpha\beta}(m^2 - E_k^2)\Big)\Big(E_k u^\lambda + k^{\langle\lambda\rangle}\Big)\delta f_k \\ &= \Delta^{\mu\nu}_{\alpha\beta}\nabla_\lambda\Big[u^\lambda \rho_r^{\alpha\beta}\Big] + \Delta^{\mu\nu}_{\alpha\beta}\nabla_\lambda \int dK E_k^{r-1} k^{\langle\alpha}k^{\beta}k^{\lambda\rangle}\delta f_k \\ &+ \Delta^{\mu\nu}_{\alpha\beta}\nabla_\lambda \int dK E_k^{r-1}\Big(\frac{2}{5}\Delta^{\lambda\alpha}k^{\langle\beta\rangle} + \frac{1}{5}\Delta^{\alpha\beta}k^{\langle\lambda\rangle}\Big)(m^2 - E_k^2)\delta f_k \\ &= \theta\rho_r^{\mu\nu} + \Delta^{\mu\nu}_{\alpha\beta}\nabla_\lambda \rho_{r-1}^{\alpha\beta\lambda} + \frac{2}{5}\nabla^{\langle\mu}(m^2\rho_{r-1}^{\nu\rangle} - \rho_{r+1}^{\nu\rangle}). \end{aligned} \tag{A.28}$$

The term $B_2^{\mu\nu}$ is little bit more complicated and it requires use of projection operator with eight indices. From definition (3.23) we can see that it can be written in form

$$\begin{aligned} \Delta^{\mu_1\mu_2\mu_3\mu_4}_{\nu_1\nu_2\nu_3\nu_4} =& \frac{1}{24}\sum_{\mathcal{P}_\mu,\mathcal{P}_\nu}\Delta^{\mu_1}_{\nu_1}\Delta^{\mu_2}_{\nu_2}\Delta^{\mu_3}_{\nu_3}\Delta^{\mu_4}_{\nu_4} - \frac{1}{84}\sum_{\mathcal{P}_\mu,\mathcal{P}_\nu}\Delta^{\mu_1\mu_2}\Delta_{\nu_1\nu_2}\Delta^{\mu_3}_{\nu_3}\Delta^{\mu_4}_{\nu_4} \\ &+ \frac{1}{105}\sum_{\mathcal{P}_\mu,\mathcal{P}_\nu}\Delta^{\mu_1\mu_2}\Delta^{\mu_3\mu_4}\Delta_{\nu_1\nu_2}\Delta_{\nu_3\nu_4} \end{aligned} \tag{A.29}$$

Using this projection operator we find out that

$$\begin{aligned} k^{\langle\alpha}k^\beta k^\lambda k^{\sigma\rangle} =& k^{\langle\alpha}k^{\beta}k^{\lambda}k^{\sigma\rangle} - \frac{6}{7}\Delta^{(\alpha\beta}k^{\langle\lambda}k^{\sigma)\rangle}(m^2 - E_k^2) \\ &+ \frac{3}{35}\Delta^{(\alpha\beta}\Delta^{\lambda\sigma)}(m^2 - E_k^2)^2. \end{aligned} \tag{A.30}$$

Now we can use relation (A.30) to write $B_2^{\mu\nu}$ as

$$\begin{aligned} B_2^{\mu\nu} &= (r-1)\Delta^{\mu\nu}_{\alpha\beta}\nabla_\lambda u_\sigma \int dK E_k^{r-2}k^{\langle\alpha}k^\beta k^\lambda k^{\sigma\rangle}\delta f_k \\ &+ \frac{2}{7}(r-1)\Delta^{\mu\nu}_{\alpha\beta}\Big(\nabla^\alpha u_\sigma + \nabla_\sigma u^\alpha\Big)\int dK E_k^{r-2}k^{\langle\beta}k^{\sigma\rangle}(m^2 - E_k^2)\delta f_k \\ &+ \frac{1}{7}(r-1)\Delta^{\mu\nu}_{\alpha\beta}\theta\int dK E_k^{r-2}k^{\langle\alpha}k^{\beta\rangle}(m^2 - E_k^2)\delta f_k \\ &- \frac{2}{35}(r-1)\Delta^{\mu\nu}_{\alpha\beta}\nabla^\alpha u^\beta(m^4\rho_{r-2} - 2m^2\rho_r + \rho_{r+2}) \\ &= (r-1)\sigma_{\lambda\sigma}\rho_{r-2}^{\mu\nu\lambda\sigma} + \frac{2}{15}(r-1)\sigma^{\mu\nu}(m^4\rho_{r-2} - 2m^2\rho_r + \rho_{r+2}) \\ &+ \frac{4}{7}(r-1)\sigma^{\langle\mu}_\sigma(m^2\rho_{r-2}^{\nu\rangle\sigma} - \rho_r^{\nu\rangle\sigma}) + \frac{1}{3}(r-1)\theta(m^2\rho_{r-2}^{\mu\nu} - \rho_r^{\mu\nu}). \end{aligned} \tag{A.31}$$

The space-like gradient ∇_λ in term $B_3^{\mu\nu}$ can be calculated similarly than comoving derivative $\mathrm{d}/\mathrm{d}\tau$ in Eq.(A.24). This way $B_3^{\mu\nu}$ can be written as

$$\begin{aligned} B_3^{\mu\nu} &= -2\Delta^{\mu\nu}_{\alpha\beta}\nabla_\sigma u^\beta \int dK E_k^r k^{\langle\alpha}k^{\sigma\rangle}\delta f_k \\ &= -2\Delta^{\mu\nu}_{\alpha\beta}\nabla_\sigma u^\beta \int dK E_k^r\Big(k^{\langle\alpha}k^{\sigma\rangle} + \frac{1}{3}\Delta^{\alpha\sigma}(m^2 - E_k^2)\Big)\delta f_k \\ &= 2(\omega_\lambda^{\langle\mu} - \sigma_\lambda^{\langle\mu})\rho_r^{\nu\rangle\lambda} - \frac{2}{3}\theta\rho_r^{\mu\nu} - \frac{2}{3}\sigma^{\mu\nu}(m^2\rho_r - \rho_{r+2}). \end{aligned} \tag{A.32}$$

Term $D^{\mu\nu}$ can be divided into equilibrium integrals $D_1^{\alpha\beta\lambda}$ and $D_1^{\alpha\beta\lambda}$:

$$\begin{aligned} D^{\mu\nu} =& \Delta^{\mu\nu}_{\alpha\beta}\nabla_\lambda \underbrace{\int dK E_k^{r-1} k^\alpha k^\beta k^\lambda f_{0k}}_{D_1^{\alpha\beta\lambda}} \\ &- (r-1)\Delta^{\mu\nu}_{\alpha\beta}\nabla_\lambda u_\sigma \underbrace{\int dK E_k^{r-2} k^\alpha k^\beta k^\lambda k^\sigma f_{0k}}_{D_2^{\alpha\beta\lambda\sigma}}. \end{aligned} \tag{A.33}$$

We can decompose equilibrium integral $D_1^{\alpha\beta\lambda}$ similarly than we did in case of vector moments:

$$D_1^{\alpha\beta\lambda} = I_{r+2,0} u^\alpha u^\beta u^\lambda - 3 I_{r+2,1} \Delta^{(\alpha\beta} u^{\lambda)}, \tag{A.34}$$

so that

$$\Delta^{\mu\nu}_{\alpha\beta}\nabla_\lambda D_1^{\alpha\beta\lambda} = -2\Delta^{\mu\nu}_{\alpha\beta}\nabla^\alpha u^\beta I_{r+2,1}. \tag{A.35}$$

The form of $I_{r+2,1}$ can be obtained by contracting $D_1^{\alpha\beta\lambda}$ with $\Delta_{\alpha\beta}u_\lambda$:

$$I_{r+2,1} = -\frac{1}{3}\Delta_{\alpha\beta}u_\lambda D_1^{\alpha\beta\lambda} = -\frac{1}{3}\langle E_k^r (\Delta_{\alpha\beta}k^\alpha k^\beta)\rangle_0, \tag{A.36}$$

which agrees with definition (3.45). Decomposition for $D_2^{\alpha\beta\lambda\sigma}$ reads:

$$D_2^{\alpha\beta\lambda\sigma} = I_{r+2,0} u^\alpha u^\beta u^\lambda u^\sigma - 6 I_{r+2,1}\Delta^{(\alpha\beta}u^\lambda u^{\sigma)} + 3 I_{r+2,2}\Delta^{(\alpha\beta}\Delta^{\lambda\sigma)}, \tag{A.37}$$

so that

$$\Delta^{\mu\nu}_{\alpha\beta}\nabla_\lambda u_\sigma D_2^{\alpha\beta\lambda\sigma} = 2\Delta^{\mu\nu}_{\alpha\beta}\nabla^\alpha u^\beta I_{r+2,2}. \tag{A.38}$$

The thermodynamic integral $I_{r+2,2}$ can be solved by contracting $D_2^{\alpha\beta\lambda\sigma}$ with $\Delta_{\alpha\beta}\Delta_{\lambda\sigma}$:

$$I_{r+2,2} = \frac{1}{15}\Delta_{\alpha\beta}\Delta_{\lambda\sigma}D_2^{\alpha\beta\lambda\sigma} = \frac{1}{15}\langle E_k^{r-2}(\Delta_{\alpha\beta}k^\alpha k^\beta)^2\rangle_0, \tag{A.39}$$

which again agrees with definition (3.45). The term $D^{\mu\nu}$ can now be obtained by combining Eqs.(A.35) and (A.38):

$$D^{\mu\nu} = -2\sigma^{\mu\nu}\Big(I_{r+2,1} + (r-1)I_{r+2,2}\Big). \tag{A.40}$$

Finally we can combine all terms from Eqs.(A.24),(A.25),(A.28),(A.31),(A.32) and

(A.40) to obtain equations of motion for irreducible tensor moments

$$\begin{aligned}\dot{\rho}_r^{\langle\mu\nu\rangle} - C_{r-1}^{\langle\mu\nu\rangle} =& 2\alpha_r^{(2)}\sigma^{\mu\nu} + (r-1)\sigma_{\alpha\beta}\rho_{r-2}^{\mu\nu\alpha\beta} - \Delta_{\alpha\beta}^{\mu\nu}\nabla_\lambda\rho_{r-1}^{\alpha\beta\lambda} \\ &- \frac{2}{5}\nabla^{\langle\mu}(m^2\rho_{r-1}^{\nu\rangle} - \rho_{r+1}^{\nu\rangle}) + 2\omega_\alpha^{\langle\mu}\rho_r^{\nu\rangle\alpha} \\ &+ \frac{2}{7}\sigma_\alpha^{\langle\mu}\Big(2(r-1)m^2\rho_{r-2}^{\nu\rangle\alpha} - (2r+5)\rho_r^{\nu\rangle\alpha}\Big) \\ &+ \frac{2}{15}\sigma^{\mu\nu}\Big((r-1)m^4\rho_{r-2} - (2r+3)m^2\rho_r + (r+4)\rho_{r+2}\Big) \\ &+ \frac{1}{3}\theta\Big((r-1)m^2\rho_{r-2}^{\mu\nu} - (r+4)\rho_r^{\mu\nu}\Big),\end{aligned} \tag{A.41}$$

where we have defined

$$\alpha_r^{(2)} = I_{r+1,1} + (r-1)I_{r+2,2}. \tag{A.42}$$

B Transport coefficients in 14-moment aproximation

In this appendix we list all transport coefficients for Eqs.(3.90)-(3.92). All transport coefficients are written in terms of thermodynamic quantities or in terms of coefficients γ and $\mathcal{A}$, which are defined in Eqs.(3.71), (3.76), (3.83) and (3.88). The transport coefficients for the bulk viscosity are:

$$\tau_\Pi = \frac{1}{\mathcal{A}_{00}^{(0)}}, \tag{B.1}$$

$$\zeta = \frac{m^2 \alpha_0^{(0)}}{3\mathcal{A}_{00}^{(0)}}, \tag{B.2}$$

$$\ell_{\Pi n} = \frac{m^2 \tau_\Pi}{3}\Big(\frac{G_{30}}{D_{20}} - \gamma_{-1}^{(1)}\Big), \tag{B.3}$$

$$\tau_{\Pi n} = \frac{m^2 \tau_\Pi}{3(\varepsilon + p_0)}\Big(\frac{\partial \gamma_{-1}^{(1)}}{\partial \ln \beta_0} - \frac{G_{30}}{D_{20}}\Big), \tag{B.4}$$

$$\lambda_{\Pi n} = -\frac{m^2 \tau_\Pi}{3}\Big(\frac{\partial \gamma_{-1}^{(1)}}{\partial \alpha_0} + \frac{n}{\varepsilon + p_0}\frac{\partial \gamma_{-1}^{(1)}}{\partial \beta_0}\Big), \tag{B.5}$$

$$\lambda_{\Pi\pi} = \frac{m^2 \tau_\Pi}{3}\Big(\gamma_{-2}^{(2)} - \frac{G_{20}}{D_{20}}\Big), \tag{B.6}$$

$$\delta_{\Pi\Pi} = \frac{m^2 \tau_\Pi}{3}\Big(2m^{-2} + \gamma_{-2}^{(0)} - \frac{G_{20}}{D_{20}}\Big). \tag{B.7}$$

The transport coefficients for the particle diffusion current are:

$$\tau_n = \frac{1}{\mathcal{A}_{00}^{(1)}}, \tag{B.8}$$

$$\kappa_n = \frac{\alpha_0^{(1)}}{\mathcal{A}_{00}^{(1)}}, \tag{B.9}$$

$$\ell_{n\Pi} = \tau_n\Big(\frac{n}{\varepsilon + p_0} + \gamma_{-1}^{(0)}\Big), \tag{B.10}$$

$$\ell_{n\pi} = \tau_n\Big(\frac{n}{\varepsilon + p_0} - \gamma^{(2)}_{-1}\Big), \tag{B.11}$$

$$\tau_{n\Pi} = \frac{\tau_n}{\varepsilon + p_0}\Big(\frac{n}{\varepsilon + p_0} + \frac{\partial\gamma^{(0)}_{-1}}{\partial \ln \beta_0}\Big), \tag{B.12}$$

$$\tau_{n\pi} = \frac{\tau_n}{\varepsilon + p_0}\Big(\frac{n}{\varepsilon + p_0} + \frac{\partial\gamma^{(2)}_{-1}}{\partial \ln \beta_0}\Big), \tag{B.13}$$

$$\lambda_{n\Pi} = \tau_n\Big(\frac{\partial\gamma^{(0)}_{-1}}{\partial\alpha_0} + \frac{\partial\gamma^{(0)}_{-1}}{\partial\beta_0}\Big), \tag{B.14}$$

$$\lambda_{nn} = \frac{\tau_n}{5}\Big(3 + 2m^2\gamma^{(1)}_{-2}\Big), \tag{B.15}$$

$$\lambda_{n\pi} = \tau_n\Big(\frac{\partial\gamma^{(2)}_{-1}}{\partial\alpha_0} + \frac{\partial\gamma^{(2)}_{-1}}{\partial\beta_0}\Big). \tag{B.16}$$

The transport coefficients for the shear viscosity are:

$$\tau_\pi = \frac{1}{\mathcal{A}^{(2)}_{00}}, \tag{B.17}$$

$$\zeta = \frac{\alpha^{(2)}_0}{\mathcal{A}^{(2)}_{00}}, \tag{B.18}$$

$$\ell_{\pi n} = -\frac{2}{5}m^2\tau_\pi\gamma^{(1)}_{-1}, \tag{B.19}$$

$$\tau_{\pi n} = -\frac{2}{5}\frac{m^2\tau_\pi}{\varepsilon + p_0}\frac{\partial\gamma^{(1)}_{-1}}{\partial \ln \beta_0}, \tag{B.20}$$

$$\tau_{\pi\pi} = -\frac{2\tau_\pi}{7}\Big(5 + 2m^2\gamma^{(2)}_{-2}\Big), \tag{B.21}$$

$$\lambda_{\pi n} = -\frac{2}{5}m^2\tau_\pi\Big(\frac{\partial\gamma^{(1)}_{-1}}{\partial\alpha_0} + \frac{n}{\varepsilon + p_0}\frac{\partial\gamma^{(1)}_{-1}}{\partial\beta_0}\Big), \tag{B.22}$$

$$\lambda_{\pi\Pi} = \frac{2\tau_\pi}{5}\Big(3 + m^2\gamma^{(0)}_{-2}\Big), \tag{B.23}$$

$$\delta_{\pi\pi} = \frac{1\tau_\pi}{3}\Big(4 + m^2\gamma^{(2)}_{-2}\Big). \tag{B.24}$$